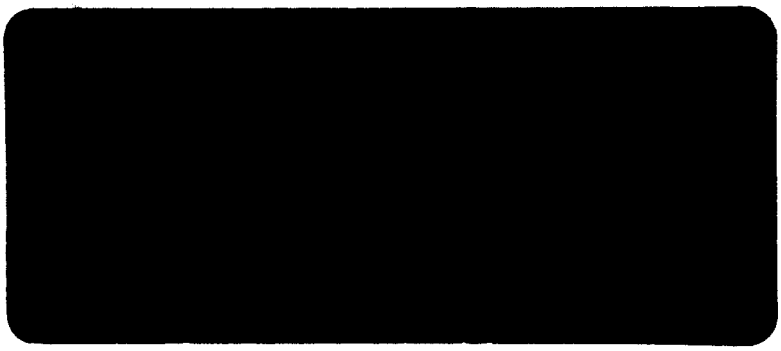

GPO PRICE $ _____

CFSTI PRICE(S) $ _____

Hard copy (HC) 4.00

Microfiche (MF) 1.00

ff 653 July 65

EXOTECH
INCORPORATED

FACILITY FORM 602

N66 26754 (ACCESSION NUMBER) — (THRU)

141 (PAGES) — 1 (CODE)

CR 75187 (NASA CR OR TMX OR AD NUMBER) — 31 (CATEGORY)

525 SCHOOL STREET, S. W. • WASHINGTON, D. C. 20024

ON THE FEASIBILITY OF RADIATION STERILIZATION OF PLANETARY SPACECRAFT

by Matthew J. Barrett and William C. Cooley

Final Report on
Contract NASW-1320

Prepared for
National Aeronautics and Space Administration
Office of Lunar and Planetary Programs

by
Exotech Incorporated
525 School St. S. W.
Washington, D. C. 20024

May 2, 1966

Technical Report TR-012

ABSTRACT

It is shown that unmanned planetary landing capsules can be sterilized by high energy X-rays or gamma rays with a dose of 5 megarads. X-rays from a 3 to 10 MeV electron accelerator are preferred for a large (2500 lb.) capsule, because of penetration requirements, but Cobalt-60 gamma rays can be used on small capsules, such as a 100 lb. Mars atmospheric probe. The most critical radiation-sensitive components are transistors which are subject to damage by surface effects and permanent degradation of current gain. Careful selection of transistor types, manufacturing processes and screening tests is recommended to select specific devices which will have acceptable changes in reverse current leakage and gain after irradiation. There is reason to believe that a capsule sterilized by radiation can be made more reliable than one sterilized by heat. Also, sterility assurance can be improved by avoiding the necessity to vent and refill with gas as is planned for a capsule which is heat sterilized. By a lowering of the dose requirement, the radiation damage effect can be reduced below the levels discussed in this report. It appears that 5 megarads may be a higher dose than required for planetary quarantine requirements. At a lower dose, near 1 megarad, radiation damage would become a much less difficult problem.

TABLE OF CONTENTS

TABLE OF CONTENTS (Cont'd)

LIST OF ILLUSTRATIONS

LIST OF ILLUSTRATIONS(Cont'd)

LIST OF ILLUSTRATIONS (Cont'd)

1.0 Introduction and Summary

1.1 Purpose of the Study and Summary of Results

In order to prevent biological contamination of other planets, unmanned planetary landing capsules must be sterilized. Present plans for the Voyager Mars exploration program are based on the use of heat sterilization. However, recent developments in radiation technology and the development of radiation resistant equipment have made it possible to perform a more definitive evaluation of the feasibility of using radiation as the sterilizing means. Therefore, the purpose of this study was to evaluate the merits of radiation sterilization in comparison with heat sterilization in order to aid in planning future sterilization technology efforts.

Although there may be synergistic advantages in using a combination of radiation and heat, the present study has not investigated this possibility.

The primary criterion for selecting the method of sterilization is to attain the desired probability of sterility with a minimum reduction of mission reliability. It is clear that the selection of components and materials for a planetary landing capsule must take into account the unique sterilization environment, whether it is heat or radiation. Therefore, a critical question to be answered is: "Can a planetary capsule which is designed for radiation sterilization potentially achieve a higher reliability than one designed for heat sterilization?" Although this report does not reach a definite answer to the question, the study gives sufficiently positive indications that further investigation is justified, particularly since the successful attainment of reliable heat-sterilizable equipment has not yet been assured.

Primary emphasis was placed on evaluating the feasibility of sterilizing a typical 2500 pound Voyager capsule in a sealed bio-canister by means of radiation and identifying the problems associated with radiation damage. It was assumed that a dose of 5 megarads would be sufficient to give a probability

of one viable micro-organism surviving the irradiation which is comparable to a dry heat treatment of 22 hours at $135^{o}C$. (Approximately a factor of 10^{12} reduction of population).

This study shows that the most promising type of radiation for sterilization of spacecraft is high energy photons. Cobalt-60 gamma rays with an average energy near 1.2 MeV are satisfactory for penetrating a small capsule such as a 100 pound Mars atmospheric probe. However, for a large capsule such as the 2500 pound Mars lander planned for the Voyager program, the use of bremsstrahlung X-rays of the order of 3 to 10 MeV in energy is preferable. A high energy linear electron accelerator can be used to produce X-rays in a heavy target material (like gold, platinum or tungsten), with an intensity sufficient to complete the sterilization in a matter of days. The use of other types of radiation sources such as a proton accelerator or combined gamma rays and neutrons from a nuclear reactor has disadvantages - in particular the production of induced radioactivity and the generation of excessive radiation damage. The direct irradiation of a capsule by electrons leads to a large dose variation with depth which would cause excessive radiation damage near the surface. Therefore, an X-ray target should be used to convert the electron energy to photons.

The selection of 1 to 10 MeV photons as the most suitable radiation for this application makes the evaluation of radiation effects on components difficult because most test data have been obtained under irradiation by neutrons, electrons, or protons, rather than high-energy X-rays. Very limited data are available for gamma ray damage alone. Accordingly, analyses were conducted which permit an estimate of X-ray damage to critical components such as silicon transistors and diodes by using experimental data obtained with electrons. This analysis includes a prediction of the electron flux and energy spectrum associated with the X-ray beam as it penetrates a capsule.

The study shows that a dose ratio of less than two to one can be achieved within a 2500 pound capsule by using 10 MeV linear accelerator (linac)

bremsstrahlung. One presently available in a facility with an adequate irradiation volume (at Hill Air Force Base, Utah) would require about two weeks to accomplish the sterilization. However, a higher power machine could accomplish the irradiation in about two days.

The radiation effects observed after the sterilizing radiation is applied are within the tolerance for specially selected radiation resistant components for use in radiation-hardened circuits. The most sensitive items will be silicon transistors and certain organic polymers. It was shown that selection of transistor type (low gain and low base transit times, or high frequency cutoff) can result in each unit losing no more than 10% of its gain, compared with the preirradiation value. Certain polymers, notably teflon, polyesters, methyl methacrylate, and polysulfide rubber were found to have unacceptable sensitivities, but satisfactory substitutes are available.

1.2 Tasks Performed

We provide here the relation between the sections of this report and the tasks set forth in the contract work statement.

Task A: Review the existing data on radiation effects and identify the spacecraft (lander) hardware items, including materials, components, systems, sensors, and instruments, which can survive a sterilizing radiation dose of 5×10^6 RADS of ionizing radiation. Particular attention will be given to review data on the long-life reliability of spacecraft hardware items after radiation. (Section 4)

Task B: Review the spacecraft hardware items and systems presently planned for inclusion in Mars landers, and identify those which are likely to be adversely affected by radiation sterilization. (Section 5)

Task C: Using the results of Tasks A and B, evaluate the merits, both inherent and relative to heat, of radiation as a technique for achieving sterility of a Mars lander. (Section 7)

Task D: Recommend appropriate methods for using radiation to achieve sterility of a Mars lander. (Sections 3, 6)

Task E: Recommended further research and development which may be required to establish the technical feasibility and the economic and operational practicality of radiation as a means of achieving sterility of a Mars lander. (Section 8, 9)

In addition, Section 2, "Selection of Type of Radiation" and Appendix A, "Elimination of Protons and Neutrons", have been provided because the extent of radiation damage is very dependent on the type of radiation used. The elimination of particle radiation as a sterilizing agent, for reasons given in that section, reduced the data available for use in the radiation effects portion of the work. A considerable body of literature exists for radiation damage from nuclear reactor radiations (mixed neutron-gamma fields). Since neutrons are judged not acceptable for sterilization, and since their effects can not be correlated accurately with those of photons, this literature is of little relevance.

Finally, Sections 8 and 9 summarize conclusions and recommendations based on the study, and Section 10 provides a list of the references used.

During the course of the study and in the preparation of this final report every effort was made to insure its accuracy and comprehensiveness. The work was discussed with outside consultants, notably Mr. R. Statler of the U. S. Naval Research Laboratory and personnel of the Harry Diamond Laboratories regarding radiation effects and Dr. C. Bruch of NASA regarding sterilization by radiation. Attendance at conferences included the radiation effects portion of the Fifth Photovoltaic Specialists Conference held on 18 October, 1965 at Goddard Space Flight Center. Discussions were also held with members of the Radiation Effects Information Center of Battelle Memorial Institute. As a result of these efforts it is believed that the principal features of the problem have been identified and accurately assessed in this report.

1.3 Radiation Sterilization Terminology

The subject under discussion - radiation sterilization of a Mars landing capsule - is of concern to technical personnel with a wide background of specialties. It is therefore appropriate that this introduction should include a brief description of the basic phenomena involved, both for review and with the intent of defining the terminology to be employed.

Radiation has been defined as an emission of energy. The types of radiation of interest here include X-rays, gamma rays, protons, electrons and neutrons. These all have the following properties:

a) The rays or particles travel in straight lines from the energy source, until they interact with matter,

b) because the particles are of nuclear size, they can penetrate appreciable depths into a solid material before striking an atom, and

c) all the energy of each particle or ray is dissipated by atomic collisions, until the particle comes to rest or is absorbed, or destroyed.

Non-nuclear sources have been developed for these radiations. Beta particles are fast-moving electrons emitted by radioactive elements, but electron accelerators are available to generate high intensity electrons of an energy which may be as high as 500 MeV. In a similar fashion, proton accelerators generate protons by non-nuclear means. Gamma rays and X-rays are electromagnetic quanta, or photons, and may be generated within the target of a particle accelerator. The earliest devices for doing this were X-ray machines, so that the photon beam generated by a target of a high energy electron accelerator is known as an X-ray, although its energy may exceed that of the gamma rays from nuclear sources.

The alpha and beta particles, neutrons and protons all are similar in that they are physical particles with a finite rest mass. The alpha particle is the helium nucleus. As its range of penetration is so small, on the order of centimeters of air, it will not be considered further. The proton, the electron and the neutron have longer ranges in matter. Proton and neutron radiations are discussed briefly in Section 2 and Appendix A and shown to be of little interest in the present problem. Electrons have limited penetration capability and can be used directly to sterilize only thin materials (less than a few centimeters).

The gamma and X-rays are composed of electromagnetic quanta, or photons. The energy per unit time (power) in the beam is simply the product of the number current of photons times the energy of each photon.

X-ray photons are formed in an electron accelerator target in two ways, both involving the slowing down of the fast-moving electron. When the electron knocks another out of its position in an atom of a target and the resultant ion is later neutralized by the capture of a local electron, the energy is emitted as one or more photons of discrete energies which are characteristic of the

atom. On the other hand, a fast moving electron can be slowed down by interactions with the electric fields of atoms and the loss of energy by the electron goes into a continuous spectrum of X-rays known as bremsstrahlung, or "braking radiation". Both processes occur when an electron hits target atoms, and the resulting spectrum of X-ray photons is a composite with a broad band (the bremsstrahlung), on which are superimposed sharp peaks (the characteristic X-rays). The sharp peaks, however, are in the eV or keV range, while the broad band extends to an upper limit almost equal to the initial energy of the electron.

Gamma-ray photons are emitted by unstable atoms, such as the fission products of uranium in a reactor, or certain artificial and naturally occurring isotopes. These radioisotopes are atoms in which the nucleus is unstable and after a random period of time will radiate a particle, generally an alpha or a beta particle, followed by one or more gamma-ray photons. Typically, gamma-ray energies are in the range of 0.1 to 1 MeV. A well-known radioisotope is cobalt-60, whose nucleus emits an electron, then two photons, becoming nickel-60. Because of the random period of time one atom may remain inert, a large number of cobalt-60 atoms will decay exponentially with time becoming atoms of nickel. The time required for half of the atoms of cobalt-60 to decay is called the half-life. With only half as many cobalt atoms remaining, the sample then emits photons at half its original rate. For cobalt-60 the half-life is 5.2 years.

Regardless of the mechanism producing it, each photon emitted travels in a straight line from its source through vacuum or through the space between atoms of a material, until it interacts with an electron. The small number of direct nuclear collisions (photonuclear reactions) that are observed can generally be neglected at photon energies below 10 MeV. Depending on the results of the impact, three types of collision are recognized. In the first, the photoelectric effect, the photon disappears. The electron acquires all

of the photon energy, leaving an electron vacancy or "hole" in the atom. Subsequently, filling of the vacancy by an electron will result in characteristic X-ray photons emitted in a random direction. In the second type of collision, the Compton effect, the photon does not disappear, but leaves the site of collision with a reduced energy and at some angle to its original path. This effect is the major one at a higher energy range than the photoelectric effect, and the electron which is hit will have a fraction of the initial photon energy as it leaves its original position. The third type of collision is called pair production. This occurs only for photons of energy over 1.02 MeV, and the photon disappears, producing an electron and a positron. The positron acts like a hole in an infinite distribution of electrons, moving as if it were an electron with a positive charge, until some electron drops into this "hole", annihilating it, and emitting 1.02 MeV as two or three photons in random directions.

Regardless of the interaction process, the energy of the initial photon appears as kinetic energy of electrons, energies of ionization of atoms, and randomly directed photons of lower energies. While a photon beam can penetrate matter, these interactions continually attenuate the beam intensity with depth of penetration. Roughly, the intensity I(x) at a depth x into a given material is reduced from the incident intensity I(o) as an exponential function:

$$I(x) = I(o)e^{-\mu x} \qquad (1.1)$$

where μ is the attenuation coefficient of the material penetrated by the beam. In a distance x equal to μ^{-1}, the intensity of the beam drops by the factor e, to 36.8% of its incident value. This distance μ^{-1} is referred to as the mean-free-path of photons in the material and is dependent on the photon energy and the material traversed. For photons in the energy range 1-10 MeV, the dependence of μ on the material is principally through the material density ρ. To a first approximation, μ/ρ is independent of type of material, and dependent only on photon energy. This fact allows an evaluation of the photon attenuation in a given capsule without regard to its material composition.

Equation (1.1) can be made exact by multiplying the right side by a factor B, called the buildup factor. It is not always easy to evaluate B from a knowledge of the various collision cross sections, but engineering approximations are available. For small values of μx (less than 1), B is close to 1, especially for the high energy photons considered here.

The ions and free electrons caused by the photon collisions enter into secondary reactions that are responsible for the observed physical effects. A free electron, for example, will have on the average a large fraction of the energy which the primary photon had, so that the material being irradiated by photons is filled with sources of energetic electrons. These electrons will scatter and cause a cascading number of ionizations. After each collision, the electron has a smaller amount of energy, until it is finally recaptured by an ion.

The ions created by the slowing down of electrons will tend to recombine to reestablish their electric neutrality. The recombinations rarely lead back to the original molecular configuration. New molecules and free radicals are formed. In a living organism some of these chemicals may be lethal. Most will be unable to perform the original biological function. In an organic polymeric material such as polyethylene, the new molecules will change the physical properties such as strength or density of the material.

A significant result of freeing electrons in crystalline solids is the possibility of collisions between electrons and the atomic nuclei. When such a collision transfers sufficient energy, an atom can be knocked out of its lattice position in the crystal. The resultant defect in the crystal lattice has a pronounced effect on the electrical properties of semiconductor materials.

Most of the energy of the incident radiation, having been divided and sub-divided during the cascade process, will appear as thermal vibrations of the atoms of the material being irradiated. (Some small amount of energy is

accounted for by molecules in higher energy states, and some is re-emitted at the surface of the material.) As a result, radiation heating is of considerable importance when the rate of energy deposition is high. The current of photons or other radiation which will form 2.08×10^9 ion pairs in a cubic centimeter of air is called a roentgen. Such a unit allows the comparison of beams of differing intensities and differing photon energies as to their ability to generate ions, and hence gives to a first approximation their biological destructiveness.

The beam energy is converted into electron energy and ion energy and the ions will recombine with electrons. Some of the energy deposited by the beam will appear as heat, some as changes in chemical bond energies. The amount of energy deposition per unit mass is measured in rads, where one rad equals 100 ergs per gram of material. Because of the units chosen, one roentgen of photon radiation produces very nearly 0.84 rad of dose for most materials.

It is important to realize that a knowledge of the number of roentgens or the number of rads is only a first step in the evaluation of the magnitude of the effect of photons in a material. Knowing the number of ions created does not solve the problems of radiation chemistry. Knowing only the number of electrons released does not automatically give the atoms that will be knocked out of their positions in a crystal lattice, and hence solve one problem of radiation damage to semiconductor materials. Knowing the number of rads of dose deposited in a microorganism does not necessarily determine the probability of its survival.

2.0 Selection of Type of Radiation

Sections 2.1 through 2.3 are concerned with presenting the results of a survey of the atomic or nuclear radiations available for sterilization. By specifying atomic or nuclear, we mean to imply that other radiations exist but are not evaluated here: e.g. ultraviolet, visible light, infrared, and microwave radiations.

2.1 Elimination of Protons and Neutrons

As discussed in Appendix A, both protons and neutrons can be eliminated from consideration because they would produce undesirable radioactivity in a planetary capsule which might interfere with scientific measurements. Also the radioactivation would pose a ground handling problem and lead to unnecessarily large radiation damage to components.

Appendix A also shows that solar flare radiation cannot be depended on for internal sterilization of a planetary vehicle.

2.2 Electron Radiation

Electron beams emitted by high voltage electron accelerators, and beta particles (electrons) emitted by certain radioisotopes are routinely used to sterilize a wide variety of materials including foods, drugs, surgical supplies, and instruments. One of the severest restrictions of electron radiation is the limited depth of penetration of the electron beam. The total penetration range of electrons of energy T is[1] in material of unit density,

$$R = 0.530T - 0.106 \text{ centimeters} \qquad (2.1)$$

for T greater than 1 MeV. To attempt electron penetration to depths of the order of 90 grams/cm^2 in this way would obviously require an unusually large electron energy.

One could take advantage of the bremsstrahlung (continuous spectrum of X-rays) created by the stopping of the electrons in the surface of the capsule being sterilized. The efficiency of bremsstrahlung production is proportional

to the electron energy, given by the formula

$$F = EZ/2000 \qquad (2.2)$$

where F is the fraction of the electron energy that is converted to bremsstrahlung, E is the initial energy of the electron, and Z is the atomic number of the material being penetrated.[2]

There are two objections to this technique. First, stopping the electrons in the capsule divides it into two distinctly different radiation zones. The outer surface zone is sterilized by the electrons; the inner zone is sterilized by the X-rays. The dose deposited in the surface zone will be the greater by far. This means that, for an acceptable sterilizing dose on the inner zone, a high dose and its concurrent damage effects will be necessary for the outer zone. The second objection, seen from equation 2.2, is that the efficiency of creation of the X-rays will be unnecessarily low, since the landing capsule is normally fabricated primarily of light, low Z materials.

Thus, electrons impinging directly on a capsule do not appear promising for the present task because of the large dose variations through the capsule and the inefficiency of conversion of electron energy to bremsstrahlung within low Z capsule materials. However, as discussed below, the use of a separate high Z target makes it possible to avoid these disadvantages. The direct use of electrons for sterilization would only be practical for small components of the order of a few centimeters or less in thickness which are to be assembled by sterile techniques after irradiation.

2.3 Photon Radiation

Of the forms of radiation studied for the sterilization of the Mars lander, electromagnetic radiation as gamma rays or high energy X-rays is the most attractive. Perhaps the most significant advantage of high energy photons (that is, 1 to 10 MeV photon energies) is their great penetration capability, which allows more uniform dose distribution that is possible with electrons,

neutrons or protons of an equivalent energy. Uniformity of dose distribution is important to prevent overexposure and unnecessary radiation damage to any part of the lander.

Other advantages of photons are also significant. In the energy range cited, they cause no significant radioactivity in low Z materials. While some materials have thresholds for photonuclear effects that are lower than 10 MeV, the cross sections for the reactions are negligible up to 10 MeV. In silicon, for example, the photoneutron threshold is 8.5 MeV, but the cross section does not become significant below 10-12 MeV, as is seen in Figure 1. Since silicon semiconductors are the elements in the lander most sensitive to radiation, 10 MeV was selected as the upper energy limit for photons to avoid radioactivation or excessive radiation damage.

The reactions of photons are primarily with electrons, so that the atomic nucleus is not displaced by recoiling from a scattering collision with a photon. This recoil, for neutron or proton scattering from nuclei leads to much larger damages to crystal lattices. The direct interaction between protons and neutrons and a nucleus transfers sufficient momentum in most cases to dislodge the nucleus from its lattice position, collide with other nuclei, dislodge them and create a whole cluster of defects. In contrast, electrons which have received a portion of the photon's energy and which collide with a nucleus transfer very little energy to the nucleus because of the small mass of an electron. An electron must have an energy greater than about 145 keV to displace an atom of silicon from its lattice. Photons or electrons therefore generate fewer crystal defects than protons or neutrons of an equal dose intensity. Neutrons in particular, since they lose all their energy by nuclear collisions, cause severe damage in a crystal, causing about 100 times as many defects as an equal dose of photons from cobalt-60.

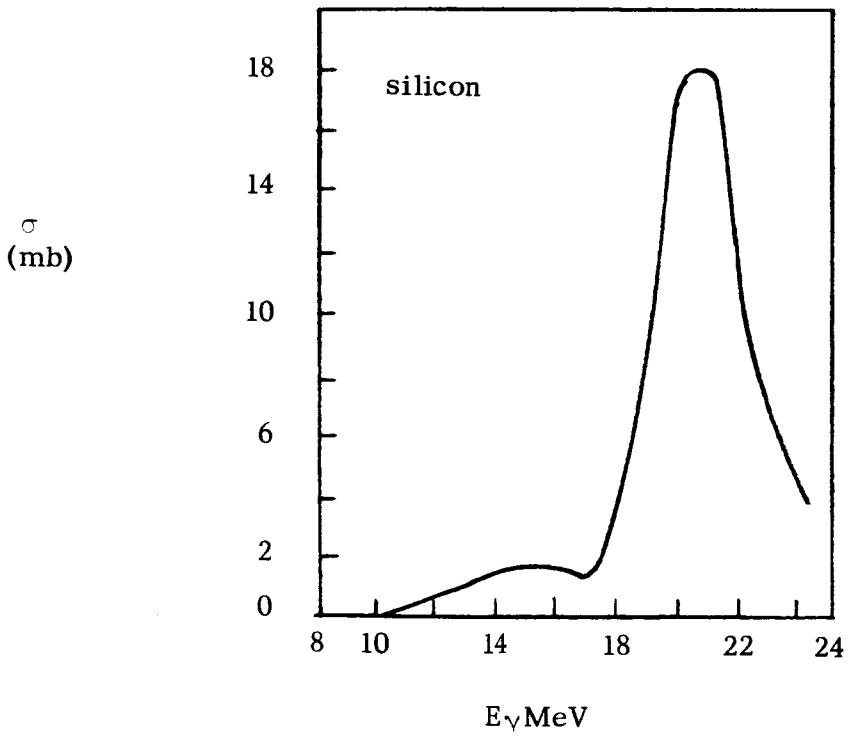

Figure 1. The cross section, $\sigma(\gamma,n)$, for neutron production by photons (3).

It is generally noticed that semiconductor materials such as silicon crystals are among the most sensitive to radiation. The electrical properties of a transistor or diode depend on the purity and crystallinity of the silicon or germanium in it. Thus, the crystal damage described above will place a limit on the allowable sterilizing dose given to the lander. This limit will be highest when the radiation is in the form of photons, particularly low energy photons which produce only small numbers of electrons which are above the threshold energy for atomic displacement.

Sources of photon radiation are readily available. The nuclear reactor, discussed in Appendix A, emits copious quantities of photons predominantly in the 1-5 MeV range. The radioisotope cobalt-60 is available as kilocurie sources, providing photons of approximately 1.25 MeV. Linear electron accelerators (linacs) readily produce X-ray spectra with upper energies in the 1-10 MeV range, or higher. These three sources: the reactor, cobalt-60, and the linac are available to produce more intense radiation beams than appear to be economically available from other sources, and the latter two of these are currently in use for sterilization applications. The nuclear reactor is not in general use for sterilization, because of the neutron component of its emission. Since neutron damage can be a significant factor and neutrons would radioactivate some capsule materials, the reactor will be disregarded in this report. However, it is conceivable that reactor radiation could be selectively shielded to reduce the neutron portion to an acceptable level. One advantage of this would be the large dose rate available. For example, a 3 megawatt reactor shielded with 8 in. of water and 16 in. of lithium hydride will give a dose rate of about 0.4 megarads per hour over a large area, with only about 1% being due to neutrons.[4]

Cobalt-60 radiation -- essentially monoenergetic photons with 1.25 MeV energy -- is available in commercial and government facilities from sources up to a megacurie. This allows fairly rapid irradiation of the capsule; times

in the order of a few days are possible, depending on the geometry of the facility and placement of the lander. The disadvantage of using radioisotopes, including cobalt-60, appears to lie in the low-energies of the photons they emit, which limits the size of capsule which can be irradiated. Photon radiation penetrating material drops off exponentially in intensity with depth of penetration (as described by eq. 1.1). The attenuation coefficient for a combination of light elements (concrete) is given in Fig. 2 as a function of the photon energy. It is apparent that the intensity at the surface of the lander would be more nearly equal to the intensity at the center if one chose photons of a higher energy that those emitted by cobalt-60. Correspondingly, the use of a source with photons of a lower average energy, would result in a worse dose distribution in the lander.

Spent nuclear fuel elements are intense sources of gamma radiation. However, the elements generally require cooling for some time after removal from a reactor. Also, the gamma spectrum includes a large amount of low energy photons, and decays in intensity rapidly with time. For these reasons, fuel elements are not generally considered as attractive sources of process radiation, and are not further considered in this report.

A long-lived fission product extracted from spent fuel and used in commercial radiation facilities is cesium-137. This isotope emits a 0.66 MeV photon; the lower energy radiation is more strongly attenuated than that of cobalt in the capsule and is therefore less desirable.

The linac (more specifically, the electron linear accelerator) accelerates electrons through a straight evacuated tube using klystrons to apply the accelerating voltage at spaced intervals along the tube. The outstanding feature of the linac is the high beam current available: machines have been designed to deliver on the order of 10^{15} electrons per second at energies over 20 MeV.[5] The electrons, striking a heavy metal target such as lead, gold or platinum,

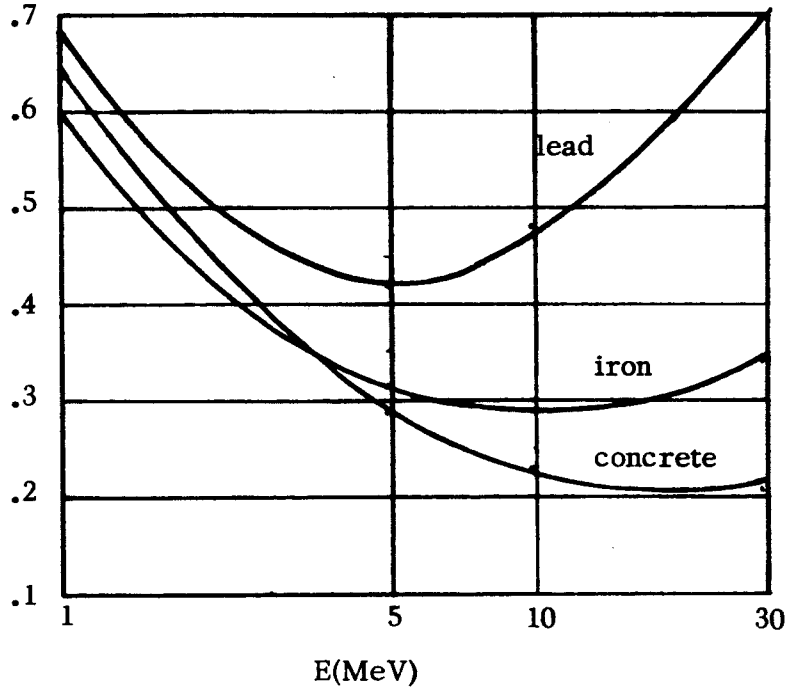

Figure 2. Attenuation coefficient, in cm^2/gm, of a low-z mix of materials (concrete), versus photon energy, in MeV

create bremsstrahlung X-rays that are radiated predominantly in the forward direction, as seen in Figure 3. The doses to be experienced in such a beam are of the order of 10^3 - 10^4 roentgens per minute (while betatrons generate doses of the order of 100-200 roentgens per minute).

The spectrum of the bremsstrahlung produced depends on a large number of parameters, such as atomic number of the target, target thickness, its lateral dimensions, coolant system, and of course, the energy of the accelerated electron. For practical purposes, however, it can be approximated by theoretical arguments,[6] and the spectrum I(E) turns out to be almost a straight line with negative slope, from a maximum at zero energy to zero at the energy of the incident electron. A small amount of shielding screens out the lower portion of the spectrum. We shall neglect this effect, since the lower portion of the spectrum is of little importance in damage calculations and we shall consider the energy distribution to be proportional to (T-E), where T is the electron energy, with a maximum energy in a range where the attenuation coefficient of most light materials is not very sensitive to energy. It is apparent from Figure 2 that the fairly constant attenuation for photons in this energy range will result in modifying the initial spectrum only slightly as the beam penetrates a capsule. Then, from equation (1.1) attenuation of the spectrum is given by essentially, a single value of μ for the spectrum. That this does indeed occur is seen in Figure 4. This result will considerably simplify the analysis to be presented in Section 3.

We conclude that the optimum radiation sterilization technique for a large Mars lander capsule will involve the use of a linac operated at approximately 10 MeV, to produce an X-ray spectrum with an upper energy cutoff just below the silicon photonuclear threshold. This, incidentally, is also below the photo-neutron threshold in aluminum (12.75 MeV), and in carbon (18.7 MeV).

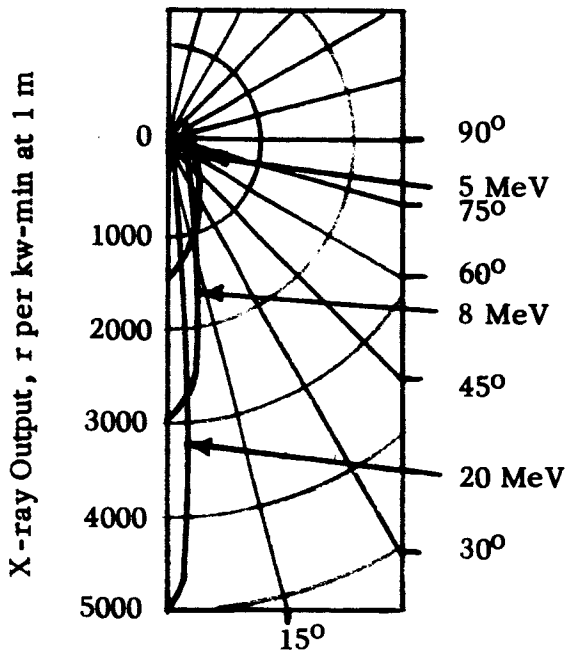

Fig. 3. X-ray Intensity Distributions for Several Electron Energies (From Ref. 5)

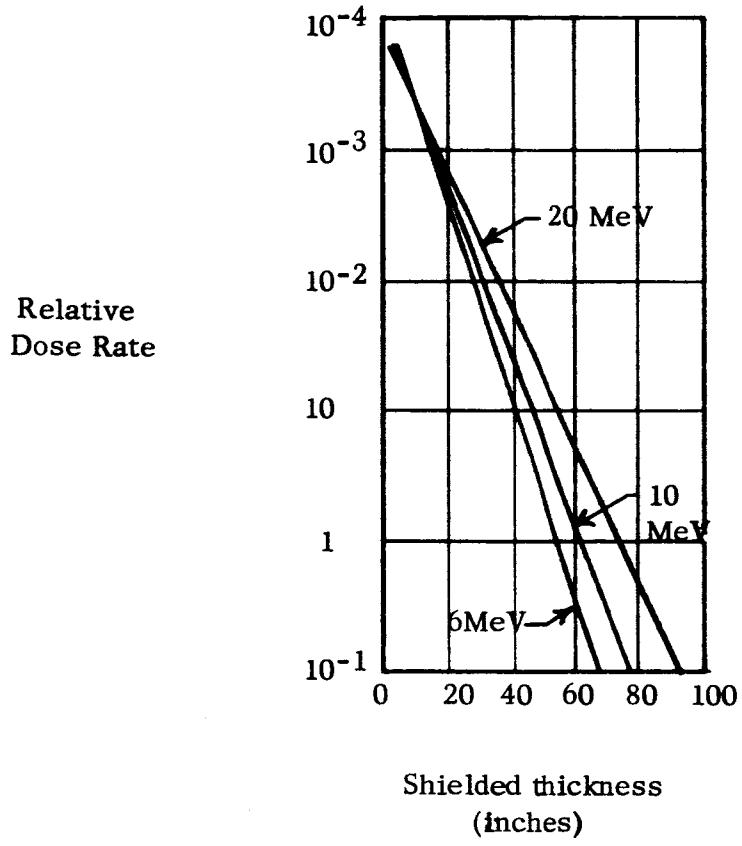

Figure 4. Attenuation of bremsstrahlung X-rays in Concrete (Ref. 7)

It will be shown that cobalt-60 gamma rays are also suitable for sterilizing small capsules, such as a Mars atmosphere probe. The possibility of irradiating a large capsule by insertion of cobalt-60 rods through bio-sealed thimbles in the capsule has not been investigated in detail because of the added complexity of design of the capsule and the difficulty of stripping the bio-barrier during flight.

3.0 Dose Variation in a Landing Capsule

One of the basic problems in the sterilization of large objects by external radiation sources is caused by the attenuation of the radiation in the object. This attenuation makes the dose in some region considerably lower than the dose accumulated in the same time in another region. Generally (but not always) the dose at the center of the object is lower than that at the surface. To irradiate the region with a minimum sterilization dose, it is necessary that other regions receive doses that may be several times this minimum. Such an exposure can exceed the threshold of unacceptable radiation damage to a semiconductor or other component.

Because of this possibility, it is generally advantageous to make the radiation exposure as uniform as possible throughout the volume of the object irradiated. Three techniques are practiced to approach uniform exposure. The first is to irradiate a spread-out array of separated components. This does not seem to be generally useful for terminal sterilization of the capsule. However, by using an assembly/sterilizer concept as proposed by General Electric,[8] it might be possible to radiation sterilize individual components and subsystems prior to sterile assembly. Second, the selection of energy spectrum can be made to provide the least attenuation of the radiation as it penetrates the entire capsule. As discussed in section 2.3, this leads to the use of high energy (up to 10 MeV) X-rays from an electron accelerator. A third technique is to choose a geometry for the sterilization (width of X-ray beam, movement of the capsule during radiation, etc.) which will optimize the uniformity of exposure. Details of this technique are discussed in the next section.

Even with such optimized practices, completely uniform exposure cannot be accomplished with sources exterior to the capsule. This suggests that the approach to be taken is first to make the distribution of the radiation dose as uniform as possible, then to arrange the more radiation-sensitive components of the capsule in places where the dose will be the minimum acceptable for sterilization.

3.1 Irradiation of a Thick Disk

The simplest method of radiation sterilization of a Mars landing capsule is to move it relative to the radiation source so that the surface, on one side of the capsule, is exposed to a reasonably uniform degree. Obviously the capsule can be turned over and the process repeated so that the other side is similarly exposed. The net result is a dose distribution that is uniform over each side and drops to some minimum value in the interior.

In Figure 5, the capsule is considered to be a thick disk and the movement of the radiation source describes two source planes, a distance a from either side. Based on a conceptual design to be discussed in section 5.0, the capsule disk has a thickness of 91 grams per square centimeter. The source movement may be time-averaged, so that the point, moving source can be represented by a stationary source covering the source planes.

By integrating the incremental doses received at point P due to sources at all incremental areas dS and dS', we arrive at the total dose. This can be readily performed for points along the disk axis, and yields a dose distribution curve that includes the maximum exposure as well as a minimum. The maximum exposure will be at the surfaces, on the disk axis and the minimum will be at the center. In the actual capsule, the minimum dose will be on the center line, since it is symmetric and the disk tapers in thickness away from the axis.

The increment of dose distribution at P due to the source at dS is determined by the angular distribution of the source emission, the thickness of material between dS and P, and the distance x intervening. Similar considerations affect the increment of dose from the source at dS'. The geometry of the sketch gives the relations

$$x^2 = r^2 + (a + z)^2 \qquad (3.1a)$$

$$y^2 = (r')^2 + (T + a - z)^2 \qquad (3.1b)$$

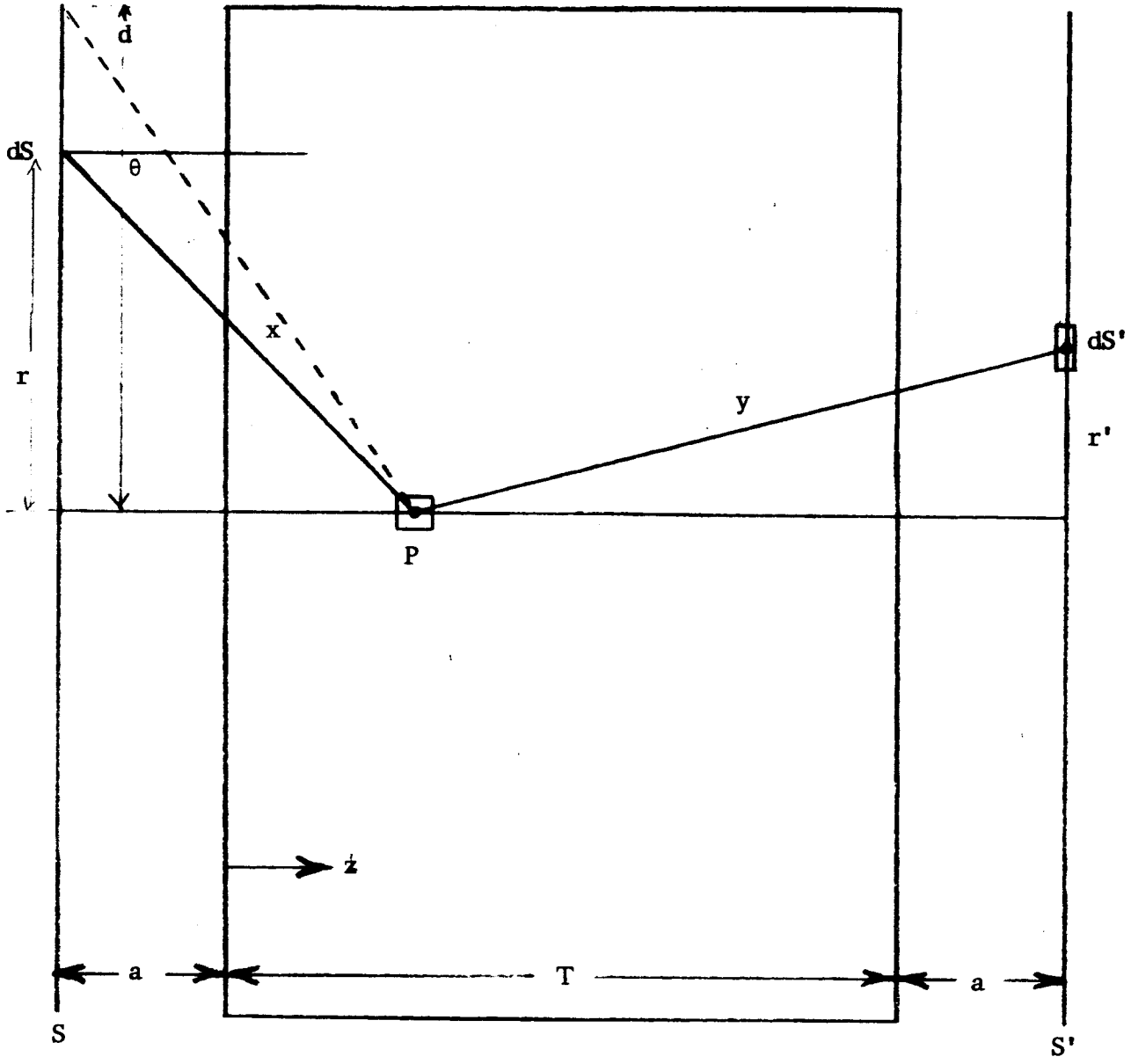

Figure 5. Construction for disk approximation of lander capsule sterilization. The incremental areas dS and dS' are on the radiation source planes; a is nominally one-three feet.

The increment of dose due to dS is

$$dD = D_0 \exp\left[-\mu(x - a \sec\theta)\right] P(\theta) x^{-2}\, dS \qquad (3.2)$$

Here, D_0 is the dose one centimeter in air from the source and is as constant for a given source intensity. The anisotropy of the source is given by $P(\theta)$, as a function of the angle θ of the ray x with the plane perpendicular. The disk is homogeneous, so that the attenuation coefficient μ in the exponential is independent of position.

A buildup factor, normally inserted in expressions such as (3.2), is omitted here. For high energy photons, and small penetration lengths, the buildup factor is close to one. A Dirac delta function $\delta(\theta)$ may be used to approximate the function $P(\theta)$ for a linac. Then the point P is irradiated only by the source at r = o, and the total dose is then

$$D = D_0 \left\{ \frac{\exp(-\mu z)}{(a+z)^2} + \frac{\exp -\mu(T-z)}{(T+a-z)^2} \right\} \qquad (3.3)$$

For large* a, this reduces to

$$D \approx D_0\, 2a^{-2} \exp(-\mu T/2) \cosh\left(\frac{\mu T}{2} - \mu z\right) \qquad (3.4)$$

Since only small amounts of heavy elements such as tin, lead, or tungsten are expected to be part of the lander capsule, the attenuation coefficient μ depends primarily on the density of material and the energy of the X-ray photons. From Fig. 4, μ for concrete and 10 MeV X-rays can be calculated to be 0.0588 cm^{-1}. Based on a concrete density ρ of 2.35, (μ/ρ) is 0.025 cm^2/gram. This figure for concrete should also apply to the capsule because of similar composition of lower Z materials, so that μT is given by (.025)(92) or 2.3. Equation (3.4)

---

* The linac target should be at a considerable distance away from the capsule such that the X-ray beam is sufficiently spread out on the capsule surface to prevent localized overheating. In section 6.0, a is taken as 90 cm and T is about 200 cm.

gives the approximate dose at a depth z into the capsule. Normalized to a unit dose at the surface of the capsule, the dose distribution from eq. (3.4) is plotted in Figure 6.

Fig. 6 shows that the minimum dose occurs at the optical center (i.e., the plane in the slab which has equal masses of material on both sides), and the maximum dose occurs at the surface. The ratio of doses D at these two positions is simply cosh ($\mu T/2$). This ratio varies with the energy of the X-ray beam used. Based on a minimum dose of 5 megarads, the maximum (surface) dose, computed from this ratio is given in Table 2.

Table 2. Maximum (Surface) Dose Deposition in "Disk" Capsule, for Two-sided Irradiation by Linac X-rays* with a Central Dose of 5 Megarads

Energy (MeV)	Surface Dose (Megarads)
4	12
6	10
10	8.3
20	7.5
30-40	7.4

* based on a capsule total thickness of 91 grams/cm^2

With cobalt-60 as the radiation source, the isotropic emission renders $P(\theta)$ as a constant equal to $1/4\pi$. The buildup factor B is given by Taylor's approximation[9] as

$$B = Ae^{\alpha\lambda} + (1 - A)\, e^{-\beta\lambda} \qquad (3.5)$$

with the constants, for aluminum, being A = 7, α = .096, and β = .015. The net effect of this approximation is to retain the form of (3.3) as an exponential, or sum of exponentials. The dose, due to the S plane is then, for the point P,

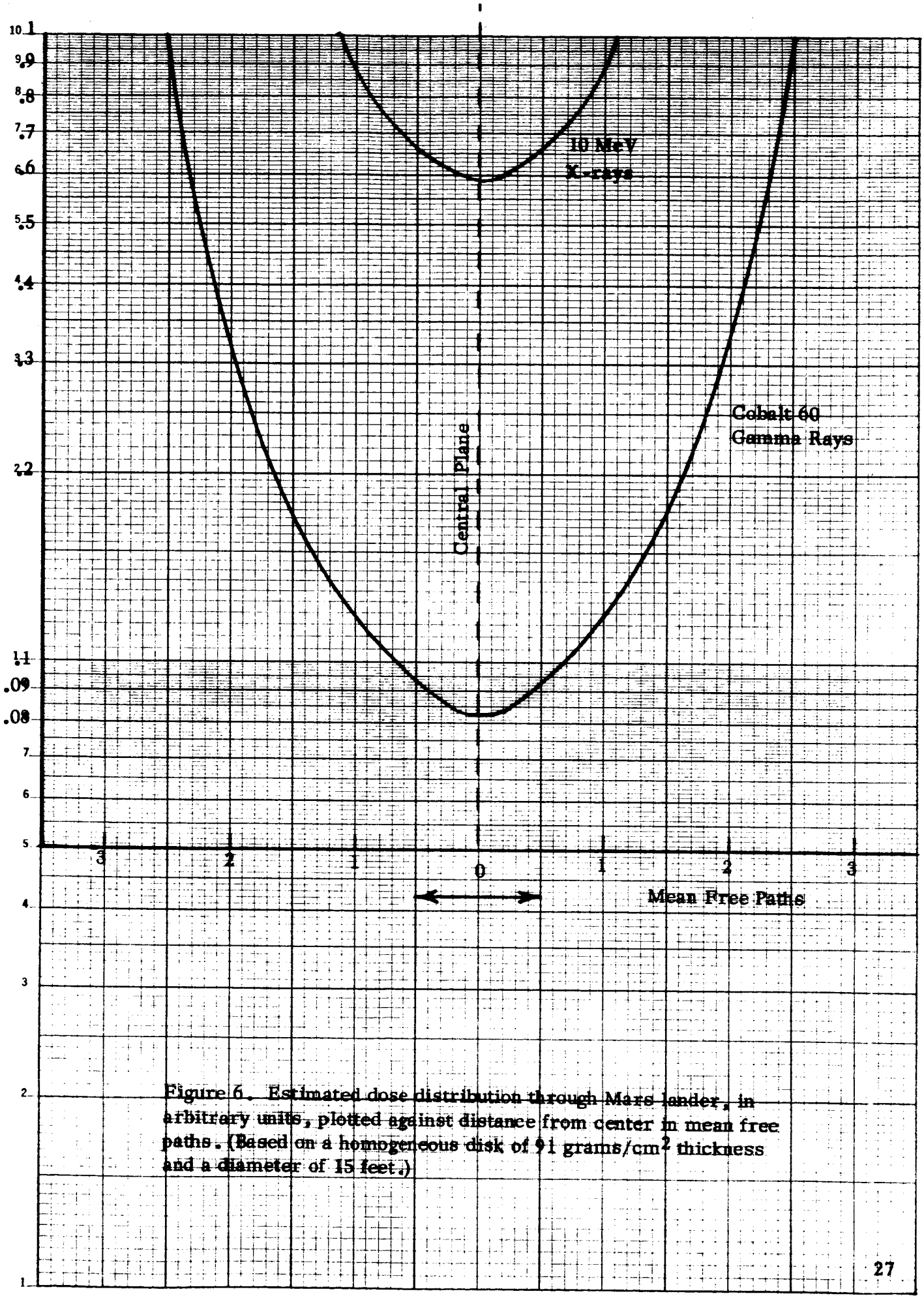

Figure 6. Estimated dose distribution through Mars lander, in arbitrary units, plotted against distance from center in mean free paths. (Based on a homogeneous disk of 91 grams/cm^2 thickness and a diameter of 15 feet.)

$$D = \frac{A}{2} \int_0^R \exp\left[-\mu_1, (x - a\sec\theta)\right] x^{-2}\, rdr$$

$$+\frac{(1 - A)}{2} \int_0^R \exp\left[-\mu_2 (x - a\sec\theta)\right] x^{-2}\, rdr \qquad (3.6)$$

where R is the radius of the source plane, μ_1 equals $(1 - \alpha)\mu$, and μ_2 equals $(1 + \beta)\mu$.

By a change in the variable of integration,

$$\int_0 \exp\left[-\mu(x - \frac{ax}{a+z})\right] x^{-2}\, rdr = \int_{a+z}^{d} \exp\left[-\frac{\mu zx}{a+z}\right] \frac{dx}{x} \qquad (3.7)$$

where d is the diagonal in Figure 5; this integral is tabulated as the E_1 function and the dose expression becomes

$$D = 3.5\left[E_1(\mu_1 z) - E_1(\mu_1 zd/a + z)\right] - 3\left[E_1(\mu_2 z) - E_1(\mu_2 zd/a+z)\right] \qquad (3.8)$$

for radiation from the S plane. Replacing z by (T-z) in this equation gives the dose at z due to the S' plane. The combination, D(z) plus D(T - z), is the dose as a function of depth z due to sterilization with cobalt-60 and is plotted in Figure 6.

Comparison of the curves in this figure show that the lander "appears" to be smaller to the linac radiation than it is to cobalt radiation. The apparent thickness for linac radiation is 2.3 mean free paths; for cobalt radiation it is 5 mean free paths. As a result, the dip at the center is more pronounced for cobalt-60 radiation. (This center is not the geometrical center of a heterogeneous slab, but rather a point which is an equal number of mean free paths from each side.)

It is seen from Figure 6, that the ratio of maximum to minimum dose in the assumed disk geometry is about 12 for cobalt-60 gamma radiation but only about 1.7 for 10 MeV X-rays. For a central dose of 5 megarads, the surface dose would be 61 for cobalt-60 gamma rays and about 8.3 for 10 MeV X-rays.

3.2 Analysis of Spherical Capsules

As seen from the previous section, the dose distribution from a planar source through a homogeneous disk is severely nonuniform when cobalt-60 is used as the radiation source and the disk is 91 grams/cm^2 thick. The central dose is low, but the arrangement in Figure 5 might be improved by allowing the source to travel completely around the cylindrical lander.

This arrangement approaches the model in Figure 7. A source uniformly irradiates the surface of a sphere. The analysis of this spherical arrangement is complicated if we allow an air space between source and sphere, as was done for the slab, so the space is assumed to be zero: the source plane is the sphere's surface.

The penetration distance x from source to detector point P is given by

$$x^2 = r^2 + R^2 - 2rR\cos\theta \tag{3.9}$$

and the dose due to dS is

$$dD = \frac{D_o e^{-\mu x}}{x^2} \tag{3.10}$$

When the surface is uniformly covered by source, the total dose is

$$D(r) = \int_0^{2\pi}\int_0^{\pi} \frac{D_o e^{-\mu x}}{x^2} R^2 \sin\theta\, d\theta\, d\varphi \tag{3.11a}$$

which is integrated to yield the dose at a distance r from the center:

$$D(r) = 2\pi D_o \frac{\mu R}{\mu r}\left[E_1(\mu R - \mu r) - E_1(\mu R + \mu r)\right] \tag{3.11b}$$

When the penetration distance x is zero, equation (3.10) is undefined. This is a consequence of approximating the source as a plane, rather than a thin shell. As a result, (3.11b) yields an undefined dose at the surface of the sphere, since the function

$$E_1(y) = \int_y^{\infty} \frac{e^{-x}\,dx}{x} \tag{3.12}$$

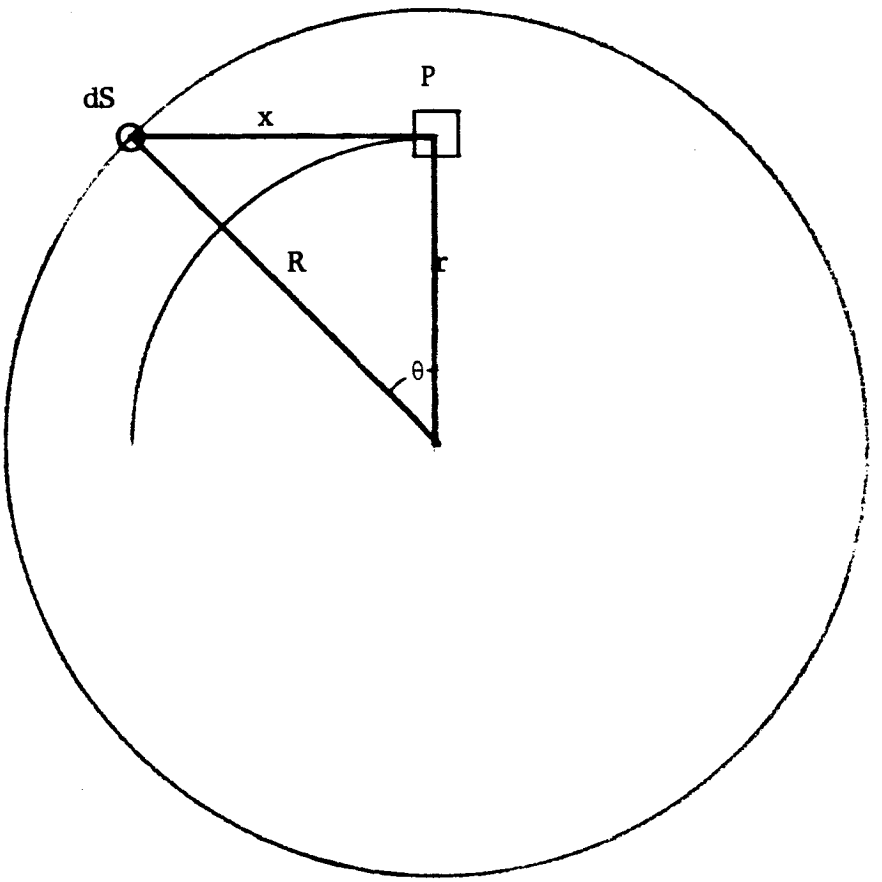

Figure 7. An incremental source at dS provides an incremental dose at P in the sphere of radius R. (Geometry for Analysis of Irradiation of Spherical Capsules)

becomes infinite for y equal zero. (This point is discussed briefly in section 5.2 of reference 10.) To avoid the difficulty, we shall assume the surface of the irradiated capsule is 0.1 mean free paths in from the source plane. With a cobalt-60 source, this is equivalent to 0.266 inches of aluminum.

At the center of the sphere, r equals zero and equation (3.11a) becomes:

$$D(o) = 4\pi D_o e^{-\mu R} \tag{3.11c}$$

which is the minimum dose in the sphere.

Examination of equations (3.11) reveals that the significant parameters which determine dose distribution in the sphere are the energy of the photons, the density of the sphere, and its radius R. This is seen by rewriting

$$\mu R = \frac{\mu}{\rho} \rho R \tag{3.13}$$

where $(\frac{\mu}{\rho})$ is the attenuation coefficient in cm^2/gram for the radiation, and is a function of photon energy. R is the radius, and ρ the density in gms/cm^3 of the sphere. The mass of the sphere is related to these parameters by

$$M = \frac{4}{3} \pi R^3 \rho \tag{3.14}$$

Numerical examples are in order. Consider first a 2500 lb. lander with an equivalent radius of 42 inches (as to be described in section 5.1), and a density of 0.221 grams/cm^3. For cobalt-60, $(\frac{\mu}{\rho})$ equals 0.055 cm^2/gram. Therefore

$$(\mu R)_1 = .055 \times .221 \times 107 = 1.3 \tag{3.15}$$

the mean free path of radiation in the capsule is 82 cm.

Consider also a 100 lb. capsule (also to be described in section 5.1) with a radius of 15.25 inches and a density of 0.186 grams/cm^3. Then, for cobalt-60 irradiation

$$(\mu R)_2 = .055 \times .186 \times 38.8 = 0.397 \tag{3.16}$$

These 2 models represent two proposed spacecraft, to be discussed more completely in Section 5. We shall refer to these, here, as the 100 lb. model and the 2500 lb. model. We shall consider solutions in the region of the 100 lb. model first.

The effect of buildup has been neglected. Buildup of dose at the center of the sphere will tend to flatten the distribution given by equation (3.11b). Thus, omission of the buildup factor leads to some conservatism in the prediction of the dose nonuniformity. This conservatism is slight for the small values of μR presently considered. Application of eq. (3.5) shows that, at the center of the sphere, where λ equals 0.397, the buildup factor B equals 1.30. That is, a 30% increase in dose over that predicted by eq. (3.11b) is to be expected. The buildup near the surface is not so large; and an over-all flattening should occur.

However, all of this is based on a homogeneous sphere. Possible streaming of radiation, localized dense materials that shield certain regions, and a non-spherical shape can all affect the value of the buildup B. A more detailed calculation is required for the selected spacecraft to be sterilized; the present results are intended only to be exploratory in nature.

Figure 8 depicts the dose distribution through the 100 lb. sphere irradiated from all directions by cobalt-60. A surface source is not necessary; the sphere can be rotated on a 2-axis gimbal turntable in front of a stationary point source so that it has covered the surface uniformly at the end of the sterilization period.

Figure 9 depicts the maximum dose in the sphere, with no point receiving less than 5 megarads, under the assumptions described above. The maximum dose is received at the surface of the sphere, and the minimum (5 megarads) occurs at the center.

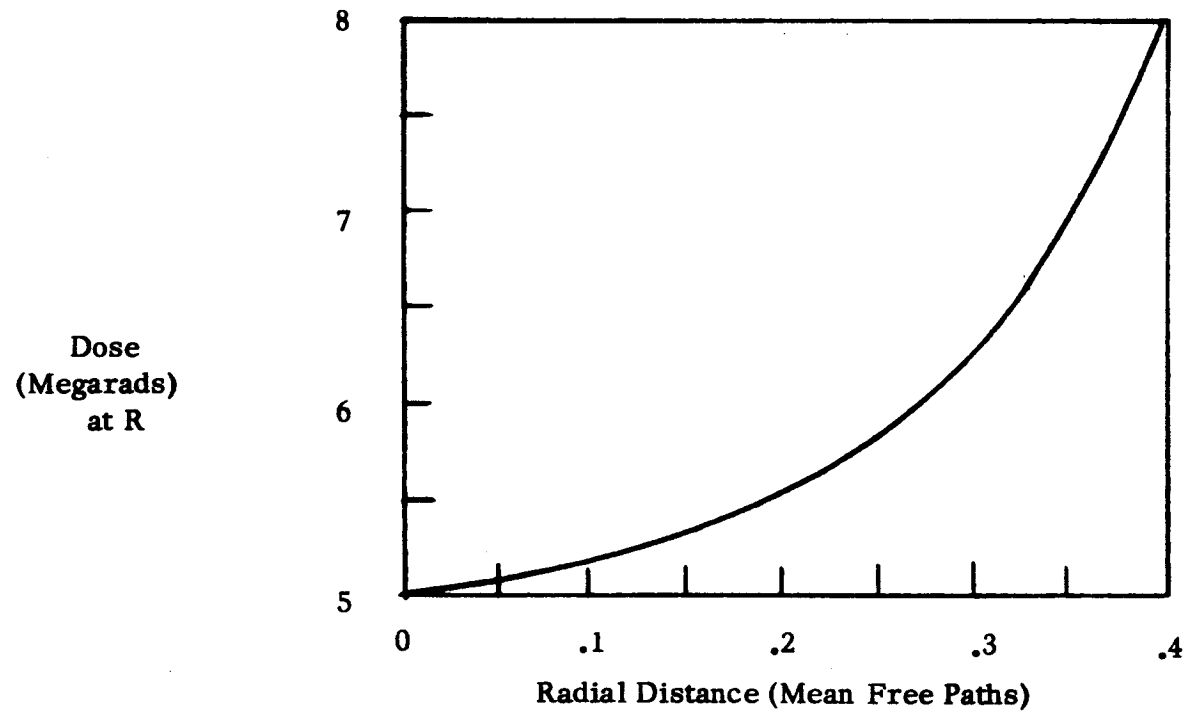

Figure 8. Radial dose distribution in a 100 lb. sphere irradiated to 5 Megarads at the center by Cobalt-60.

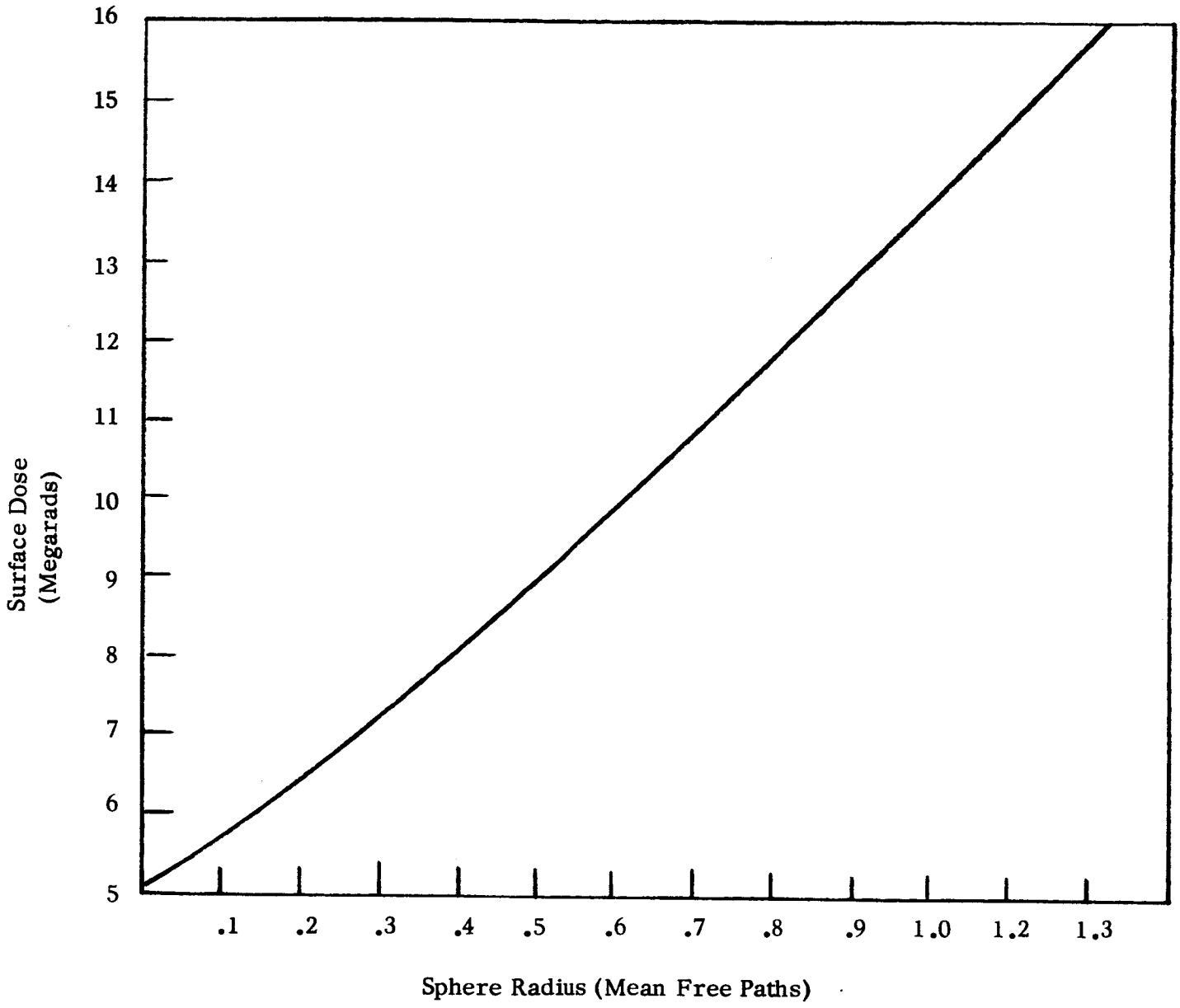

Figure 9. Dose required from Cobalt-60 at surface of sphere in order that dose at center of sphere equal 5 megarads.

The dose distribution in the 2500 lb. model, because of the greater value of μR, is more nonuniform. The distribution is shaped similar to that shown in Fig. 8, but reaches, at the outer surface, a dose of 20 megarads required for that at the center to be 5 megarads.

It will be recalled that, in section 3.1, the slab analysis for the 2500 lb. capsule called for a surface dose of 61 megarads when cobalt-60 is used. The reduction from 61 to 20 megarads is not entirely due to the spherical model used here: the slab thickness μT represented a chord through the thickest part of the model capsule being investigated. A chord through a thinner portion of the capsule would call for a lower surface dose.

An analysis as above was also performed for a spherical capsule using linac radiation. Figure 10 is a summary graph showing the effect of capsule size and type of radiation on the maximum surface dose required to give a minimum dose of 5 megarads.

It is seen that cobalt-60 gammas can achieve a maximum dose of less than 10 megarads for capsule radii up to 2 feet. The 10 MeV linac gives a maximum dose of 8.3 megarads with a capsule radius of 3.5 feet, which approximates a 2500 lb. capsule.

3.3 Rotation Methods for Dose Flattening

As seen from the examples of radiation sterilization of a slab by an isotropic surface source, the distribution of dose through the sterilized object is severely nonuniform when cobalt-60 is used as the radiation source.

A technique, used in medical radiation therapy, to provide a large dose at an internal position on the object while not over-irradiating other portions, is called rotational therapy. The object is rotated while in a narrow beam of radiation. If the beam diameter is small compared with the diameter of the rotated object, a peak results in the dose distribution.

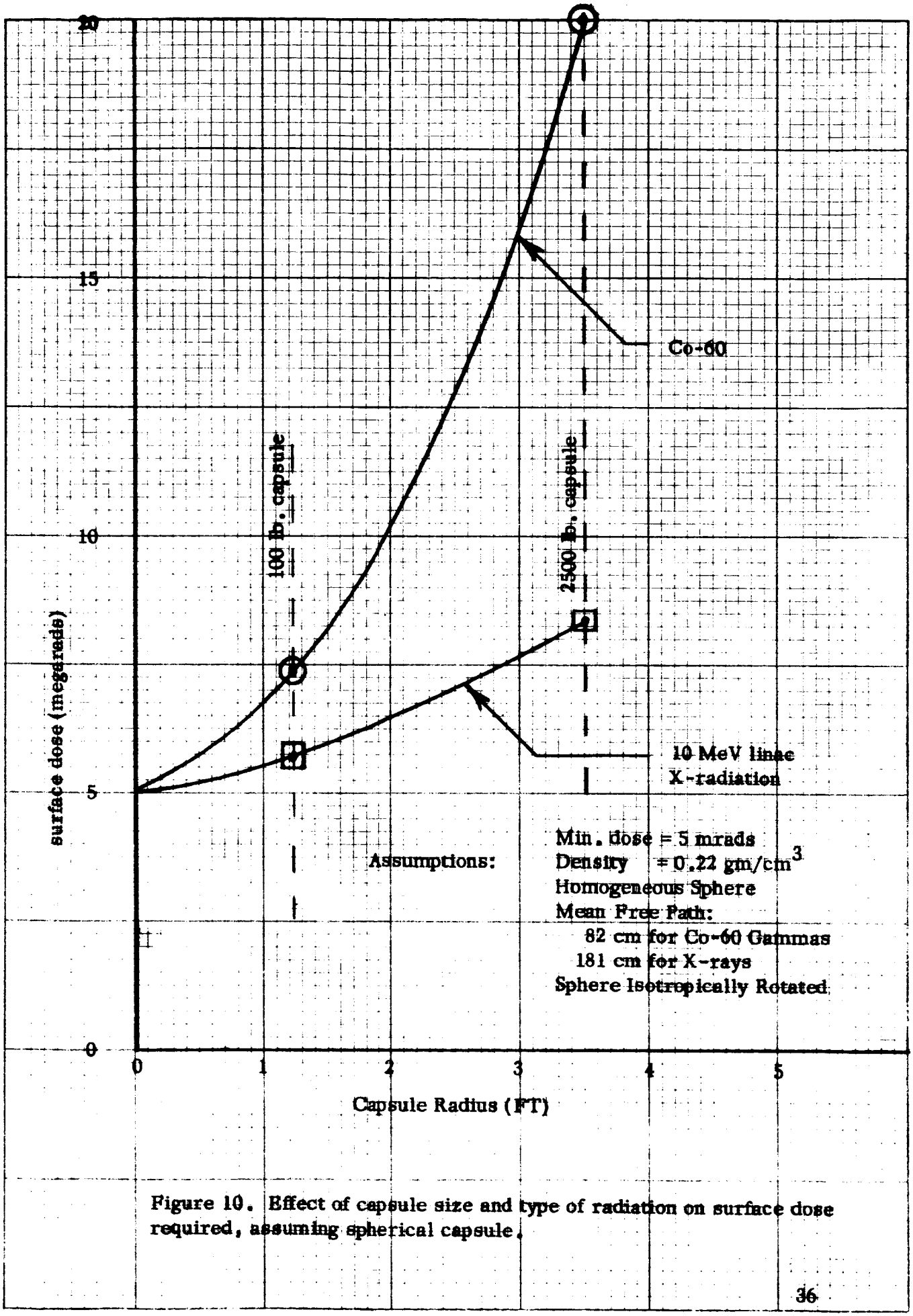

Figure 10. Effect of capsule size and type of radiation on surface dose required, assuming spherical capsule.

Evaluation of the dose distribution for rotational therapy, prior to irradiation, is performed by the use of "dose-depth" tables. Since the human body is fairly anisotropic, the laborious use of tables has been preferred over the use of a simpler mathematical model. Plaster or water models with imbedded detectors have also been employed to obtain experimental data.

Since a narrow-beam results in a dose peak at the center of the object, and a broad beam results in a maximum dose near the surface of the object, then apparently a beam of intermediate diameter should result in dose flattening.

The arrangement, shown in Figure 11, involves placing the capsule in a two-axis, gimbal turntable intercepting a narrow beam or cone of photons formed by placing the source behind a beam-defining slit. For mathematical simplicity the capsule is treated here as being spherical. Should a very heavy payload be used, it could be irradiated in this manner to flatten the dose.

Lacking dose-depth tables, we assume uniform density for the sphere and develop a mathematical model. The relation between source photon energy and sphere weight is assumed to be such that the sphere radius R is 6 mean free paths. This is equivalent to the weight of the presently considered lander (2500 lbs.) with cobalt-60 photons. A heavier lander with reactor or linac radiation could be matched for the same value of R. For simplicity, the effects of buildup are not considered; the generality of the analysis makes this a second order detail. Buildup of dose at the center, and the non-circular shape of the lander capsule both tend to decrease the dip in dose distribution. Therefore, disregarding these effects results in a simplification that is conservative. More detailed analysis would require the use of dose-depth curves and a realistic design for the capsule.

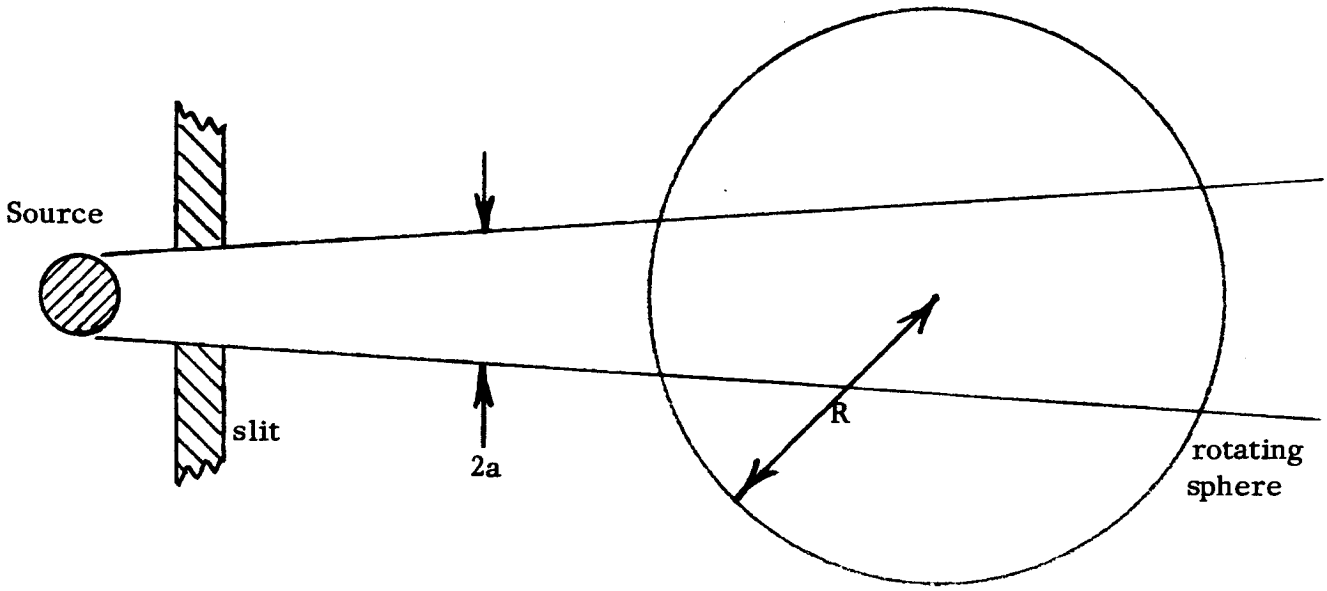

Figure 11. Spherical model of spacecraft on 2-axis-gimbal turntable.

The problem now is to determine the relative dose rate D(r) at a radius r in the rotating spacecraft, due to a beam of radius a and of energy such that the spacecraft radius is R mean free paths. This problem was solved analytically. A brief discussion of the analytic approach follows.

Geometric relationships which are obvious from the illustration are:

$$m = r \sin\theta$$

$$v = r \cos\theta \qquad \text{(see Figure 12)}$$

$$(u + v)^2 + m^2 = R^2$$

Elimination of m and v from these equations gives an expression for u which is the depth of penetration a beam photon must travel to reach the point P at arbitrary radius r and angle θ. With the source at a considerable distance from the sphere, the rays are essentially parallel and the dose is Ie^{-u}, where I would be the unshielded dose. If the volume considered is on the hemisphere away from the source, then the dose is $Ie^{-(u+v)}$. The portion of the shell which is at an angle θ to the beam is given by $\sin\theta$. The average dose over the shell is

$$D(r) = \frac{I}{2}\left[\int_0^{\sin^{-1} a/r} e^{-u} \sin\theta + \int_0^{\sin^{-1} a/r} e^{-(u+2v)} \sin\theta d\theta\right] \qquad (3.17)$$

for shells with radius r greater than a. Otherwise, the upper limits of the integrals are simply $\pi/2$. Integration yields:

$$D(r)\left[e^{-R}\sinh r - e^{-\alpha}\sinh\beta + \frac{1}{2}(R^2 - r^2)\left[E_2(R-r) - E_2(R+r) + E_2(\alpha+\beta) - E_2(\alpha-\beta)\right]\right] \qquad (3.18)$$

where

$$\alpha = \sqrt{R^2 - a^2} \text{ (if } r > a\text{), or } \sqrt{R^2 - r^2} \text{ (if } r < a\text{)} \qquad (3.19a)$$

$$\beta = \sqrt{r^2 - a^2} \text{ (if } r > a\text{) or } 0 \text{ (if } r < a\text{)} \qquad (3.19b)$$

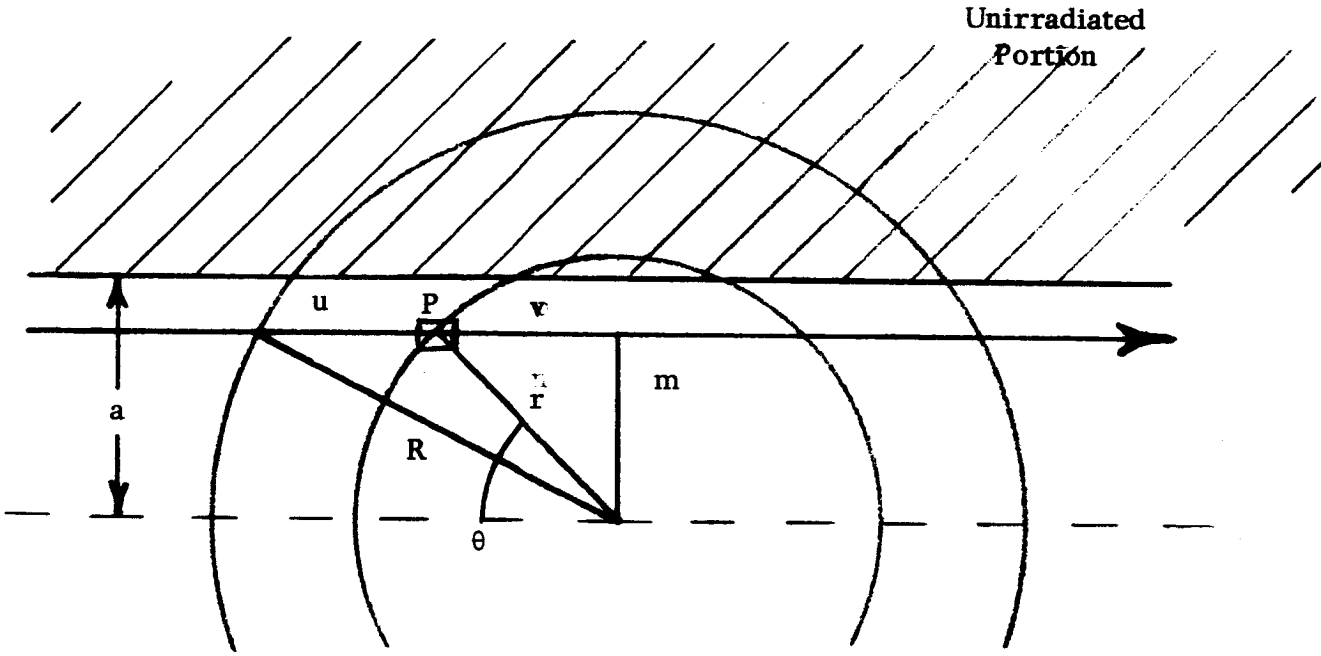

a = half-width of beam

R = radius of capsule

All dimensions in mean free paths.

Figure 12. Construction for irradiation of a spherical capsule by a narrow beam of radius a.

For the special case where r equals zero (the center of the sphere); u becomes R and v vanishes, so that (3.17) gives, for the dose at the center,

$$D(o) = 2Ie^{-R} \tag{3.20}$$

These expressions are applicable when the sterilization arrangement is as depicted in Figure 11. The source can be either cobalt-60 or a linac target. Since the sterilization arrangement of Figure 7 assumes an isotropic source at the surface of the lander, it is not directly applicable to linac radiation and (3.18) should be used in such a case instead of (3.11). In summary, three expressions are provided: (3.3) for the situation depicted in Figure 5; (3.11) for the situation depicted in Figure 7; and (3.18) for the situation depicted in Figure 11.

For the dose at the surface of the sphere, (3.18) gives

$$D(R) = \frac{I}{R}\left[R - \sqrt{R^2 - a^2} + \frac{1}{2}(e^{-2\sqrt{R^2 - a^2}} - e^{-2R})\right] \tag{3.21}$$

The ratio of (3.21) and (3.20) is of interest, since frequently the maximum dose occurs at the surface, while the minimum occurs at the center. This ratio is

$$\frac{D(R)}{D(o)} = \frac{1}{2R}\left[(R - \alpha)e^{R} + e^{-\alpha}\sinh(R - \alpha)\right] \tag{3.22}$$

where the first term is the dominating one and α equals $\sqrt{R^2 - a^2}$.

The minimum dose does not always occur at the center of the sphere. For R equal 6, the curves for three different beam widths a are given in Figure 13. We see, for the narrow beams, the emergence of a central plateau, which is the effect sought in rotational radiation therapy.

From this figure, it can be concluded that a flattening of the dose distribution can be achieved by the use of a narrow beam, a rotating table, and selection of an appropriate beam energy. Better results may be possible by the superposition of two beam widths, as suggested in the figure.

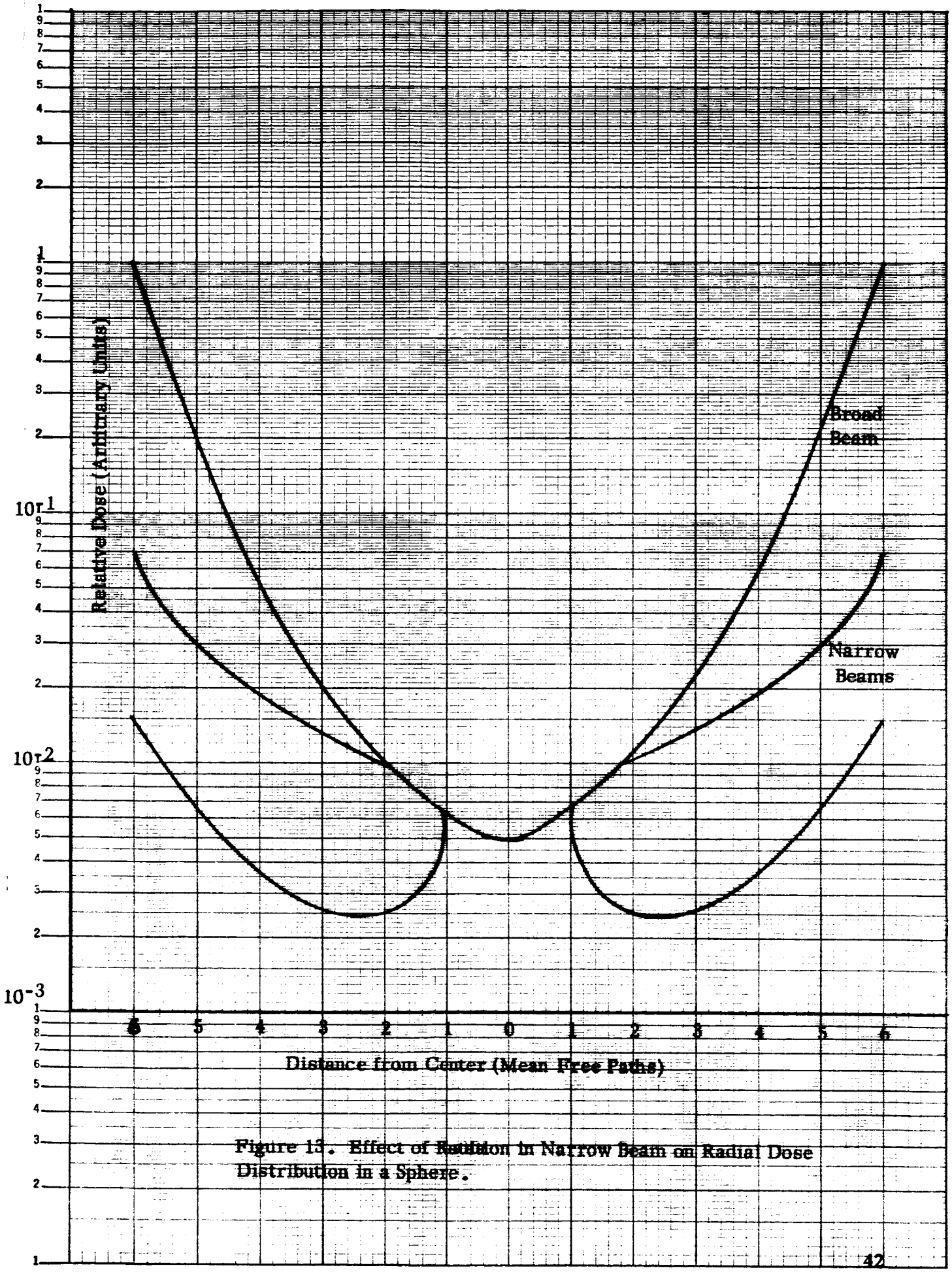

Figure 13. Effect of Radiation in Narrow Beam on Radial Dose Distribution in a Sphere.

There is little point in a further optimization study based on this model. Along with the approximations discussed above, it must be remembered that the model is considerably oversimplified, taking no account of the true geometry and heterogeneity of the lander capsule. The possible existence of air spaces extending for considerable lengths through the spacecraft may introduce radiation streaming paths that would increase the dose at the center.

If these refinements could be introduced into the dose distribution calculation, they would provide a correction term to Eq. (3.18) that would permit more effective flattening. The purpose here is not to find a precise estimate, but rather to demonstrate that the ratio of maximum to minimum dose can be brought to a tolerable level by the rotational technique, either when cobalt-60 radiation is used, or when the lander capsule to be sterilized is significantly more massive than the 2500 pound model assumed in this report.

3.4 Relation of Photon Fluence to Dose

Exposure to a fluence (time integrated flux) φ per square centimeter, of photons of energies in the range 1-10 MeV, is related to the dose in roentgens by

$$\varphi = 1.84 \times 10^{9} E^{-3/4} \text{ photons/cm}^2 - r \qquad (3.23)$$

where E is the photon energy in MeV. As an example, cobalt-60 radiation has an average E of 1.25; $E^{-3/4}$ is therefore 0.85, and a fluence of 1.56×10^{9} of these photons per square centimeter results in a dose of one roentgen.

From Figure 6, the surface dose in a lander to be irradiated to 5 megaroentgens at its center by cobalt-60, is seen to be $5 \times 10^{6}/.08$, or 6.25×10^{7} r. The required fluence is therefore 9.75×10^{16} photons/cm^2.

A linac target emits a bremsstrahlung spectrum of X-ray photons with energies up to a maximum equal to the kinetic energy T of the accelerated electrons in the beam. If we know this spectrum dN/dE, then the number of photons per unit area of the beam can be related to the dose through the use of (3.23).

Since the exact shape of the spectrum depends on the various arbitrary considerations discussed in section 2.3, an approximate expression will be used here. This is based on the intensity spectrum I(E) being given by C(T - E) where C is a constant for a given total intensity. The number spectrum P(E) is therefore C(T/E - 1), with some effective cutoff at low energies due to target assembly self-shielding. The number φ of photons/cm^2 required from this spectrum, for a dose D is then given by

$$\frac{\varphi}{D} = \frac{\int_a^T P(E)\, dE}{\int_a^T \frac{P(E)}{\varphi(E)}\, dE} \qquad (3.24)$$

where a is the effective cutoff energy. Integration yields

$$\varphi = 1.84 \times 10^9 D \left[\frac{T \ln T/a - (T - a)}{0.762T^{1.75} - a^{1.75}(1.33T - 0.562a)} \right] \qquad (3.25)$$

For a linac operated at 10 megavolts, T equals 10 and (φ/D) equals 8.56×10^8 photons/cm^2 per roentgen if the cutoff energy is 1 MeV. For a cutoff energy of 0.5 MeV, φ/D equals 10.7×10^8 photons/cm^2 per roentgen. These numbers give, for a dose of 8.3 megarads, a flux of 7.1×10^{15} or 8.8×10^{15}. Averaging these numbers gives an estimate for φ of 8×10^{15} photons/cm^2 to produce 8.3 megarads dose on the surface of a capsule.

This number is used as a basis for the calculations of radiation damage by 10 MeV bremsstrahlung to electronic components, in Section 4.

4.0 Radiation Damage to Components: Transistors and Polymers

In Section 2, the radiation for capsule sterilization was selected to be photons in the 1-10 MeV range, with the higher energies deemed best for the thicker capsules. The photon energy, method of irradiation, and capsule size were related to the uniformity of dose distribution in section 3. For the specific case of a 15 foot diameter disk-type capsule, an electron linac operating at a 10 megavolt potential, producing bremsstrahlung to irradiate the capsule from both sides, gives the capsule a surface dose of 8.3 megarads when the least-exposed portion receives the 5 megarad dose that is the sterilization criterion of this report. More elaborate techniques were presented for larger capsules, and lower energy photons were shown to be adequate for smaller capsules.

In this section, the most deleterious effects of the 8.3 megarad dose of 10 MeV X-rays are studied. The effects are less for lower doses or lower energies. It should be emphasized that damage effects are <u>not</u> determined only by the magnitude of dose. The nature of the radiation (photons, neutrons, etc.) plays an important role.

Comparison of these results with dose levels for nuclear radiation damage, as from fission sources, shows that the photons are considerably less harmful to electronics than fast neutrons from nuclear fission, for which the data on radiation damage have been used to generate broad conclusions on thresholds for equipment failure. Parallel information for high energy X-ray exposures is less complete since there has been little practical inducement to measure radiation damage by the high energy X-rays proposed herein for sterilization of Mars landing capsules.

To provide quantitative predictions of the damage to the semiconductor electronic components of the capsule, which are certainly the most sensitive components, it is necessary to analyze the mechanism of interaction on an atomic scale. As discussed in section 1.3, the principal effect of X-ray photons

in material is to free electrons and provide them with various amounts of kinetic energy. The kinetic energy of each free electron will be, of course, some value that is less than that of the photon that released it. In Figure 14, we plot the spectrum of X-ray photons emitted by a linac target[10]. The electron spectrum produced by this photon spectrum in a landing capsule will be shifted to lower energies.

As a function of photon energy, the rate of interaction - and hence the rate of production of free, fast electrons is the mathematical product of the intensity of photons (Figure 12) and the attenuation coefficient (Figure 5). The interactions of interest are Compton collisions, for which there exist analytic forms of both the differential and the total cross section. The photoelectric effect is neglected at these high photon energies.

The electrons resulting from pair production are also neglected, although it is realized that a careful analysis should include them. There are three reasons to suspect that such electrons represent a second-order effect. The first, exhibited in Table 3, is the relative size of the pair production and Compton

Table 3 Aluminum Cross Sections for Compton and Pair Production, in $cm^2/gram$.

Photon Energy	Compton σ	Pair σ
1 MeV	.062	0
2	.046	.0008
3	.033	.0018
5	.024	.0042
7	.018	.0062
10	.014	.0085

cross sections. The magnitude of the former appears to be, for the X-ray spectrum, about a factor of 5 lower than the latter. A second reason is that the maximum electron energy obtainable is roughly (E-1)MeV, where E is the photon energy

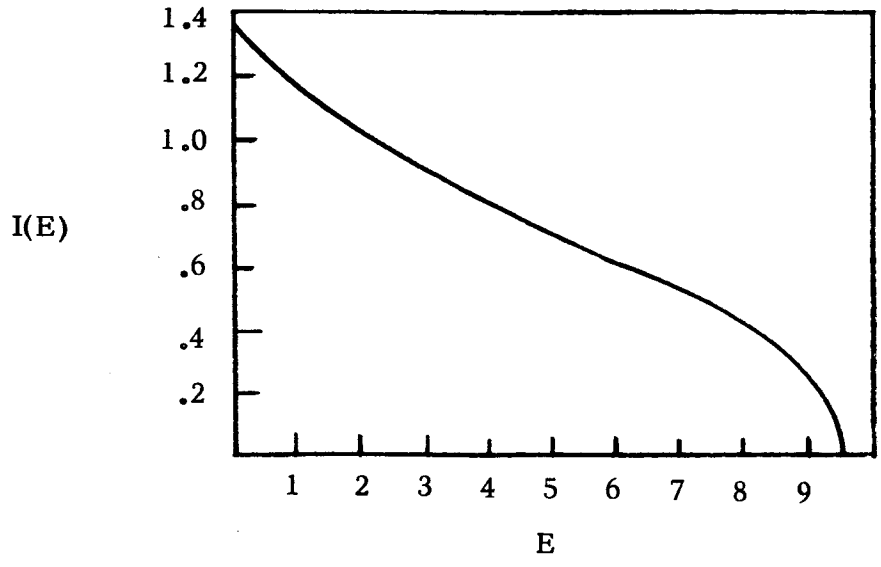

Figure 14. Intensity of radiation, in arbitrary units at energy E, versus photon energy E for 10 MeV electrons in a lead target. (After Ref. 10)

(Ref. 61, p. 704). The maximum, for Compton collisions, is roughly (E-1/4). A third reason is that the electron energy spectrum produced in the pair effect is approximately flat, while the spectrum produced in the Compton effect is peaked at the maximum energy. For a first approximation, with emphasis on the faster and more damaging electrons, the electrons resulting from pair production are neglected in the following discussion. However, when total ionizations are the damage mechanism, it is relatively easy to include that due to pair production, and this is done.

There is, then, a temporary source of free, fast electrons throughout the capsule material. The number of these electrons is equal to the number of primary ionizations. From this, it can be concluded that the damage due to an X-ray beam is composed of two parts. One is the damage due to the primary ionizations, where ions are formed which lead to subsequent chemical reactions, just as happens when the material is irradiated with any other type of radiation. Ionization damage is, for example, the principle effect of the lower energy photons from gamma sources, and the effect of lower energy electrons incident on the material. The second component of the damage in the present case is that due to the freed fast electrons which can cause atomic displacements in crystal lattices. In principle, therefore, damage due to high energy X-rays can be related to lattice damage due to fast electron sources, plus ionization damage.

The fast electrons, because of their greater momentum, are capable of elastic scattering collisions with the atomic nuclei in the medium. The recoil of the atom, if sufficient, displaces it from its position in a crystal lattice. Atomic displacements are of primary concern in the damage to semiconductor materials. These materials, because of the high purity required for transistor and diode action, are therefore among the most sensitive to radiation. In section 4.2, the effect of atomic displacements is linked to the damage

observed in transistors. The relationship involves application of experimental data for fast electrons. Then, in section 4.3, results of this analysis are applied to evaluate the gain degradation to be anticipated in transistors.

The general class of materials known as organic polymers is also highly sensitive to radiation damage. Here it is the number of ionizations, and not the energy of the ions and electrons, that is of primary importance. This subject is discussed in section 4.6 and sensitive polymers are identified.

4.1 Electron Spectrum Produced by Photon Flux

The Klein-Nishina cross section of $(\frac{d\sigma}{dE})$ for Compton collisions gives the probability per electron in a medium, that a photon traversing one centimeter of the medium will be scattered, and go from an energy E_0 to a lower energy E_1. Per cubic centimeter of medium, the number of such reactions is therefore

$$S(\epsilon_0) = NZ\varphi_\gamma \left(\frac{d\sigma}{d_E}\right)_{E_0,E_1} \tag{4.1}$$

where N is the density of atoms, Z their atomic number and φ_γ the number of photons incident on each square centimeter. Each scattering reaction releases an electron from its bond in the medium; the kinetic energy of the electron is closely given (neglecting electron binding energy) by the difference between E_o and E_1; so that $dS(\epsilon_0)$ can also be taken as the number of electrons released per cubic centimeter, with an energy ϵ_o given by

$$\epsilon_0 = E_0 - E_1 \tag{4.2}$$

The electrons so created lose energy as they travel through the medium, being recaptured after traveling a distance R from the point of origin. For ϵ_0 between 1 and 20 MeV, an empirical relationship frequently used is

$$R = aE_o - b \tag{4.3}$$

where a and b are constants, being 0.195 and 0.035 respectively, for the range in centimeters of aluminum. From this equation for R, it can be seen that an

electron which has an energy ϵ after traveling a distance r started off with an initial energy ϵ_0 given by

$$\epsilon = \epsilon_0 - r/a \tag{4.4}$$

provided that ϵ is within the interval of applicability of the equation (4.3), namely 1 to 20 MeV.

The flux of free electrons of an energy ϵ in the irradiated medium can now be found. If $S(\epsilon_0)$ electrons of energy ϵ_0 are freed in a unit volume a distance r from the detector volume, and these electrons are radiated isotropically, then $S(\epsilon_0)/4\pi r^2$ electrons will strike a detector with an energy ϵ. The number of electrons with energy ϵ striking the detector from all directions is then

$$N(\epsilon) = \iiint \left[S(\epsilon_0)/4\pi r^2\right] dV \tag{4.5}$$

In spherical coordinates, this becomes

$$N(\epsilon) = \int_0^\infty S(\epsilon_0)\, dr \tag{4.6}$$

The condition that the electrons are radiated isotropically can be relaxed, since (4.5) involves an integration over all directions. As is well known, specifying the incident photon energy E_0 and electron energy ϵ_0 will specify the angle of emission, through the Compton relation so that for parallel beam photons, a Dirac delta function is usually included in (4.5). This direction dependence is of concern only when the scatter volume does not completely surround the detector to a distance given by the maximum range R. To reduce a complex problem to one that may be handled by first considerations, we neglect the spread in R implied by (4.3). Straggling does, however, cause fluctuations of individual electron ranges about the mean value R. That is, for an electron whose initial energy was some differences from the energy ϵ_0 required by (4.4), there is some probability $P(\delta)$ that the electron will travel a distance r and arrive at the detector with the required energy ϵ. We shall assume that

$$\int_{-\infty}^{\infty} S(\epsilon_0 + \delta) P(\delta) d\delta = S(\epsilon_0) \tag{4.7}$$

so that $N(\epsilon)$, which is strictly speaking formed with the left side of (4.7) as the kernel of the integral in (4.6), will be approximated by the simpler form. Finally, electrons in a material do not travel in straight lines, but in zigzags, where each sharp detour in the electron path is due to elastic scattering from an atom. This has the effect of bending the path traveled by an individual electron so that generally its end point is closer to its source than the distance R cm covered by a straight path. In an infinite medium with uniformly distributed sources, the amount of bending should have no effect on the electron flux.

The energy E_1 that the photon must retain to contribute an electron to the integral in (4.6) is

$$E_1 = E_0 - (\epsilon + r/a) \tag{4.8}$$

Therefore, a substitution of variables is allowed, By differentiation,

$$a\, d\, E_1 = -dr \tag{4.9}$$

and using the analytic form of the cross section in (4.1) for $S(\epsilon_0)$ to be placed in the integral, we have

$$N(\epsilon) = a\, NZ\varphi_\gamma \pi r^2 mc^2 E_0^{-2} \int_{(E_0 - \epsilon\,\mathrm{Max}) = \alpha}^{(E_0 - \epsilon) = \beta} \left[\frac{E_0}{E_1} + \frac{E_1}{E_0} + \frac{1}{E_0} - \frac{1}{E_1} + \frac{1}{4}\left(\frac{1}{E_0} - \frac{1}{E_1} \right)^2 \right] dE \tag{4.10}$$

where the lower limit on E is defined by the maximum energy an electron can receive in a collision with a photon of energy E_0. The integral is integrated to give

$$N(\epsilon) = a\, NZ\varphi_\gamma \pi r^2 mc^2 E_0^{-2} \left[(E_0 - 1 - \frac{1}{2E_0}) \ln \beta/\alpha + (\beta^2 - \alpha^2)/2E_0 + (\beta - \alpha) \right.$$
$$\left. (4E_0 + 1)/4E_0^2 + (\beta - \alpha)/4\alpha\beta \right] \tag{4.11}$$

where β equals $(E_{0_2} - \epsilon)$ and α equals $(E_0 - \epsilon)_{max}$. For high energy photons, α approaches $mc^2/2$, where mc^2, the rest energy of the electron, is 0.51 MeV. The classical cross section of the electron, πr^2, is 0.248 barns. (1 barn is 10^{-24} cm^2)

Figure 15 shows the calculated energy spectrum, in aluminum, of electrons generated by a unit flux of either 5 or 10 MeV photons, according to (4.11). The product a N in the formula is independent of density; thus the ratio of electron flux to photon flux in the irradiated capsule does not depend on the void fraction. This ratio is to be found by integration over ϵ of (4.11); the result is

$$\varphi = A\left\{E_0^2 - E_0 - 3/4 \ln \gamma - 5/6\, E_0^2 + 3\, E_0 - 1/6\, E_0^2 \left[6\gamma^2 + 3\gamma - 2\right]\right\} \quad (4.12)$$

where γ equals $(4E_0+1)$. The integration includes that portion of the electron flux spectrum below 1 MeV, assuming the formula for $N(\epsilon)$ is not seriously incorrect. It is therefore increasingly conservative as E_0 approaches 1 MeV. In (4.12), A equals the expression on the right side of (4.11) outside the brackets:

$$A = a\, N\, Z\, \varphi_\gamma\, \pi r^2\, m\, c^2/E_0^2 \quad (4.13)$$

The ratio φ_e/φ_γ of electron fluence (integrated over energy) in equilibrium with photon flux increases about as the square root of the photon energy. The calculated ratio is seen in Figure 16. The contribution of low energy electrons due to electron cascade in the material is not included in the figure. It is seen that there is only about one electron for every 100 to 500 photons in equilibrium as a beam penetrates a solid.

The photon fluence from section 3.4 is about 8×10^{15} per square centimeter for a dose of 8.3 megarads. The electron fluence is therefore about 3×10^{13} per square centimeter.

4.2 Radiation Damage to Semiconductors

Below the threshold of photonuclear reactions, the direct interaction between photons and atomic nuclei is minor (nuclear Compton scattering) and leads to no lattice displacements. Indirectly, however, energetic photons free electrons as

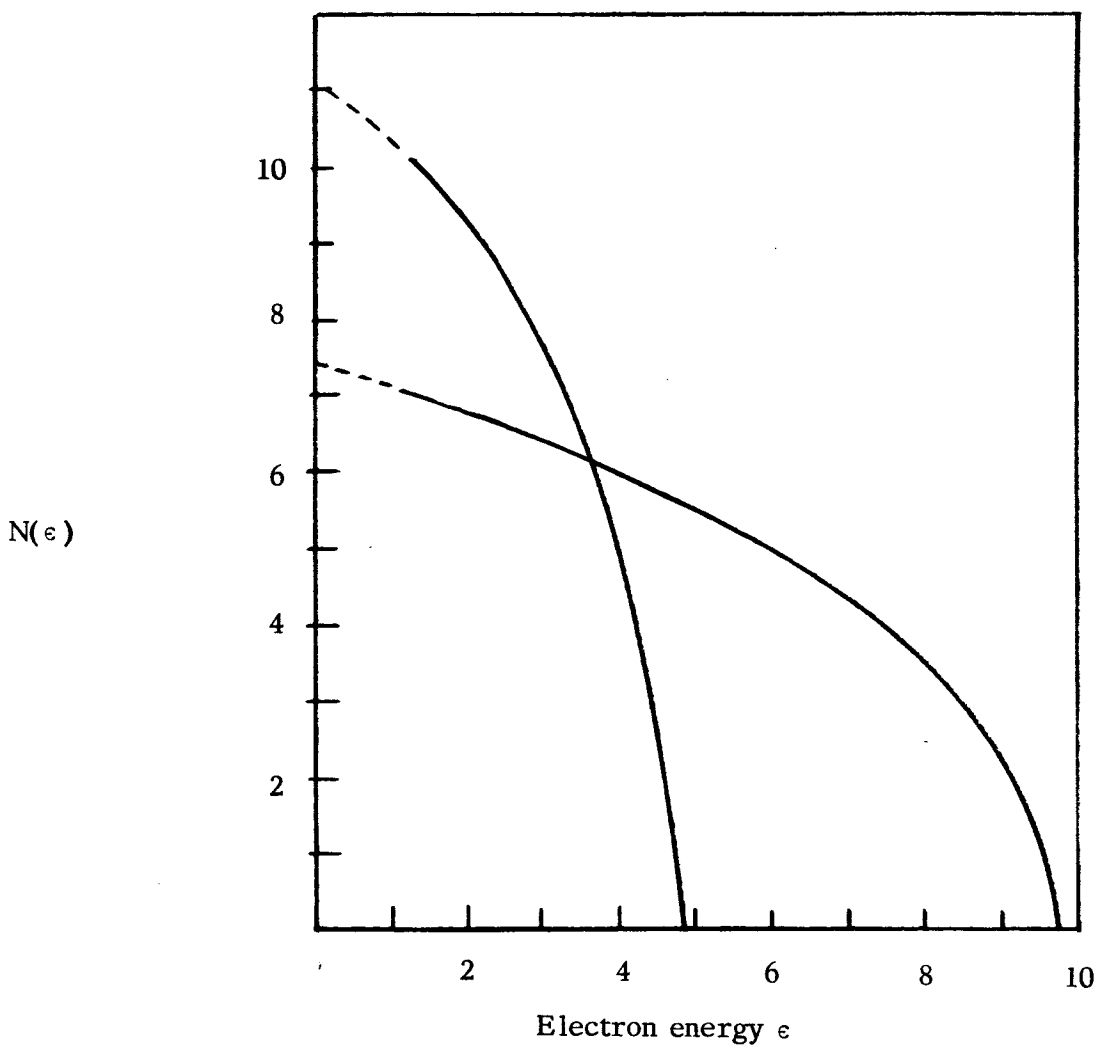

Figure 15. N(ϵ), the energy spectrum of electrons (e/cm^2-MeV), generated per 1,000 photons of 5 MeV or 10 MeV in aluminum

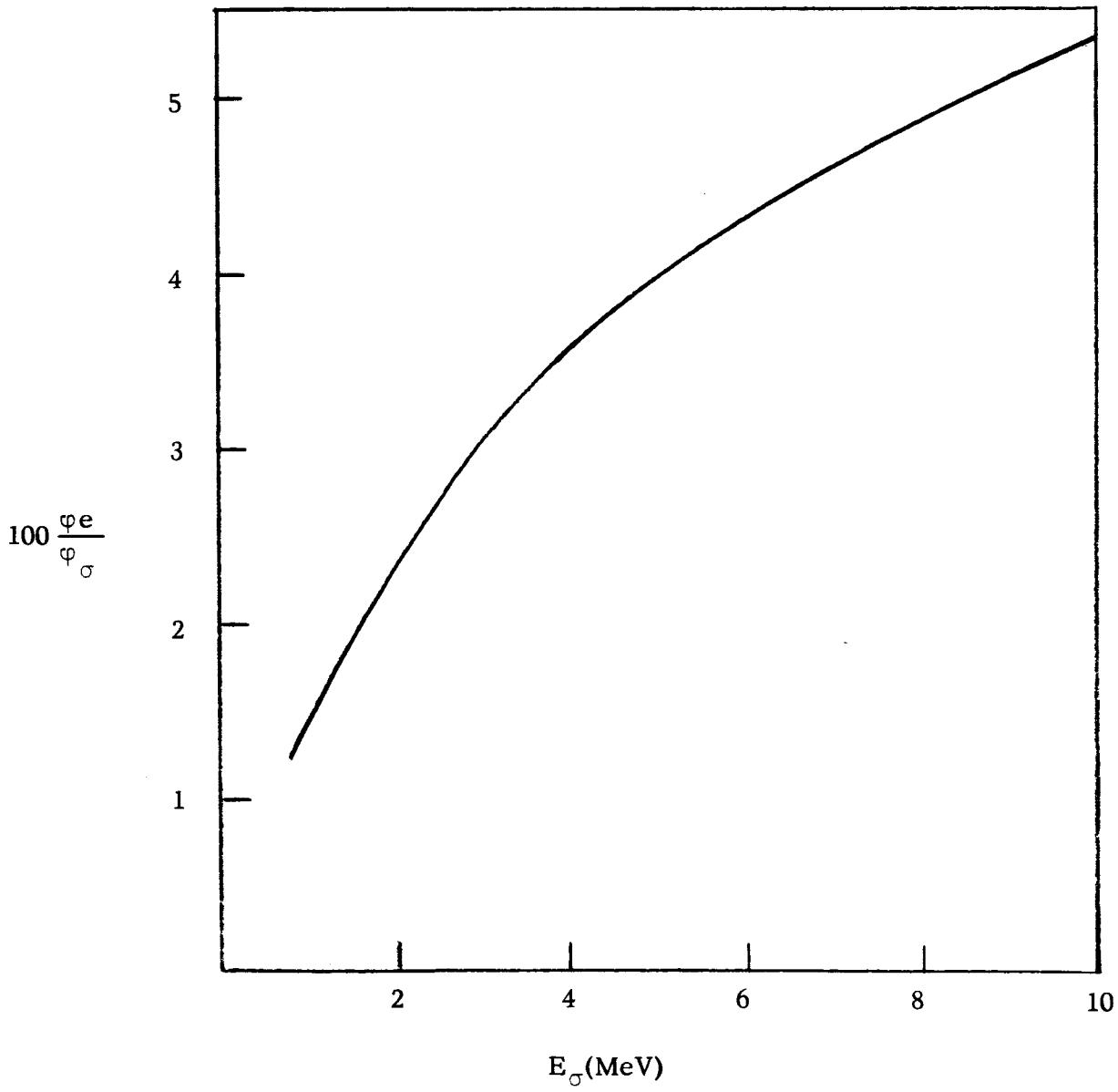

Figure 16. Ratio of electron flux to photon flux in aluminum, in equilibrium. Pair electrons and cascade effects neglected.

described in the previous section, and these electrons do scatter in the electric field of the nucleus so that lattice displacements can and do occur.

The resulting vacancy at a lattice site -- and the atom at some interstitial position -- leads to the bulk radiation damage in semiconductor devices. The damage increases as the radiation fluence is increased. In addition to this damage, there is also a surface effect on transistors which is poorly understood, but is believed to be due to charge deposition in the surface layer of the device under the influence of radiation. A significant property of surface radiation damage is that it saturates. That is, after a certain amount of radiation exposure (on the order of several megarads) the surface radiation damage reaches an upper limit.[11]

Many of the vacancy-interstitial pairs formed by recoil from the electron scattering collisions immediately recombine at room temperature with the aid of thermal vibrations. Temperature obviously plays a critical role in this annealing. When the repair of the vacancy-interstitial pair is not immediate, the vacancy can diffuse away, from atom site to atom site, seeking a stable position. The surface of a crystal is one such position, leading to a redefinition of the crystal boundary and no observable vacancy. Another is an association with some impurity atom, normally present in silicon, to form a stable configuration that will act as a recombination center for electrons and holes.

The distance a conduction electron can travel, before recombining with a hole, is inversely proportional to the concentration of these recombination centers in the crystal. Radiation-induced permanent defects form recombination centers which provide allowed energy levels in the otherwise forbidden energy gap of a semiconductor. Crystal surfaces also provide recombination sites, but if we neglect these for the moment, we can say that the lifetime τ of an electron in the conduction band is given by

$$\frac{1}{\tau} = \sigma v(N_0 + N_1) = \frac{1}{\tau_0} + \sigma v N_1 \qquad (4.20)$$

where v is the electron velocity, σ the cross section for recombination of minority carriers, N_0 the number of centers originally in the crystal, and N_1 the number generated by radiation-induced displacements. Before irradiation, τ is equal to τ_0, and the measured value of τ_0 will include not only the effect of the N_0 defects but also the surface recombination effect.

Since N_1 is proportional to the radiation fluence (time integrated flux) φ, this equation can be rewritten as

$$\frac{1}{\tau} = \frac{1}{\tau_0} + K_\tau \varphi \qquad (4.21)$$

where K_τ is the "lifetime damage coefficient" and depends on the type and energy spectrum of the radiation. The N_1 centers are stabilized by impurities, hence K_τ depends also on the initial concentrations of impurities, or dopants, in the semiconductor. The higher the impurity concentration in a semiconductor, the higher the conductivity and generally, the larger the value of the damage coefficient. This suggests that some radiation hardening of a device can be achieved by reducing the concentration of impurities in the crystal, or by selecting dopants which will combine with the radiation-created defects to form weak centers for electron-hole recombination.[12][13]

The lifetime τ is related to the electron's diffusion length L by

$$\tau = L^2/D \qquad (4.22)$$

where D is a diffusion coefficient, typically 38 cm^2/sec for electrons and 13 cm^2/sec for holes, in silicon at 300^oK[14]. The diffusion length decreases with radiation since τ decreases. Multiplication of (4.21) by 1/D gives a formula for this decrease. The expression K_τ/D, often written as K_L, is known as the diffusion length damage coefficient.

Measured values[15] of K_L for fast electrons in p-type silicon are plotted as Figure 17. The trends with electron energy E and sample conductivity are seen to conform with the above statements. One can write

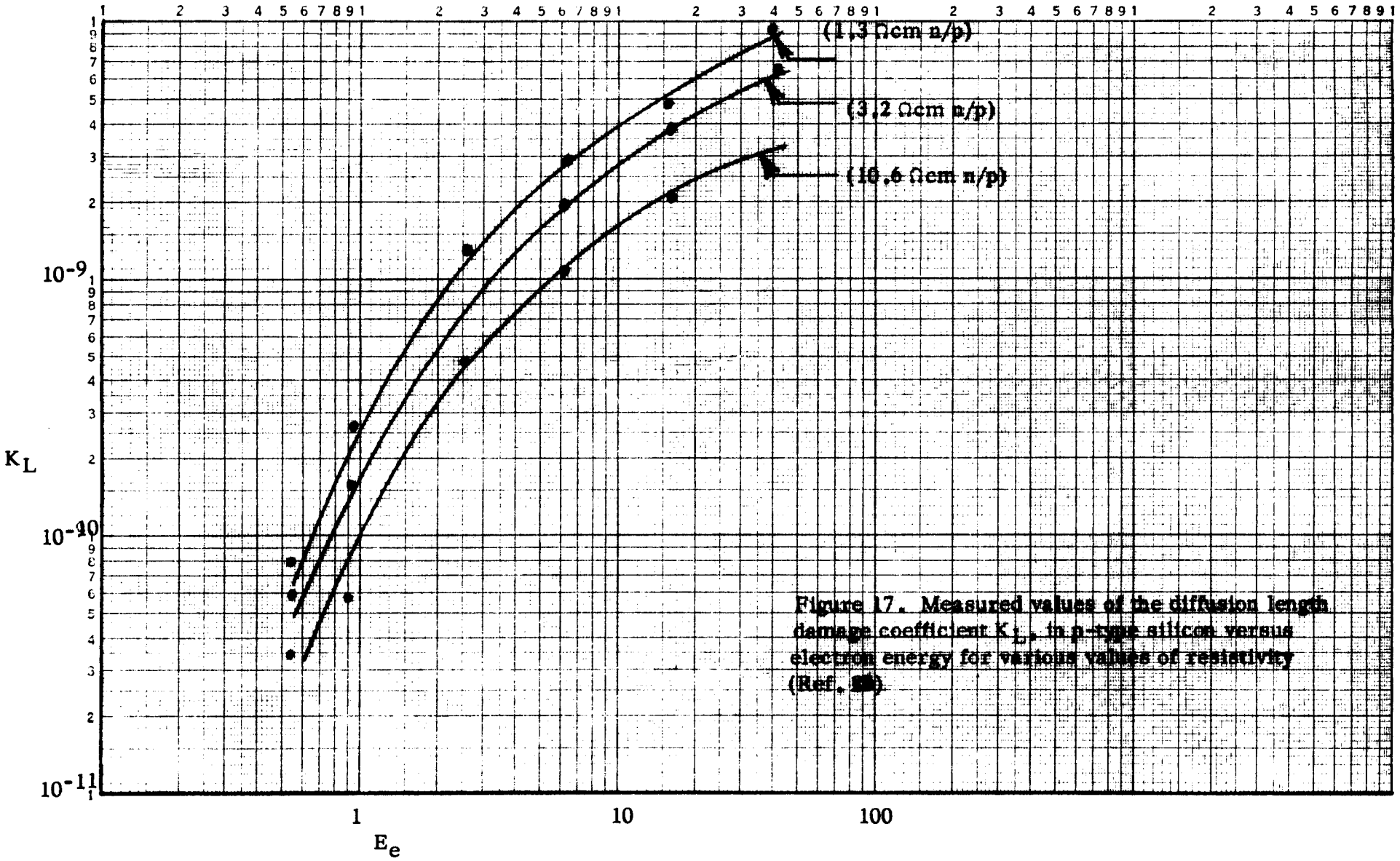

Figure 17. Measured values of the diffusion length damage coefficient K_L, in p-type silicon versus electron energy for various values of resistivity (Ref. 28).

$$K_L(E) = \left[N \sigma_d(E) \nu(\epsilon) v / D \right] \sum_i P_i \sigma_{ai} \qquad (4.23)$$

where N is the number of atoms per cubic centimeter (5.22×10^{22}) for silicon, $\sigma_d(E)$ is their cross section for displacement, as a function of the energy ϵ of the colliding particle, and $\nu(\epsilon)$ is the number of permanent vacancy-interstitial pairs created per recoil, and the product $N\sigma_d(E)\,\nu(\epsilon)$ equals the number of atom displacements generated per unit fluence φ. The average electron velocity is v and the diffusion coefficient is D. The summation is over the probabilities P_i that each of the various stable configurations, such as the A center, will occur, multiplied by the cross section of the configuration for minority carrier recombination.[16]

The number N_1 of recombination centers equals the number of atom displacements multiplied by $\sum_i P_i$, which is the total probability a displaced atom will develop a center. The significant centers are due to the lattice site, from which the atom was ejected, diffusing in the lattice until it forms a stable configuration; with an impurity atom. The configuration can be dissoci ated generally by increasing the temperature. As a result, the number of centers can be decreased by a suitable thermal annealing of the irradiated material.

For example, consider the A center. This is a recombination center with an energy level 0.17 eV below the conduction band; it is the predominant effect of gamma radiation on n-type silicon containing oxygen as an impurity.[17] The annealing energy for this center is about 0.93 eV, so that substantial reduction in N_1, and consequent annealing of the damage to n-type silicon is possible at temperatures of 100°-200°C.[18] Annealing the radiation damage while continuing the sterilization by heat is a promising procedure in this case. Alternatively, post-irradiation heating of the transistors alone by electrical heating deserves evaluation. The results of five minute annealing periods with such heaters are shown dramatically in Figure 18, for temperatures of 200°C-500°C.

SILICON TRANSISTORS TYPE CDQ 19119

H_{FE} VS φ , I_C = 10 ma; V_{CE} = 5 Volts, T = 25°C

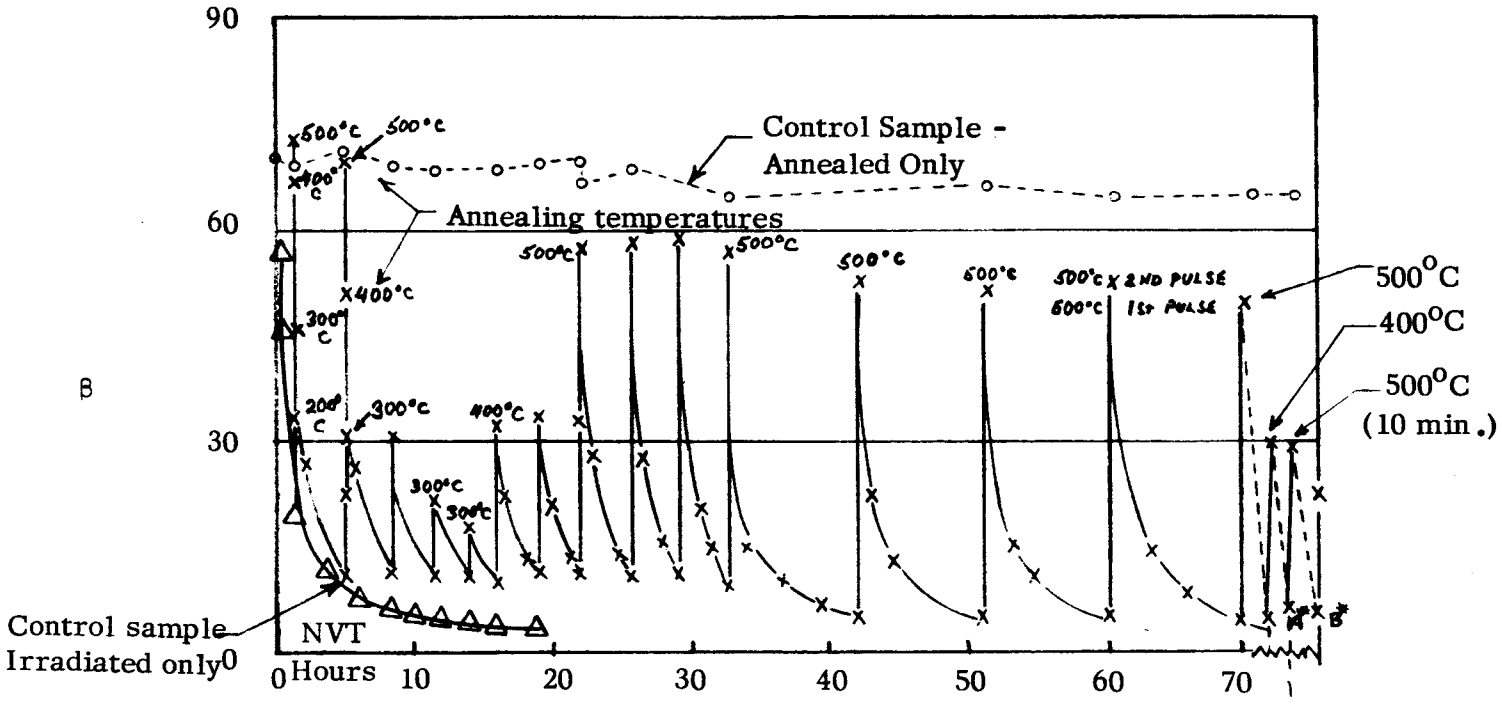

Normalized Total Exposure in Hours at 2.0×10^{10} Neutrons/cm^2/sec (E > 0.4 ev)

* Notes:

1 - Points "A" & "B" were reached by simultaneously irradiating at 2×10^{12} n/cm^2/sec and annealing at 400°C and 450°C respectively.

2 - All annealing pulses were 5 minutes in duration unless otherwise noted.

3 - Transistor CDQ 19119 is electrically similar to type 2N2900.

Figure 18. Effects of repeated annealing of radiation damage in a silicon semiconductor (Ref. 19).

Unfortunately, major recombination centers produced in p-type silicon have annealing energies in the 200^{o} - 350^{o}C range.[18] Hence, the base material of pnp transistors may be annealed at lower temperatures than are required for the annealing of npn transistors. Offsetting this advantage is the fact that the initial damage for a given dose to n-type silicon is greater than to p-type silicon, apparently due to a greater minority-carrier capture cross section σ_{ai}.[20]

The understanding of the annealing process does not appear to have reached a reliable state allowing quantitative predictions. Rather than an attempt to incorporate annealing considerations in the present report, we merely point them out as a possible cure when an application requires that the transistor damage is minimal.

A principal figure of merit, affected by radiation damage, is the common emitter dc current gain β (or h_{FE}) in hybrid terminology). For a junction transistor, this gain is related to the minority carrier lifetime in the base of the transistor. Specifically, a radiation-induced change in lifetime τ of minority carriers in the bulk material of the transistor base results in a change in β. The two changes are related[21] when the radiation damage is not excessive by the expression

$$\Delta \frac{1}{\beta} = t\,\Delta\left(\frac{1}{\tau}\right) = K_{\beta}\varphi \qquad (4.23)$$

where t is the base transit time for minority carriers, and K_{β} is the gain damage coefficient per unit fluence, φ.

Most transistors on the Jet Propulsion Laboratory Preferred Parts List[22] are of the npn silicon type, where electrons are the minority carrier in the base region. The base transit time is often simply related to construction parameters. The relation is[23]

$$t = W^2/2D \text{ for a uniform base transistor} \qquad (4.26a)$$

$$t = W^2/4D \text{ for a linear graded base transistor} \qquad (4.26b)$$

where W is the width, in centimeters, of the base and D is the diffusion constant for the minority carrier in the base material.

Obviously, then, the changes in the reciprocals of the current gain β, the lifetime τ, and the diffusion area L^2 are all proportional to the fluence φ, and the damage coefficients are simply interrelated by

$$K_\beta = tK_\tau = tDK_L \tag{4.27}$$

As an example, consider one n-p-n silicon transistor on the JPL Preferred Parts List, the 2N1613 transistor as manufactured by Fairchild. Measurements of gain decrease due to 2 MeV electrons give[21] a value of 4×10^{-17} for K_β. An independent measure of t is 1.7 nanoseconds.[24] Using the value of 38 cm^2/sec for D, we obtain

$$K_L = 4 \times 10^{-17}/1.7 \times 10^{-9} \times 38 = 6.2 \times 10^{-10} \tag{4.28}$$

which agrees with a point for p-type silicon of resistivity of about 2 ohm-centimeter resistivity as plotted in Figure 17. This provides a confirmatory check of transistor damage against damage coefficient of p-type silicon as measured in solar cells.

Data are available[25] on $\Delta(1/\beta)$ for several other transistors as a function of electron fluence at 1 MeV. Table 4 presents the points for an electron fluence of $3 \times 10^{14}/cm^2$. The wide variation in K_β with component is obvious. But when we multiply observed K_β by design alpha cutoff frequencies $f_{\alpha\beta}$, the results are considerably closer for all the transistors studied.

Table 4. Change in the reciprocal of gain for 3×10^{14} electrons/cm^2

Transistor	Type	$\Delta(\frac{1}{\beta})$	$f_{\alpha\beta}$ (Mc/sec)	Product: $(f_{\alpha\beta})(\Delta \frac{1}{\beta})$
2N2102 planar	npn	.02	60	1.2
2N1132 planar	pnp	.013	100	1.3
2N1486 mesa	npn	0.18	1.25	2.3
2N1132 mesa	pnp	0.33	60	2.0

That the product $f_{\alpha\beta}\Delta(\frac{1}{\beta})$ should be fairly constant stems from the relation of the alpha cutoff frequency to base width W and diffusion coefficient D:

$$f_{\alpha\beta} = 1.22D/\pi W^2 \qquad (4.29)$$

as that $f_{\alpha\beta}$ is proportional to the reciprocal of t. The base transit time t, measured for several transistors, is presented in Table 5.

Table 5. Mean Base Transit Time t (Nanoseconds) at 35°C for Various Currents (Milliamperes)[24]

Transistor Type	Manufacturer	t(o)	t(10)	t(30)	t(100)
2N694	TI	2.020	1.707	1.704	1.904
2N3439	RCA	6.4792	6.053	8.155	-----
2N1613	Bendix	0.970	0.737	0.662	0.710
2N914	Fairchild	0.339	0.311	0.336	0.414
2N709	Fairchild	0.156	0.158	0.175	0.320
2N1613	Fairchild	1.713	1.444	1.398	1.486
2N708	Fairchild	0.332	0.324	0.374	0.653
2N3227	Motorola	0.215	0.203	0.236	0.601
2N835	Motorola	0.406	0.357	0.375	0.519
2N2218	Motorola	0.510	0.414	0.367	0.392
2N1613	PSI(TRW)	0.886	0.682	-----	-----
2N744	TI	0.334	0.375	-----	-----
2N916	Motorola	0.496	0.452	0.473	3.140
2N1893	TI	1.684	1.477	1.529	2.179
2N2784	Sylvania	0.095	0.071	0.083	0.126
2N3014	TI	0.324	0.274	0.272	0. 367
2N1506A	TRW	0.808	0.584	0.495	-----
2N1893	TRW	1.125	1.006	.965	1.241
2N2656	TRW	0.388	0.379	0.452	0.848
2N916	Fairchild	0.365	0.368	0.481	-----
2N780	TI	0.679	0.880	-----	-----

It is to be observed, from Table 5, that the mean base transit time t depends not only on the transistor type, by serial number, but also on the operating value of the collector current and on the manufacturer's current technique of fabrication. There are, for example, three different manufacturers represented for the 2N1613 transistor tested, and the tested devices all have different t. As well, apparently

identical units from a single manufacturer will differ. The result of these differences is clearly, from the relation of t to K_β, a wide difference in the radiation damage sensitivities of the units.

As a result, we must conclude that an evaluation of transistor performance after irradiation cannot be based on transistor type alone. Rather, the initial gain β_o, the base transit time t (or the equivalent information from $f_{\alpha\beta}$), and the composition and resistivity of the base material, together determine the final performance.

4.3 Approximate Transistor Damage

The permanent damage to electronic circuits due to the use of high energy X-rays for sterilization is primarily due to a degradation of transistor gain β. This is the ratio of collector current to base current when the transistor is connected as a common-emitter amplifier. Should the transistor be connected in a common-base arrangement, the ratio α of the collector current to the emitter current is of interest. The well-known relation

$$\beta = \alpha/(1 - \alpha) \qquad (4.30)$$

allows one to determine radiation effects on α if radiation effects on β are known.

Since the circuits of the lander will not be energized during irradiation, surface damage to the transistors will be minimal.[26]* In this case, all the background for an evaluation of the effects of radiation sterilization has been presented in the previous sections. The sequence of calculations for such an evaluation is:

a) Determine the total fluence of photons incident on the transistor. For the sterilization process, this was computed in section 3.4 to be $8 \times 10^{15}/cm^2$ for 8.3 megarads dose of 10 MeV bremsstrahlung.

b) Determine the photon energy spectrum N(E). This was shown in section 2.3 to be roughly (T/E - 1), where T is 10 MeV, and more precise shapes are given in Figure 12.

---

* as discussed in section 4.4, component selection to insure minimal surface damage is also contemplated.

c) Calculate the equilibrium electron spectrum $N_E(\epsilon)$ to be found in the lander capsule in equilibrium with photons of several energies E in the incident photon spectrum, using the methods of section 4.1.

d) Calculate the damage coefficient K_L for photons of energy E via secondary reactions of electrons, with the formula

$$K_L(E) = \int K_L(\epsilon) dE \qquad (4.31)$$

where $K_L(\epsilon)$, the damage coefficient for electron collisions, is obtained from Figure 15, and $K_L(E)$ is the damage coefficient for photons. Since the damage by electrons and photons is qualitatively the same, the same symbol K_L is used here.

e) Calculate the average damage coefficient per photon in the spectrum being used, with the formula

$$K_L = \left(\int K_L(\epsilon)\, \varphi(E) dE \right) / \left(\int \varphi(E)\, dE \right) \qquad (4.32)$$

f) Finally, obtain the reduction in reciprocal gain by obtaining K_β from eq. (4.27) and multiplying it by the photon fluence in eq. (4.23).

A sample calculation of $K_L(E)$, for monoenergetic 10 MeV photons, is given in Table 6. A straight-forward use of Simpson's rule for numerical integration permits rapid evaluation of the integral.

Table 6. Damage Coefficient for 10 MeV Photons in p-type Silicon of 1.3 ohm-cm resistivity

E	$10^3 N(\epsilon)$	$10^9 K_L(\epsilon)$	Product			
0	---	0	0	x 1	=	0
1	7.2	.25	1.80	x 4	=	7.20
2	6.8	.74	5.03	x 2	=	10.06
3	6.5	1.25	8.12	x 4	=	32.50
4	6.0	1.72	10.32	x 2	=	20.64
5	5.5	2.15	11.82	x 4	=	47.30
6	5.1	2.50	12.75	x 2	=	25.50
7	4.5	2.80	12.60	x 4	=	50.40
8	3.75	3.05	11.44	x 2	=	22.88
9	2.5	3.30	8.25	x 4	=	33.00
10	0	----	0	x 1	=	0
						249.48

$$K_L = 1/3 \times 249.48 \times 10^{-12} = 8.3 \times 10^{-11}$$

$$K_\tau = 38 \times .83 \times 10^{-10} = 3.15 \times 10^{-9}$$

Similar calculations at lower energies yield a smoothly varying function $K_L(E)$ of the photon energy E. Because of the approximations in determining the electron spectrum, the derived function can be expected to be of doubtful accuracy around an energy of 1 MeV. Therefore, the theory is used at the higher energies and this curve is extrapolated through a measured value[19] of K_β (1.25 MeV), divided by t D in accordance with eq. (4.27). The resulting curve is presented as Figure 19.

Step (e) of the calculation requires that $K_L(E)$ be folded into N(E), values of which were presented in Figure 15. The result is a damage coefficient for 10 MeV linac radiation:

$$K_L = 1.24 \times 10^{-11} \text{ per photon,} \qquad (4.33)$$

This value as shown on Fig. 19, is equivalent to the value for 3 MeV monoenergetic photons and is a factor of 6.7 lower than the damage coefficient for monoenergetic photons of 10 MeV as calculated in Table 6. The result is that 10 MeV linac radiation has a value of K_L just twice as large as the K_L for cobalt-60 photons. In section 3.3 it was indicated that a sterilizing dose of cobalt-60 requires over 10 times as many photons as 10 MeV linac radiation. The cobalt-60 damage, at the capsule surface, is therefore over 5 times the linac damage at the surface. On the other hand, an electronic component at the center of the capsule would see only 5 megarads in either case and be less damaged by cobalt-60 radiation than by a 10 MeV X-ray spectrum. The density of the capsule and the placement of the semiconductor units determine the optimum energy choice for minimizing electronics damage. It appears this choice would, except for extremely small capsules, be near 10 MeV. (Other considerations in sections 4.4 and 6.2 will reinforce this choice.)

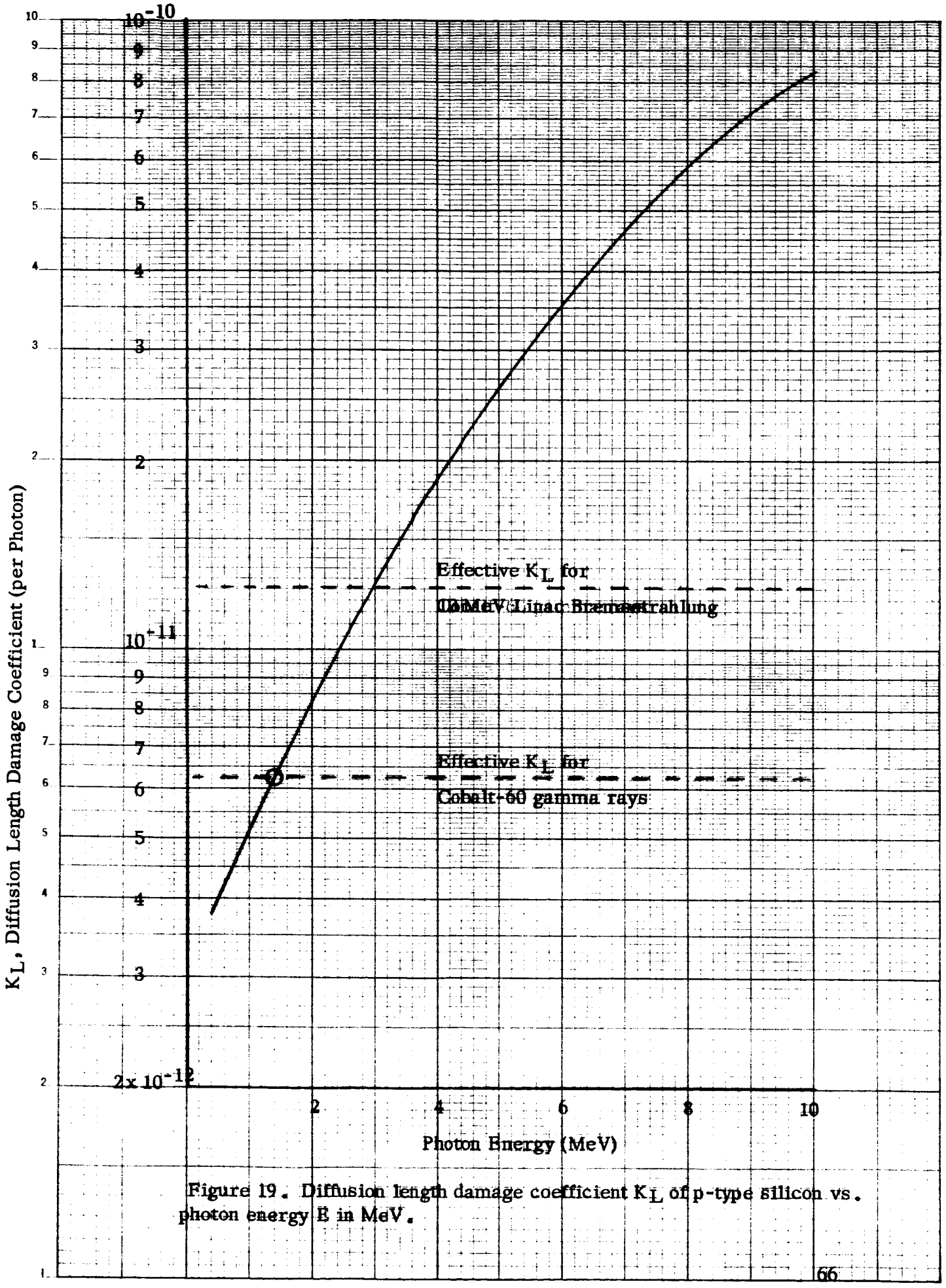

Figure 19. Diffusion length damage coefficient K_L of p-type silicon vs. photon energy E in MeV.

K_L can now be used to evaluate the gains α and β of any surface-passivated silicon transistor after linac sterilization, provided E is known. As an example, consider a 2N1613 transistor with β originally 50 and t equal to 1.7 nanoseconds. The gain β becomes, after exposure, 38. This is 76% of its original value. Circuit design using this transistor must be such as to tolerate this decrease in addition to the thermal and other effects normally anticipated.

A summary graph showing the expected degradation of transistor gain as a function of transistor location in a 3.5 foot radius spherical capsule is given in Figure 20 for irradiation by both Co-60 gammas and 10 MeV linac X-rays. It is seen that 2N1613 transistors will lose only 20% in gain if located near the surface of the capsule and radiation-sterilized with a 10 MeV linac. However, with cobalt-60 gammas, the gain degradation would be 40% for the surface location. Therefore high energy X-rays are preferable for sterilizing a large capsule.

A simple method for transistor selection can be generated on the basis of the analysis. We suppose that the operation of a particular circuit stage requires that the gain ratio β/β_o after irradiation is specified. Combining the above equations gives

$$\frac{1}{\beta} = \frac{1}{\beta_o} + tDK_L\varphi \tag{4.34a}$$

Solving for β/β_o, we have

$$\frac{\beta}{\beta_o} = \frac{1}{\beta_o tDK_L\varphi) + 1} \tag{4.35}$$

Figure 21 is a plot of the function β/β_o. Of the factors affecting β/β_o, the product, $(DK_L\varphi)$ is evaluated to be 3.8×10^6, for 8.3 megarads, and the others depend on the choice of transistor. Rapid evaluation of the radiation damage to a particular transistor is possible by the use of this graph. One notes, for example, that if the product gain times transit time ($\beta_o t$) is less than 30 nanoseconds, the

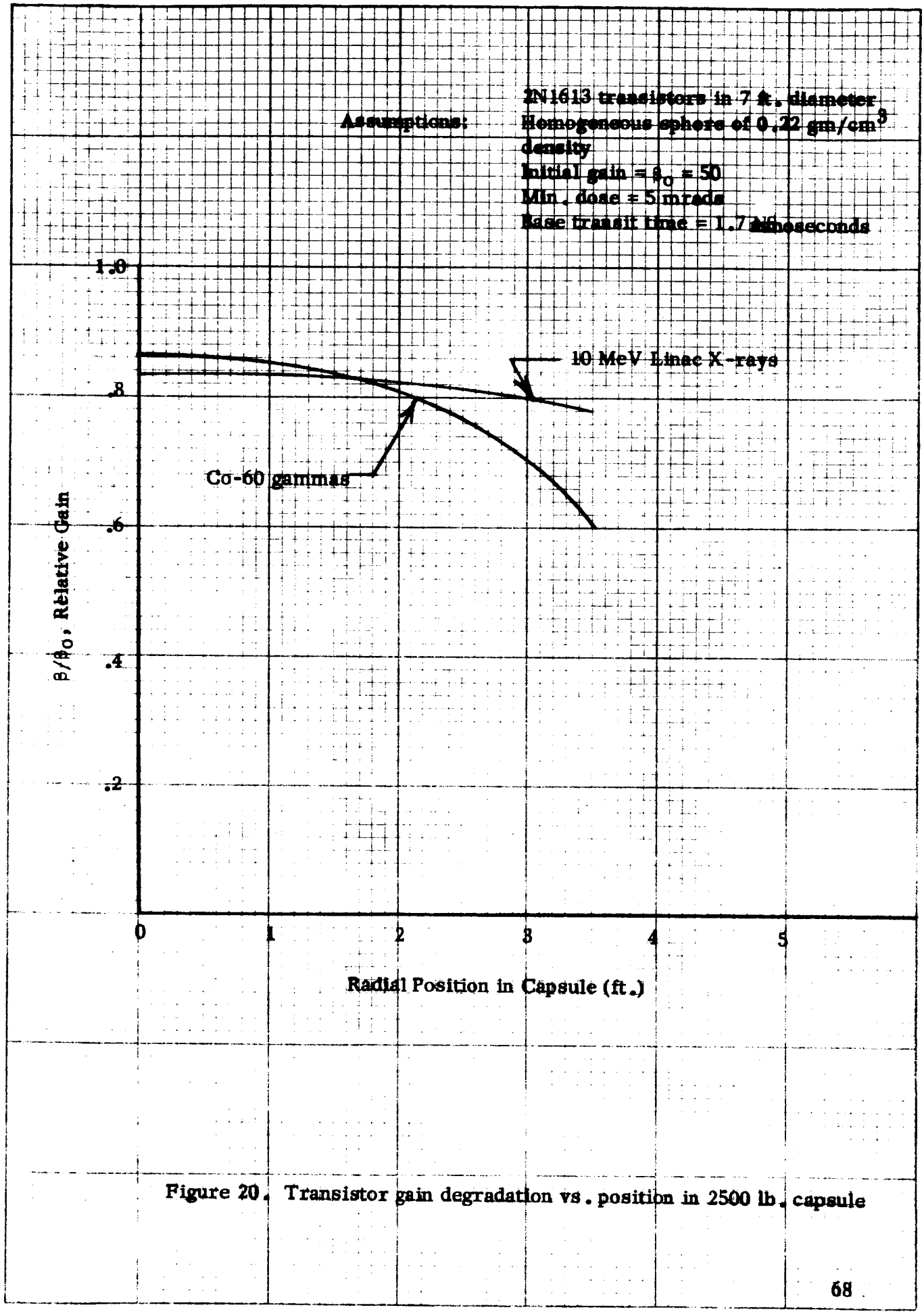

Figure 20. Transistor gain degradation vs. position in 2500 lb. capsule

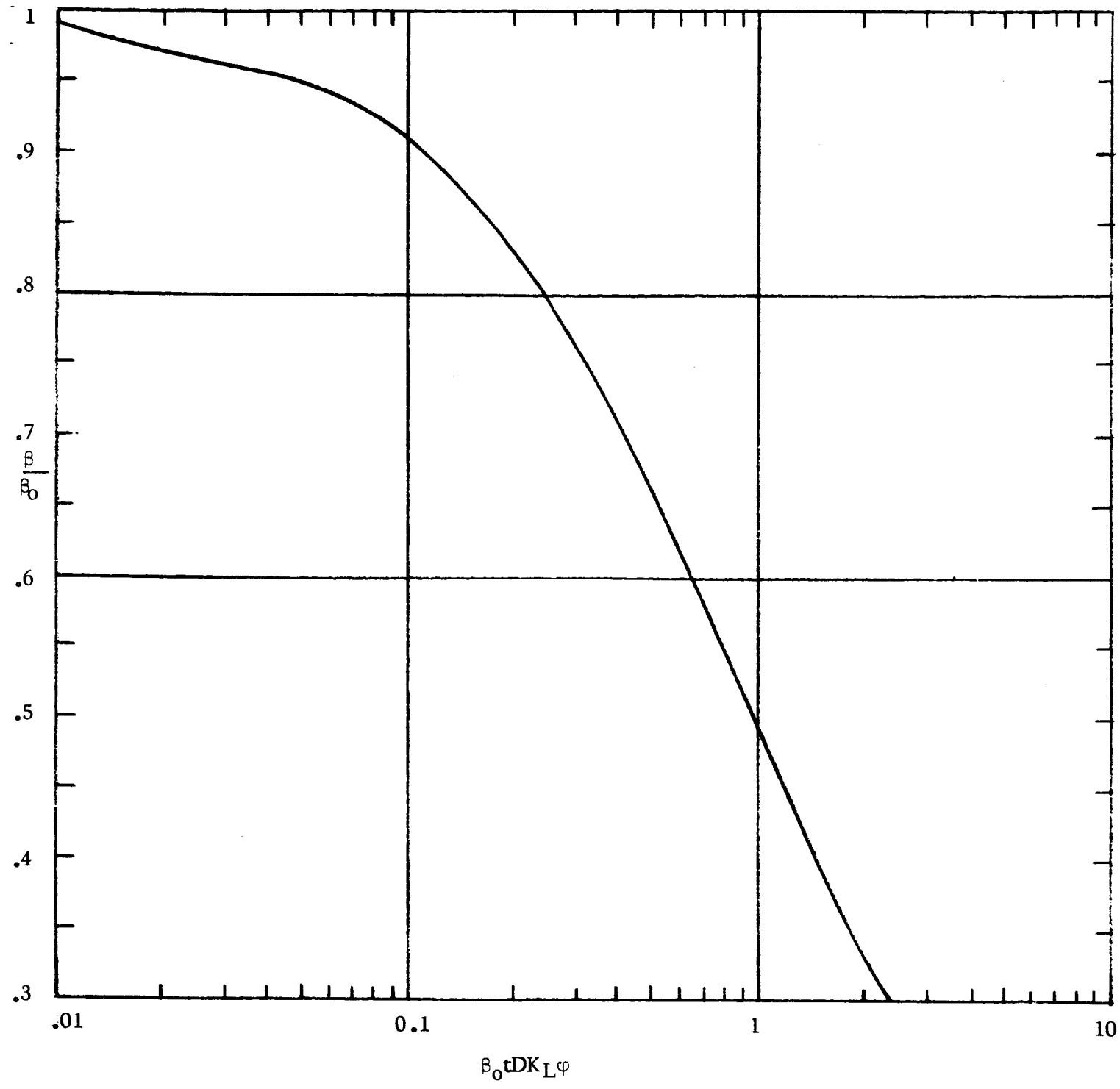

Figure 21. Ratio of gain β after radiation to gain β_0 before radiation as a function of transistor parameters and radiation parameters ($\beta_0 tDK_L\varphi$) defined in text.

transistor will lose less than 10% of its gain after radiation sterilization. For the transistors of Table 5, this limits the maximum gain allowed to 17.6-316, depending on t, if we neglect the first two units (2N697 and 2N3439) which are undoubtedly radiation sensitive, due to their large t.

In conclusion, it appears that the gain of most transistors (with surfaces stabilized against surface effects) does not drop significantly with an 8.3 megarad sterilizing dose of radiation from a 10 MeV linac. A change in β of up to 50% is sometimes expected during the lifetime of a transistor, and designs are customarily stabilized against this by proper use of feedback.

4.4 Surface Effects on Transistors

Most transistors which are presently available, show some effects of radiation on reverse current leakage and current gain at doses in the range of 0.1 to 1 megarad. These effects are very complex but are associated with radiation effects on the surface oxide layer which is generally used to passivate the transistor surface. At doses above one megarad, permanent damage to the gain usually is dominated by degradation of minority carrier lifetime in the base region, as discussed in section 4.3 above.

The most critical problem in radiation sterilization is the avoidance of excessive radiation surface effects on transistors. This problem is still in a very unsatisfactory state with respect to scientific understanding of the surface chemistry and physics involved. The surface effect phenomena are also the main source of unreliability in transistors which are not exposed to radiation.

The reliability of transistors in general is controlled primarily by phenomena at the surface of the semiconductor, particularly in the region where a p-n junction reaches the surface.

Early transistors with etched surfaces (e.g. mesa and alloy constructions) were not surface-protected and their characteristics were found to depend on surface contamination. Under irradiation, mesa transistors exhibited surface effects which were associated with gas ionization in the transistor can while the device had voltage applied. This effect could be essentially eliminated by evacuating the can and maintaining very clean surfaces.[26] However, the techniques for maintaining the required cleanliness and evacuating transistors have not been widely adopted by the industry. Instead, the use of dielectric insulating coatings has been widely adopted (e.g. planar, surmetic and annular transistors). These insulating coatings are usually thermally grown oxides. These passivating layers may still not prevent effects of the environment on and beyond the coating.

The complicated effects of radiation on transistors are believed to be due primarily to electrical charge deposition within such dielectric coatings. Therefore one can predict that radiation surface effects on transistors might be reduced or eliminated by

1. Eliminating the surface insulating layer,
2. Maintaining very clean silicon surfaces, and
3. Evacuating the can.

Whether this approach could be practically implemented by the semiconductor industry remains to be evaluated, because it would undoubtedly require drastic revision of present production practices. Also, it is not clear that all the transistor types required for a planetary capsule could be made using the mesa or alloy technique which is most applicable for implementing this suggested approach.

Despite the substantial improvement in stability attained by passivating the surface, the reliability of transistors in operating environments is still limited by these surface phenomena. This is particularly true for transistors which are to operate during or following irradiation. Therefore

it is recommended that a serious evaluation be made of the feasibility of eliminating radiation surface effects either by eliminating the surface oxide layers which are responsible for the effects, or improving the quality of the surface layer.

Screening test procedures for selecting transistors which are relatively immune to radiation surface effects have been developed by Bostian and Manning[27].

4.5 Microcircuits

The effects of radiation on the performance of microcircuits can be predicted in terms of the individual components in the microcircuit. Where transistors are present, the most significant effect to the circuit is via the damage mechanisms discussed in the previous sections; thus transistor gain and base transit time are the significant factors. Passive microcircuits, without transistors, are less sensitive to radiation, their sensitivity depending first on the semiconductors (diodes) present, and then on the remaining parts to a lesser degree. Thus, microcircuit damage is related to the mechanisms previously discussed, primarily the decrease in minority carrier lifetime τ.

When the circuit elements are indistinguishable, this analysis by parts is not possible. Nevertheless, the qualitative conclusion that the damage is no greater than that experienced by transistors still holds true.

With the rapid developments in microcircuit design and the random nature of the radiation effects studies reported, it would be meaningless to interpret experimental results here. In one test,[28] 80 microcircuits of 16 types were irradiated with 3 MeV electrons. Failure occurred after a fluence of 7×10^{14} to 2×10^{16} e/cm^2. This would indicate that these particular designs would withstand the 3×10^{13} e/cm^2 generated by an 8.3 megarad sterilization dose in the capsule (section 4.1). The provisions, however, to this conclusion are that the definition of failure used in the experiment be no less stringent than the criterion used in the capsule electronics and that the 3 MeV electrons can be equated to the electron spectrum generated by the sterilization.

Before capsule sterilization, it is therefore recommended that a statistically meaningful sample of each of the microcircuit designs to be used in the capsule be irradiated in an aluminum shell to the maximum sterilization dose, and the resultant damage measured to verify acceptable performance of the part of the capsule electronics.

4.6 Solar Cells

A simple calculation based on the damage coefficient K_L developed in section 4.3 allows us to estimate the reduction in maximum power output from a solar cell, should it be included in the sterilized capsule.

Consider a typical diffusion length L_o of 125 microns (1.25×10^{-2} cm) for n/p silicon cells with 1 ohm-cm base resistivity. The product $K_L\varphi$, from the results of the previous section, for a sterilization dose of 8.3 megarads, is 9.92×10^{4}. From the equation

$$\frac{1}{L^2} = \frac{1}{L_o^2} + K_L\varphi \qquad (4.36)$$

these figures indicate that the diffusion length after exposure is 24.6% of its original value. Reference 14, page 38, indicates that this decrease will result in the solar cell maximum power output after radiation being 80% of its initial value.

These calculations are based on a silicon resistivity of 1.3 ohm-centimeter. Currently, solar cells are being constructed of p-type base material of greater resistivity, up to 10 ohm-centimeters. As can be seen from Figure 17, this will decrease the damage coefficient K_L, and improve the resistance to radiation.

4.7 Polymeric Materials

Radiation damage to organic polymers is principally due to ionization. The radiation breaks covalent bonds; the subsequent recombination of the free radicals is random and leads either to smaller molecules (scission) or to a union of adjacent molecules (cross-linking). When scission predominates, the degradation of the polymer is more pronounced. This occurs in polymers such as Teflon, Kel-F, and polymethyl methacrylate. Cross-linking does not affect the material properties so strongly; this occurs in polystyrene, polyethylene, mylar, silicone, epoxy and natural rubber.

Cross-linking increases the viscosity of liquids, and the hardness and brittleness of solids. Scission, on the other hand, decreases viscosity and softens solids. Both of these modes of radiation damage can occur simultaneously in a given material, but one generally dominates. Hydrogen gas is also generated which may have deleterious effects.[29]

Evaluation of the acceptability of a polymeric material after irradiation to the sterilization dose depends on a number of considerations. The use to which the material is put will determine the acceptable level of degeneration of a given property. The level of degeneration, for the given dose, is dependent to some extent on such factors as the temperature and atmospheric pressure, the inclusion of trace impurities such as antirads, the level of cure of a rubber, and the molecular size of the polymer. Without delving into these considerations, only broad ranges can be given for the radiation damage in individual polymeric materials.

Two such lists are reproduced here as Table 7. The materials are listed with the dose that will give approximately a 25% loss in a salient property. These lists are intended for survey use; they indicate that, most likely, some materials are unacceptable, and some are quite safe.

Table 7a. Order of Magnitude of Dose (in Megarads) for Significant Damage[29]

Base Oils (damage is usually to viscosity or acidity)

5000	polyphenyls
1000	polyphenyl ethers, alkyl aromatics
100	polyglycols, mineral oils, methylphenyl silicones, aryl esters
50	silicates, disiloxanes, alkyl diesters
5	phosphates, alkyl silicones, olefins

Plastics (damage is usually to tensile strength)

4000	polystyrene, phenol formaldehyde filler
400	polyester (mineral filler)
100	polyvinyl chloride, polyethylene
50	urea formaldehyde
20	monochlorotrifluoroethylene, cellulose acetate
10	phenol formaldehyde
1	methyl methacrylate, polyester (unfilled), teflon (in air)

Elastomers (damage is usually to tensile strength)

90	polyethylene
25	polyisoprene (natural rubber)
10	styrene-butadiene
7	nitrile rubber
6	neoprene, silicone rubber
4	butyl rubber, fluoroelastomers
3	acrylate rubber
2	polysulfide

Table 7b. Order of Magnitude of Dose (in Megarads) For Significant Damage[30]

Polymers	
1000	polystyrene, aromatic silicone, polyethylene
100	epoxy, melamine-formaldehyde, urea-formaldehyde, mylar, natural rubber
10	silicone elastomers, polypropylene, polycarbonates, polyvinyl chlorides, nylons, synthetic rubbers
1	Kel-F, polyurethanes, polymethacrylates, polyacrylates

The extreme sensitivity of halogenated polymers is immediately apparent. Gaseous breakdown products, often corrosive, are liberated. Teflon and Kel-F both fluorocarbon polymers useful as dielectric and insulating materials, lose resistivity at the levels quoted, embrittle, and generate volatile fluorocarbons. In the case of Teflon, it has been established that the presence of oxygen is partly responsible for its extreme sensitivity. When the irradiation is carried out in a vacuum, the dose for significant damage to Teflon is about 10^6 rads. Lacking tabulations of thresholds for damage in vacuo or inert gas one may use the presented compilation to indicate conservative values of radiation sensitivity.

The part played by fillers or inert additives is to reduce the radiation effect. These fillers, such as carbon black, silica, glass fiber, cellulose fiber, talc, asbestos, and wood flour used to reinforce the polymer or merely to be an economical extender, absorb part of the dose and thereby reduce the radiation damage.[29]

The table indicates that the selection of rubber (elastomeric material) is significant for control of radiation damage effects. Butyl rubber is quite sensitive, natural rubber is rather resistant, and nitrile rubber falls somewhere between. The molecular rearrangements that lead to these widely different sensitivities to radiation are not the same. In natural rubber, the polymer molecules tend to cross link under radiation exposure. In butyl rubber, on the other hand, the polymer molecules tend to undergo chain scission, and a sticky gum results. This latter effect is more critical to the elastomeric properties, hence the greater sensitivity of butyl rubber. Figures 18 and 19[29] show the resultant changes in physical properties for butyl and natural rubber.

Nylon, also with a fairly low threshold, has a high ratio of chain scissions to cross linking when irradiated. This makes it more sensitive to radiation than is polyethylene, with respect to retention of strength and elongation.

In conclusion, those materials with threshold damage doses less than 10 megarads as given in Table 7 should be rejected from the capsule unless

tested to verify acceptable performance. Those materials with threshold damage doses of 10 megarads or greater would appear acceptable for consideration. However, when a material is described as having a threshold around 10^7 rads, discretion in its use or rejection is required, due to the fact that there is generally no sharp threshold for damage, but rather a gradual deterioration with accumulated dose. Many organic materials may be radiation hardened with additives or by slight changes in their fabrication.

Organic materials in the lander can include lubricants, insulation dielectrics, culture media, ablative heat shields, thermal insulations and battery cases and separators. Insulation dielectrics in use in the aerospace industry have been listed by their radiation damage threshold[30]; the ones with damage thresholds below 10 megarads are silicone rubber and polysulfide. In the same report, aerospace lubricant radiation damage is listed; all those tested survived over 10 megarads of cobalt-60 radiation. Of the lubricants, only silicones fail at less than 10 megarads.

The presence of organic materials in the Mars lander encourages the use of high photon energies for the sterilization. Organic damage is, in general, simply proportional to dose. The dose at all points in the lander should be no greater, as a result, than that acceptable for sterilization. This indicates the need for uniformity of dose, which is best obtained by using high photon energies. On the other hand, electronic semiconductor material damage was shown to be proportional to dose and to increase with photon energy. Should an electronic component specification be unable to tolerate the damage described in section 4.2, that damage could be reduced by lowering the photon energy from the 10 MeV cutoff, but at the expense of increasing damage to organic materials. Further study is needed to optimize the selection of photon energy, considering the specific semiconductor and polymer materials and components to be used.

5.0 Radiation Damage to Components Other than Transistors or Polymers

The Mars lander capsule is to be sterilized as a unit. During and after sterilization, it will be encapsulated in a sterilization canister to prevent reinfection. Since this canister is not to be opened until the spacecraft is outside the earth's atmosphere, there must be assurance that all components of the capsule safely retain their operational characteristics during the sterilization process, and will reliably perform their functions on Mars after a launch and approximately a nine month mission. In this reaction, we relate the radiation damage observations of Section 4 to the specific components and subsystems of a conceptual design of the Mars lander capsule.[31]

5.1 General Description of the Mars Landing Capsules

While the design of the Mars lander has not been finalized, it should not differ radically from present concepts. One proposed lander is fairly large, with dimensions and shape approximately as shown in Figure 22. The forward end of the capsule, when entering the Martian atmosphere, is to the left; this is covered, inside the sterilization canister, with a heat shield.

The sterilization canister is composed of two parts: the blunt-cone "base" and the disk-shaped "lid". These fit together with an airtight seal that must be broken at the time of separation. This canister, although only 30 mils thick, represents one-seventh of the total lander capsule weight, so that its design is critical. For example, heat sterilization calls for a gas-filled lander to insure good heat transfer during the baking process. The gas pressure will increase with heating, and the canister must either be built to withstand this pressure or must be valved to relieve it. With radiation sterilization, there is negligible pressure increase.

The entry shell is covered with a heat shield; chopped cork in a silicone binder has been suggested. The shell itself is of beryllium face sheets bonded to a stainless steel honeycomb core, and it has an explosive charge for separation.

Under the entry shell, supported by radial, aluminum beams, is the landed capsule and its parachute. The capsule, essentially an oblate spheroid in shape, will be of laminated fiberglass and honeycomb to a depth of about 15 inches to take the landing shock,an inch of bumper material, probably balsa wood, below this, and the capsule proper with its payload at the center of this shock-absorbing and distributing system.

The total assembly pictured in Figure 22 will weigh about 2500 lbs., but the landed capsule (including its fiberglass-honeycomb-balsa covering) weighs only 595 lbs. The densities of the capsule alone and of the total lander can be computed from these figures. Approximating either as an oblate spheroid,

$$V = (4/3)\,\pi a^2 b \qquad (5.1)$$

where V is the volume, a the semimajor axis, and b the semiminor axis. For the lander (a = 90 in., b = 40.5 in.), the volume is 794 cubic feet and the overall average density is 0.0505 grams/cm^3. For the capsule alone (a = 44 in., b = 27 in.), the volume is 127 cubic feet and the average density is 0.0754 gms/cm^3. Two centers of high density can be identified in the design; these are the rocket and the payload. Thus, four macroscopic regions of different densities can be determined, to give the density distribution shown in Figure 23.

Electronic assemblies are particularly vulnerable to radiation damage, as discussed in section 4.0-4.8. The attitude control system (ACS) electronics and gyros are alongside the rocket motor. The bulk of the electronics, however, are the internal payload inside the landed capsule and the external payload, outside the landed capsule but inside the entry shell. Thus, electronic assemblies can be pictured as being distributed throughout the lander.

Therefore, we have looked, in section 3.0-3.3, for the ratio of maximum/minimum dose, regardless of where they occur in the lander. The beam of radiation through the lander which cuts through the greatest mass is clearly that line which bisects Figure 23 horizontally. Adding homogenized

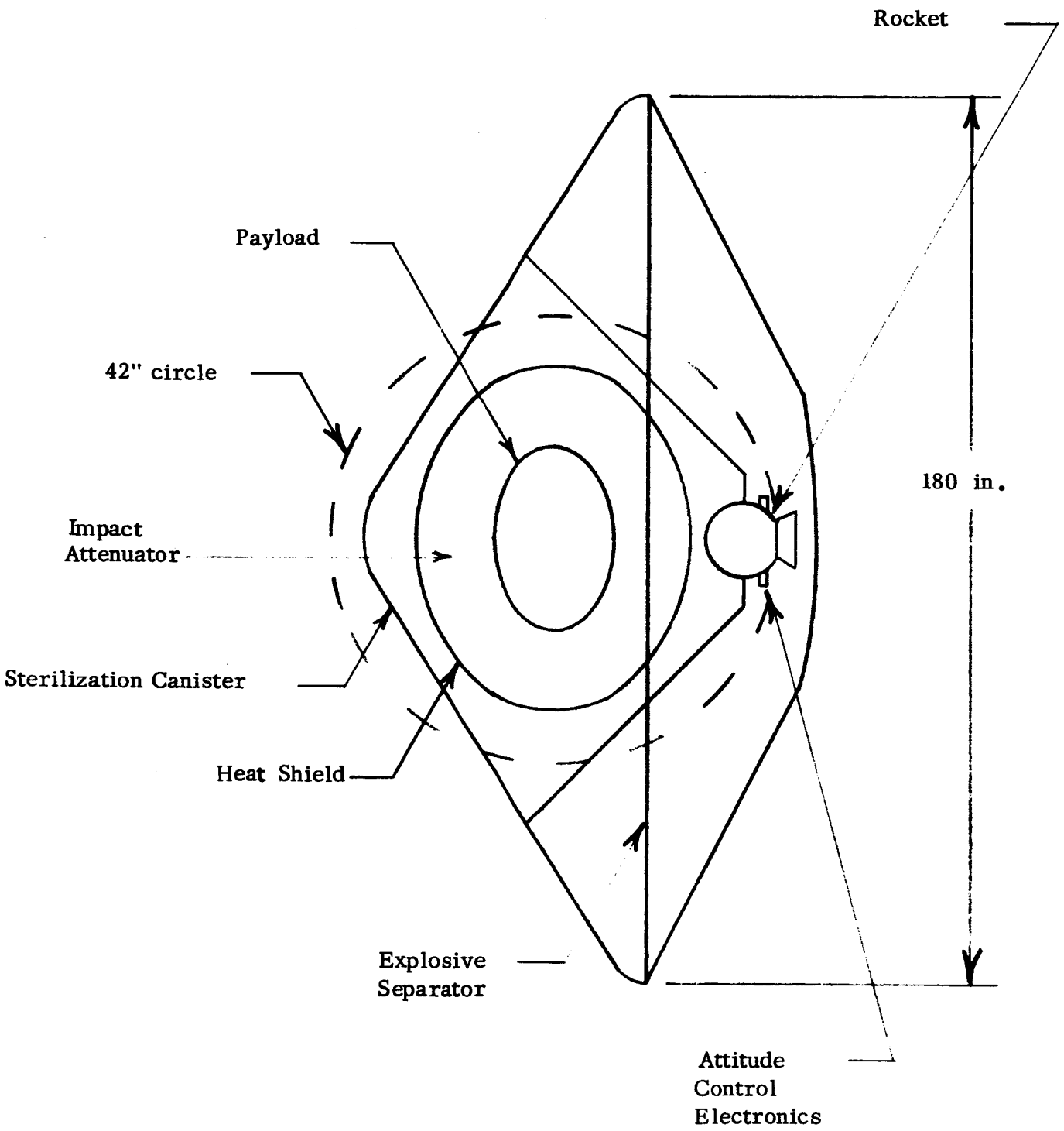

Figure 22. Design Concept of the Mars Lander[31]. The superimposed 42 in. radius sphere is for shielding approximations of section 3.

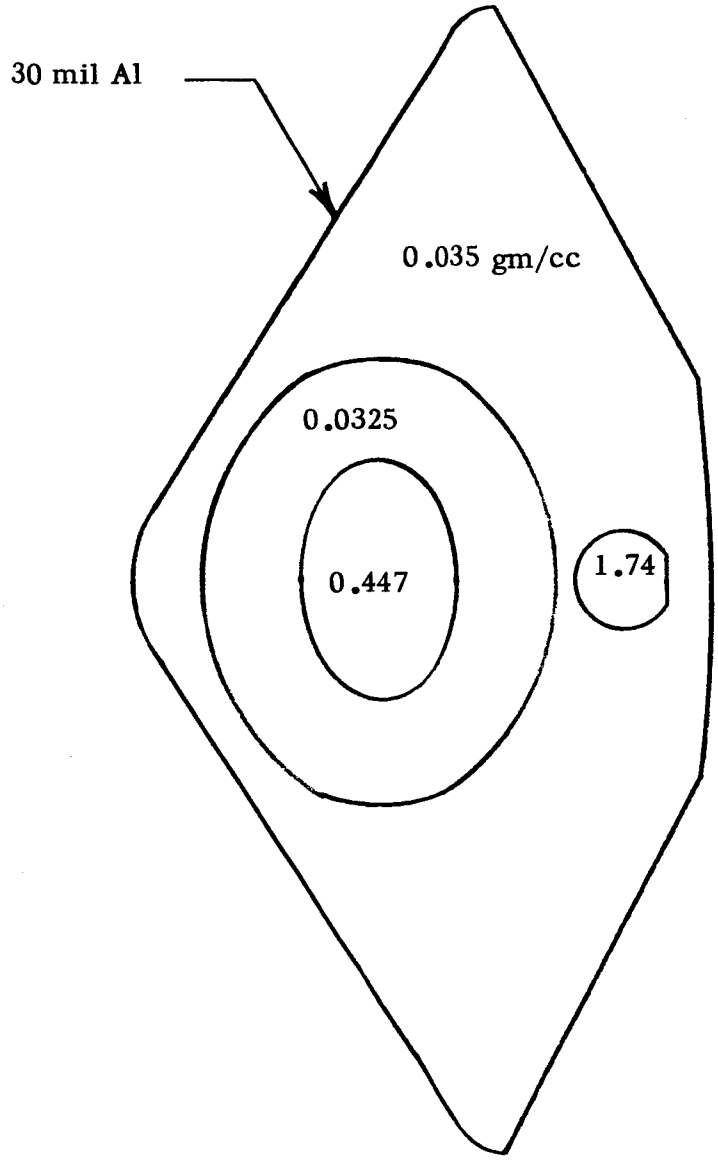

Figure 23. Density distribution, semi-homogenized, of the Mars Lander.

density-depths along this line gives a total thickness of 91 grams/cm^2. This figure was used to derive the maximum/minimum dose ratios for slab-type irradiations of the lander (section 3.1). Penetrations along lines other than this will involve smaller masses per unit area and smaller maximum/minimum dose ratios.

Another concept presently proposed[33] is depicted in Figure 24. This capsule weighs only 107 pounds, including a propulsion rocket. The sterilization canister alone weighs 50 lbs., the entry vehicle inside weighs 38.7 lbs. The diameter of this capsule is 30.5 inches. The approximate density of the capsule, assuming it to be a sphere of this diameter, is 0.186 grams/cm^3. With no impact attenuator, such as the 2500 lb. lander contained, this sphere is destroyed upon impact with the planet's surface, and is useful only for atmospheric measurements during its descent.

5.2 Radiation Sterilizability of Sub-Systems and Components

The sub-systems which are most sensitive to radiation damage are those employing transistors and those with organic polymers. These two classes of materials have been discussed in detail in sections 4.0-4.6. Other systems, to a lesser degree, are degraded by the sterilization dose, and are discussed in this section. Considerable detail for this survey was provided by a report of the radiation testing of SNAP components,[34] which were required to withstand 100 megarads of gamma radiation and a heavy dose of neutrons. The devices that qualify for this level of radiation should qualify for a lander that is to be irradiated with less than 10 megarads.

Optical Systems: Glasses

Glasses darken upon prolonged exposure to radiation. Color centers are produced by the displacement of atoms from their normal position in the crystal or glass matrix. Often, these centers exhibit luminescence as well as scattering light; the effect may be reduced by annealing near the α-β transition temperature[35].

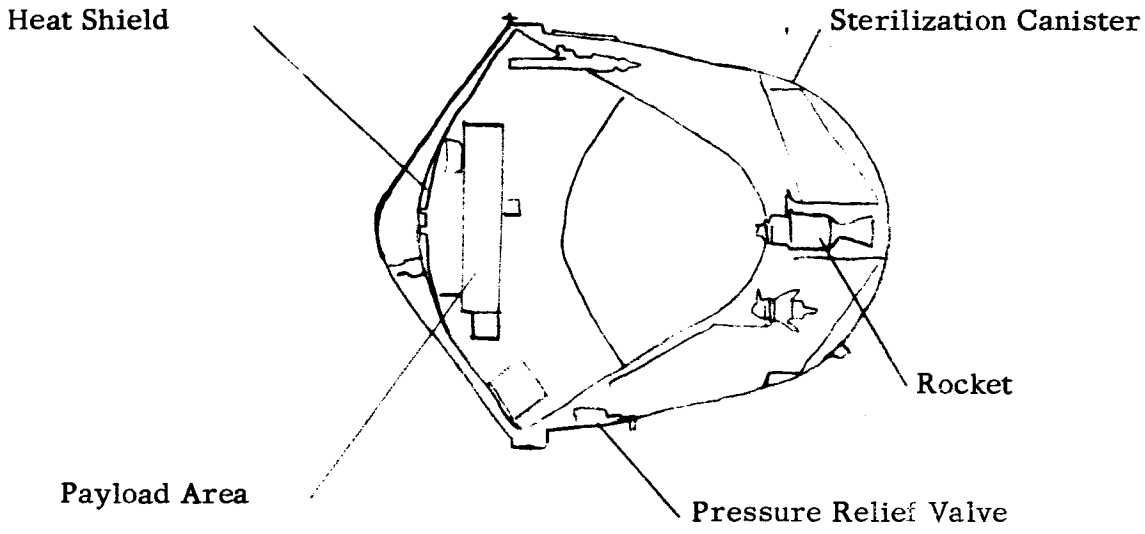

Figure 24. 100 lb. Proposed Mars Capsule (Ref. 33)

The optical transmission of glass degrades linearly with radiation dose. This degradation appears to be the major limiting factor for photomultiplier tubes and lamps, and is significant in lens-bearing systems and glass-protected solar cells. The glass selected has a strong influence on the rate of degradation; ordinary glass may be protected by the addition of cerium, for doses up to 10^8 rads.[35, 36] Table 8 presents experimental data to provide an indication of the relative merits of glasses.

Diodes

The following diodes are affected by less than 5% in their current and forward voltage parameters after an exposure to 100 megarads of cobalt-60 radiation. The manufacturer is given in parentheses: TI means Texas Instruments; GE means General Electric, H means Hoffman, D means Dickson, U means Unitrode; M means Motorola.

1N551 (TI); 1N1202 (GE); 1N914 (TI); UZ810 (U); and the Zener diodes 1N723 (H); 1N751A (IRC); 1N1590A (IRC); 1N1593A (D); 1N1601A (IRC); 1N1604A (IRC); 1N1604A (H); 1N2974B (H); 1N2498A (D); 1N2974B (D); 1N3042B (IRC); 1N3042B (D); 1N3330B (M); 1N3330B (D).

Power diodes are affected (principally by the neutron component) and were not used for SNAP systems. Neither were transistors. For the smaller, neutron-free dose discussed in this report, however, it was shown that transistor degradation is not severe. It is generally believed that semiconductor diodes are about 2 orders of magnitude less sensitive to radiation than are transistors.[38] Thus, it appears that diode degradation will not be severe after the sterilization dose.

Resistors

A variety of types of resistors are available for a wide range of circuit parameters. These include carbon, deposited carbon film, metal film, wire-wound, and ceramic. Of these, the most radiation resistant is the wire-wound

Table 8. Effects on Glass of 1.2 MeV Electron Irradiation to An Exposure of 2.7×10^{15} e/cm^2 (about 230 Megarads)(37)

Manufacturer	Material	Type	Thickness in.	Wide-band transmission loss, percent
	Plate glass	Soda lime	0.250	26*
Blue Ridge Glass Corp.	Feurex	heat-resistant borosilicate	0.250	25.2
Pittsburgh Plate Glass Co.	Solex	heat-absorbent glass	0.250	2.7
Corning Glass Works	Vycor	------	0.250	59*
Corning Glass Works	0211	micro-sheet	0.026	7.6
Corning Glass Works	7940	fused silica	0.125	0
Linde Co., Div. Union Carbide	Linde sapphire	sapphire	0.080	0
Dynasil Corp.	dynasil	optical grade	0.125	0
General Elec.	GE104	----	.0935	0.8
General Elec.	GE 105	----	.0935	30
General Elec.	GE 106	----	.0935	28.6

* These losses correspond to an exposure of 1.7×10^{15} electron/cm^2.

construction of metal, ceramic and epoxy. These are unaffected by SNAP radiation of 100 megarads. Metal film resistors are also unaffected provided that they are on ceramic bobbins rather than glass.

Of the other commonly used resistors, all exhibit mild-to-moderate damage after 10 megarads.[27]

Capacitors

A survey of the effects of radiation on capacitors of common construction types indicates[27] that mild-to-moderate damage can generally be expected with 10 megarads of exposure. Exceptions are glass and ceramic types, having no measurable effects, while electrolytic capacitors can exhibit severe damage.

Immediately after the sterilization, the capacitance of an electrolytic capacitor is typically at a minimum, from which it partially recovers with a time lapse on the order of days. In one test[40], tantalum electrolytic capacitors were submitted to 5.9 megarads of gamma radiation, plus neutrons, and the capacitance dropped an average of 9.7 percent. After 10 days, the capacitors had recovered to a value 4.7 percent below the initial value.

Dry-film Mylar capacitors with epoxy end seals are unaffected by SNAP radiation of 100 megarads and are to be preferred over oil-film Mylar capacitors.

Magnetic materials are not affected significantly by SNAP radiation of 100 megarads. Preferred insulation materials are fiberglass, Mylar, epoxy, and ML; these and a leadout wire insulation of irradiated polyolefin were unaffected by SNAP radiation.

Electromechanical Timers

Timers made by the Haydon Timer Co., Waterbury, Ct., were modified by replacing nylon and Teflon parts with phenolic, diallyl phthalate, epoxy-glass, and Mylar. The standard motor lubricant was used. The lead wire insulation

was irradiated polyolefin. SNAP radiation of 100 megarads did not affect the unit's switch timing beyond the tolerance of 2 percent.

Electromechanical Relays

Available radiation-hardened relays have no significant changes after SNAP irradiation. These include

Leach Relay: model M234-E2-112-6633

Leach Relay: model M254-A2-112-5634

G.V. Controls Relay: thermal time delay

Penn Keystone Ball Relay: AA7100-P.

Insulation and Potting Materials

Tests in SNAP radiation environments gave the following results for these insulating materials.

Unaffected were PRE-ML; ML (heavy) insulated wire; Poly (heavy) insulated wire; epoxy-glass board; epoxy-glass covered magnetic core, and diallyl phthalate.

Satisfactory were polyester webbing, nylon paper, and TRT insulated wire.

Mylar took a slight set after 100 megarads but was otherwise unaffected.

Potting materials tested were Stycast 1095, Sylgard 182, and Eccobond 182. These were found suitable for SNAP radiation.

A survey [27] of insulation materials concludes that the commonly-used inorganic insulations exhibit no effects or very mild effects after 10 megarads of X-radiation. Of the organic insulations commonly used, all have measurable damage at this dose level (although the above-mentioned tests showed the insulation properties of several organic materials are unaffected). Thus, inorganic insulations are preferable from a radiation damage viewpoint and organic insulations are to be used with caution.

Infrared Detectors

A survey of experimental results is reported in Ref. 39. Lead sulfide and lead telluride films lose 50% or more of their sensitivity to infrared after receiving 4 to 8 megarads, and hence are unsuitable for the present application. Indium antimonide cells, on the other hand, showed no change in performance with doses up to about 34 megarads. The discussion on glasses is pertinent to the lens portion of infrared detectors. Silicon, used extensively in infrared optics, develops an absorption band at 12 microns[30].

Mechanical Units

Because of the extreme lack of sensitivity of metals to photon radiation, mechanical units, such as latches, pin-pullers, erection devices, fans, and structural elements normally present no radiation damage problem. The lubricants on moving parts are more sensitive, and some care in their selection is required, as was indicated in Table 7 of section 4.6. The associated electric motors also can exhibit some radiation sensitivity. For the SNAP system, motor generators were hardened by an interlayer insulation of ML with fiberglass, a potting varnish of ML, leadout wiring insulation of irradiated polyolefin, and bonding of stator laminations with an epoxy cement.

Where plastics are used in mechanical units, the discussion of section 4.6 applies. The use of nylon gears, for example, is indicated in Table 7b to be marginal.

Explosives

A survey of radiation damage to explosives indicates that the sterilization dose can be tolerated without significant deterioration of explosive parameters. In particular[30], TNT, tetryl, and lead styphnate evolved gas during a 220 megarad gamma exposure but lost none of their explosive power, while lead azide and diazodinitrophenol lost some explosive power after 130 megarads. Of the explosives tested, only mercury fulminate lost its explosive power for a dose under 100 megarads. These doses, however, are an order of magnitude greater than the sterilization dose.

Silver-Zinc Storage Batteries

Experimental work has not reached the point where the radiation damage to silver-zinc batteries can be predicted.[41] It is known that silver electrodes immersed in a 40% KOH electrolyte are slightly soluble as the oxide. The damage mechanism appears to be a reduction of this oxide, and a noticeable precipitation of silver metal at doses as low as 10^5 rad. If the electrode is not charged during irradiation, the precipitate does not form.

Indications are that storage batteries will be found acceptable for radiation sterilization. Separator plates should be preferably a radiation-polymerized polyethylene, rather than Teflon; Lockheed has successfully irradiated a battery with this substitution to a gamma dosage of 120 megarads and obtained 409 ampere-hours of current at 23.4 volts after the exposure.

6.0 Feasibility of Radiation Sterilization

6.1 Mode of Irradiation: The Linac

As shown in Figure 3, the radiation from a linac target is highly anisotropic. Since it was concluded in section 2.3 that a linac, operated at 10 megavolts to produce bremsstrahlung photons of energies up to 10 MeV, appears to be the best source for radiation sterilization of a large capsule, as far as minimizing radiation damage is concerned, then it is necessary to evaluate the mode of operation of this source, to estimate the time needed for complete irradiation and to explore effects of varying the X-ray beam geometry relative to the capsule.

There are several parameters which affect the outcome of the irradiation. First, the choice of linac and linac target will fix the upper limit of dose rate obtainable. Considering the limitations of several presently-available accelerators, we base our preliminary calculations on a modest dose rate of 25,000 rads per minute, one meter in front of the target. (This is based on a radiography linac located at Hill Air Force Base.)

Space must be available to place a landing capsule in position, and access to this space must allow the entire bulk of the capsule to be removed without disassembly. These criteria will disqualify a large number of presently-available linear accelerator facilities (but not the one mentioned above).

For a model landing capsule, the concept described in section 5.1 can be used. This is approximately a disk, tapered at the rim, with a radius of 7.5 feet. Because of its thinness, it would seem reasonable that the X-ray beam be directed at its center, along its axis. The lander should be placed a distance away from the linac target that puts it far enough away so that the dose rate on its surface is not greatly nonuniform, yet close enough so that an appreciable fraction of the X-rays from the target are used in sterilizing the lander. The results of placing the lander 3 meters (9.8 ft) from the target are that the dose rate on the axis is 2800 r/min; and is

1300 r/min at an angle of 15^{o}

357 r/min at an angle of 30^{o}

235 r/min at an angle of 37.5^{o}.

This last dose rate is at the rim of the lander. At this rate, the rim would receive a sterilizing dose of 5 megarads in 355 hours, or 14.8 days of continual operation. Since the capsule is thin at its rim, the dose profile through interior, under the rim, will be flat, essentially constant at 5 megarads. The dose profile along the axis, on the other hand, will not be flat. Turning the lander over, halfway during the 14.8 day exposure will result in a dose profile as described in section 3.1, for the axis, with the minimum dose in the interior considerably above 5 megarads.

The placement of the lander for the results described above is sketched in Figure 25a. A way of providing a more equalized dose is sketched in Figure 25b. Here the beam from the linac target is directed at a point halfway between rim and axis and the capsule is spun slowly on its axis so that the point traces a circle.

Determining the surface dose rate for this second alternative can be accomplished by using the results of the first, concentric arrangement. The dose rate at a distance r from the beam axis drops off with r due to two effects. These are the anisotropy of the beam and the inverse square relation, the dropoff can be estimated for a plane three meters from the source and is given as Figure 26. For the spinning disk, each point traces out a circle of various distances from the beam axis. Thus the average surface dose rate at several representative points is

730 r/min at the center

823 r/min on the beam axis

307 r/min on the rim.

In this arrangement, the rim is still the region where the longest irradiation is necessary for a selected sterilization dose. For 5 megarads to the surface, the rim dose rate calls for 11.3 days of irradiation in this mode. During this time, the surface on the axis of the lander receives a dose of 13 megarads.

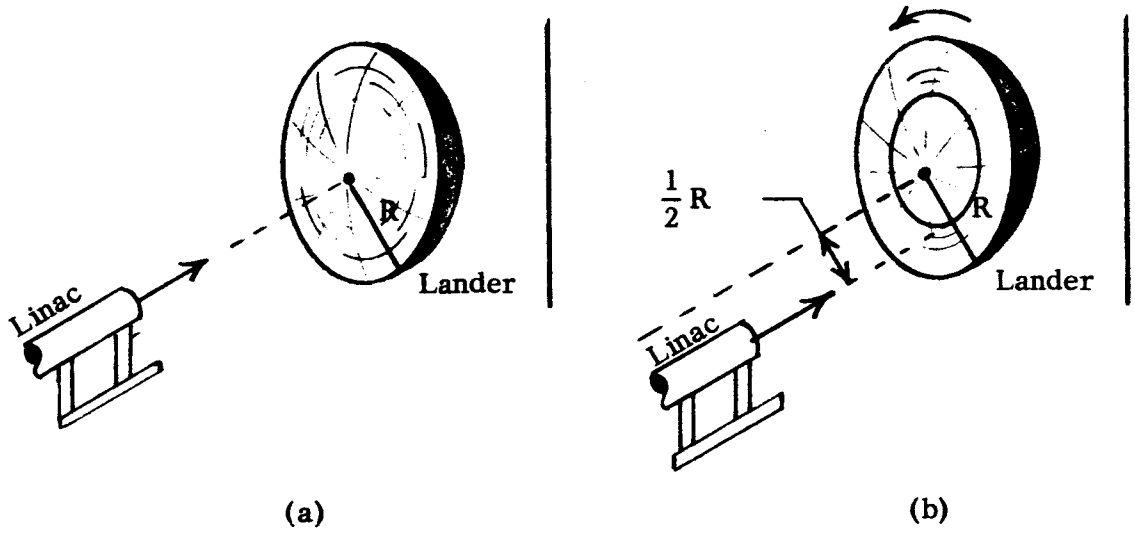

Figure 25. Alternative simple arrangements for radiation sterilization of the Mars lander by a 10 MeV linac.

For reasons given in section 3.1, the dose at any surface point on the lander must be greater than the selected dose for sterilization. Where the mass thickness (grams/cm^2) is small, the two values approach each other. As the lander will most probably have its weight concentrated along its axis, the surface dose on the axis will need to be larger than required farther away, as on the rim. For the axis of the model chosen for study in section 5.1, and the selected dose for sterilization of 5 megarads, it was shown in section 3.1 that a surface dose of 8.3 megarads is required at the axis of the lander. Along the rim, the mass thickness is vanishingly small (Fig. 23), so that 5 megarads seems sufficient.

Halfway during the irradiation, the lander must be reversed so that the opposite face of its disk is exposed to the irradiation. This increases the time required for a sterilizing dose, especially for those parts of the lander where the X-rays must penetrate the greatest mass thickness, i.e., the center.

The axis of the 2500 lb. lander capsule is 2.2 mean free paths thick (section 3.1). Thus, while one side is irradiated by the linac, the other is receiving an intensity that is a factor $e^{-2.2}$ less than this. The time-average dose rate on the surface, assuming the capsule is flipped over midway through the irradiation, is $1/2\,(1 + e^{-2.2})$, or 0.55 times the dose rate on the surface while facing the radiation source. The average dose rate at the capsule surface is therefore not 730 r/min (the instantaneous dose on the source-facing side), but 400 r/min.

For the interior (along the axis) to receive a minimum dose of 5 megarads, the surfaces, irradiated at a time-averaged dose rate of 400 r/min, must each accumulate a dose of 8.3 megarads. This occurs in 14.4 days (for the linac being considered) i.e., 7.2 days irradiation on each side. In this time, the surfaces of the rim accumulate 6.36 megarads.

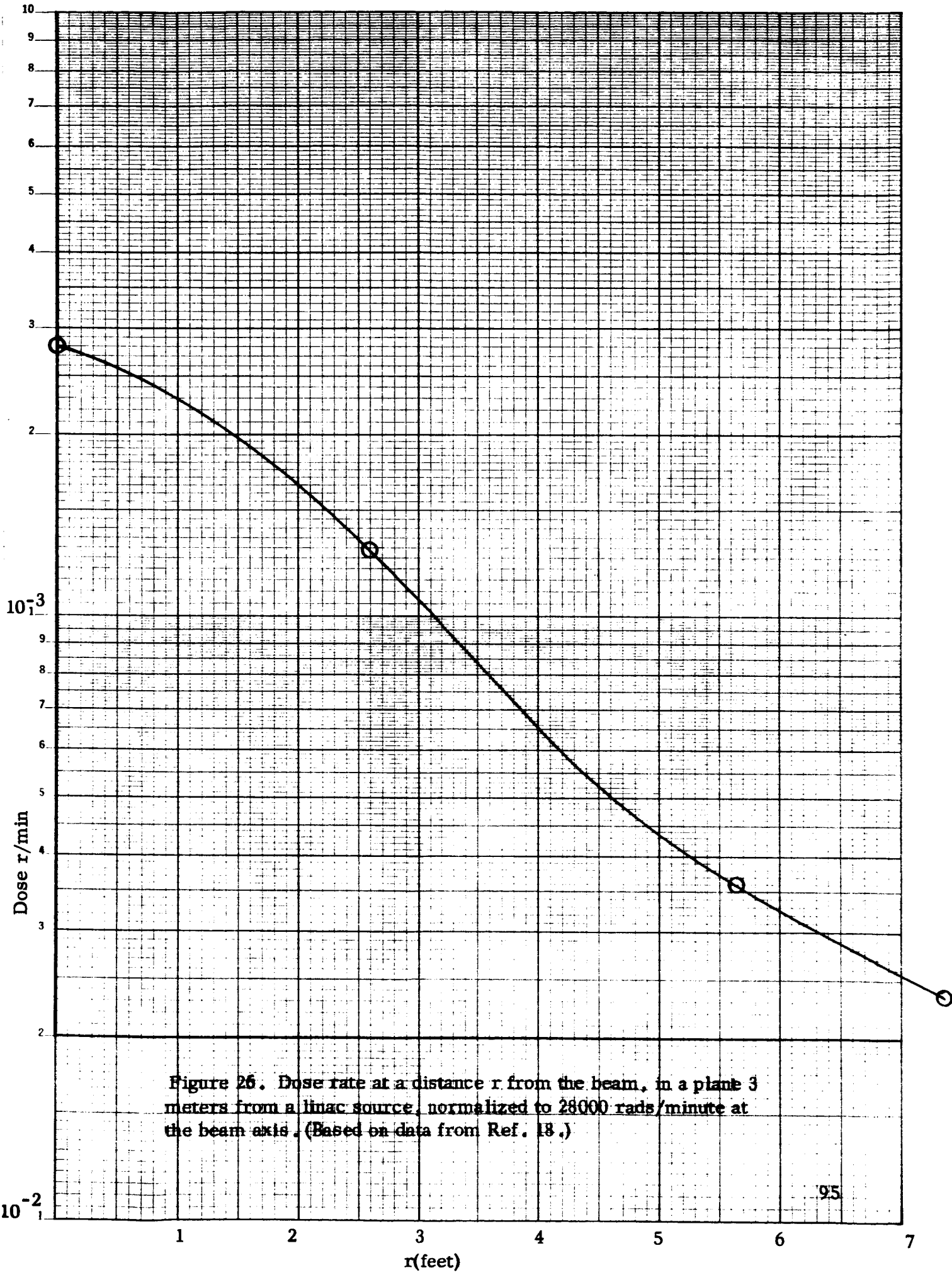

Figure 26. Dose rate at a distance r from the beam, in a plane 3 meters from a linac source, normalized to 28000 rads/minute at the beam axis. (Based on data from Ref. 18.)

These approximate calculations can be refined to derive (a) the most efficient arrangement of the X-ray beam relative to the lander and (b) a precise evaluation of the time required for sterilization. Alternatively, a dummy lander, with material arranged to duplicate the mass distribution in the time lander and with small dosimeters positioned in its interior, can be irradiated to verify the dose distribution after sterilization.

All these dose rates can now be scaled to the machine selected. This is done, in the next section, to obtain an estimate of the exposure time required.

6.2 Irradiation Time Versus Intensity

The approximate calculations of the previous section demonstrate a method for the calculation of irradiation time to sterilize the lander. The intensity of the linac X-ray radiation is a governing factor for the irradiation time; in section 6.1 an intensity of 25,000 rads/min was assumed 1 meter in front of the target.

The X-ray intensity is proportional to the product of the electron beam current and the efficiency of X-ray production, per electron striking the linac target. Of these, the first factor decreases and the second factor increases as one increases the accelerating potential for a given machine. An optimum accelerating potential T results from these considerations; it is[42]

$$T = 0.125 \left[(3T^* - 1) + \sqrt{(3T^* - 1)^2 + 8} \right] \qquad (6.1)$$

where T^* is the maximum voltage the machine is designed for. To design a machine that produces a maximum intensity of X-rays at 10 MeV, the design maximum voltage T^* should be 13.7 megavolts.

The choice of an accelerating potential of 10 megavolts was made in section 2.3 as a compromise between the advantage of high energies from a shielding viewpoint and the appearance of photonuclear effects above 10 MeV.

Aside from the shielding viewpoint, another advantage exists. This is that the X-ray production efficiency increases with energy, so that the most efficient -- and highest intensity -- machines produce X-rays at high energies. Thus, selecting an energy just below the photonuclear effect threshold insures minimum attenuation in the lander and maximum efficiency of bremsstrahlung production by the machine.

The calculations of section 6.1 were based on the capabilities of a linac at Hill Air Force Base. This is a mobile machine. A stationary machine could be constructed with an X-ray intensity (at 10 MeV) a factor of 8-10 greater; a linac being built for Argonne National Laboratory will be capable of generating around 165,000 r/min one meter from the target.[43] This intensity is a factor of 6.6 greater and use of this machine would reduce the capsule irradiation time from a total of 14.4 days to approximately 52.5 hours.

Operated at 10 MeV, a linac of beam power P in kilowatts gives a dose P times 3300 r/min, one meter in front of a suitable target. In section 6.1, a lander 3 meters from a target emitting 25,000 r/min at the one meter mark, required a total of 14.4 days for sterilization. This can be scaled to provide the time T, in days, for sterilization by a linac operating at power P, in kilowatts:

$$T\,(\text{days}) = \frac{110}{P} \qquad (6.2)$$

assuming, of course, continuous operation at the power P, and a lander of the size and shape considered here.

6.3 Mode of Irradiation: Cobalt-60

For a small capsule such as the one in Figure 24, the penetration capabilities of linac X-rays are not necessary and, as discussed in section 3.2, cobalt-60 radiation can be used without serious nonuniformity of dose.

Further, it was shown in section 4.3 that this radiation causes less degradation to transistors than do linac X-rays. Therefore a mode of irradiation with cobalt-60 is evaluated below.

Typical cobalt installations contain 10^5 to 10^6 curies of source.[44] The dose rate one foot from a source of 10^6 curies is a little over 1 megarad per hour, depending on source geometry and self-shielding at the particular facility.

With these figures, an approximate evaluation can be made of the time required for irradiation of a 100 lb. capsule. To allow for source radius and a capsule radius of 15.25 inches, the capsule is centered approximately 2 feet from the source center. A two-axis gimbal holds the capsule so that it may be rotated for a uniform surface dose. The dose deposition is given by Figure 8, when the irradiation is complete. The center of the capsule, however, has been continually irradiated at some constant dose rate D such that the product Dt equals 5 megarads, where t is the time of irradiation.

The dose rate D is given, in megarads per hour, as

$$D = \frac{1}{4} \exp(-0.5) \qquad (6.3)$$

where the factor 4 is the inverse-square attenuation by distance, and the exponential is the shielding of the center of the capsule. Thus, D is 0.15 megarads per hour, and the time t required for complete irradiation is 33.3 hours, if a source of 10^6 curies is used.

6.4 Estimated Facility Cost

The cost of sterilization of the Mars lander depends on the availability of facilities with adequate working space and adequate beam intensity. Should there be a sufficient number of capsules to be sterilized, and e.g.,

facilities not conveniently available, it may be necessary to construct a facility for the task. The high-powered Argonne National Laboratory machine mentioned above costs about $790,000, but some of this cost is associated with instrumentation for precise physics requirements. The Hill AFB machine costs about $250,000. Table 9 shows estimated costs for an entire linac facility to operate at 37 kilowatts (requiring about three days for a lander sterilization).

Table 9. Cost Estimate for a 10 MeV Linac Facility[45]

Capital	
Equipment	$400,000
Facility	$ 50,000
Operating	
2000 hours	$ 30,000
TOTAL	$480,000

The costs of a cobalt facility can be estimated by the equation

$$C = 0.75R^{0.38} + 0.55R \qquad (6.4)$$

where C is the cost, in millions of dollars, and R is the source rating in megacuries. The first term is based on an analysis[44] of costs of existing facilities; the second term represents the cost of the cobalt-60 source itself. Here, we are assuming 50 cents per curie and 5 cents per curie for post-reactor encapsulation. Future prices of cobalt-60 are expected to drop to the neighborhood of 30 cents per curie. However, based on eq. (6.4), the megacurie facility assumed in section 6.3 would cost 1.3 million dollars. A facility with 5×10^6 curies would cost $850,000 and perform sterilization of the 100 lb. capsule in 66.6 hours. From this preliminary

study, it appears that linac radiation is cheaper than cobalt-60 radiation at present, but it is realized that if an existing facility can be used, many factors not considered here will enter into the cost of renting rather than buying.

In conclusion, mention should be made of the NASA-owned Space Radiation Effects Laboratory. This facility, near the Langley Research Center (Hampton, Va.), includes an electron linear accelerator with an electron beam energy in the 3-12 MeV range, a beam current (averaged) up to 0.5 milliamperes, thus a beam power P up to 5 kilowatts. From equation 6.2, this indicates that sterilization of the large lander capsule would require 22 days in the beam. The target area, with removable concrete block walls, is adequate in size and readily accessible.

7.0 Comparison of Radiation and Heat Sterilization

7.1 Effects on Component and System Reliability

In general, the effects of radiation occur at the atomic or intra-crystalline level, whereas the effects of heat treatment occur at the inter-crystalline (macroscopic) level as well as within the material crystals due to atomic diffusion. In this respect, radiation does not affect some of the failure mechanisms which are temperature-dependent and which often lead to failures of typical electronic components. For example, the effect of a 10 megarad dose of radiation on the mechanical properties of a stressed soldered joint are expected to be negligible. However, a heat sterilization treatment may cause thermal stresses or change in physical properties of the joint which could lead to failure either during or following a heat sterilization exposure.

Radiation degradation of the minority carrier lifetime of silicon semiconductor devices is a "wear out" failure mechanism. In this regard, radiation is a preferable sterilizing medium, because its effects occur predictably during the sterilization and any further irradiation during a planetary mission is so small that it will contribute a negligible decrement of the wear out life. This is not the case with heat sterilization, because the heat exposure accelerates the same temperature-dependent failure mechanisms which control the wear-out life and which affect random failures during the mission environment.

There are several components which apparently will withstand radiation sterilization better than heat sterilization, although test data are needed for verification. One of the present critical problems is the development of heat-sterilizable silver-zinc batteries. In solving the problem, it has been found that radiation-treated battery separators are preferred. The plastic separators are typically pre-treated with 10 to 20

megarads of radiation. Therefore it appears that a terminal radiation sterilizing dose of 5 to 8 megarads may have a relatively small effect on the properties of the separator. However, tests are needed to determine the effects of irradiation while in contact with KOH solution in the battery.

Similarly, experiments are needed to determine whether liquid culture media which are not heat sterilizable can be satisfactorily sterilized by radiation.

7.2 Effects on Capsule Weight

The weight of a capsule which is to be heat-sterilized must be increased to provide for the internal gas pressure build-up in the bio-canister which would occur during heat sterilization. If vents were provided to relieve this pressure, the sterility assurance would be compromised. On the other hand, radiation sterilization would cause a negligible pressure increase in a bio-sealed capsule. Therefore, a potential weight saving or improved sterility assurance by avoidance of venting and re-fill plumbing is possible.

In addition to a possible weight saving on the bio-canister, if a liquid propellant retrorocket were used, it is probable that the weight increase for gas pressure buildup in the propellant tanks during irradiation would be less than for heat sterilization.

7.3 Effectiveness of Sterilization Treatment

There is rather limited research data on the effectiveness of radiation sterilization as compared to heat sterilization. Based on a personal communication from Dr. Carl Bruch of NASA Headquarters, it has been assumed in this study that a dose of 5 megarads would give the same destruction of microorganisms as a dry heat treatment[46] of 12 D values, namely a reduction in population by a factor of 10^{12}. The usual sterilization

dose for pharmaceuticals and hospital supplies is 1.8 to 2.5 megarads of ionizing radiation although 1.5 megarads are adequate to destroy the most resistant organism in a concentration sufficiently higher than normal contamination.[47] Also Trump[48] states that 1.3 megarads would attenuate an initial count of 10^7 spores (B. subtilis) per milliliter so the last organism would have one chance in 10^6 of surviving. (See Figure 27.) He states that "quite commonly, sterilization doses of 1 to 2 megarads are given to insure a completely adequate margin of dose against all possible uncertainties". On the other hand, Silverman at MIT has found survivors after larger exposures.[49] Proper selection of the dose of radiation must take into account the types of species which are likely to be present in a planetary landing capsule. Also the possible effect of spore environment and recovery medium on the survival probability should be investigated. Further research is clearly needed. At this time it can only be surmised that 5 megarads has at least as much effectiveness as the presently specified heat treatments which are predicted to yield a survival probability of 10^{-4} for B. subtilis var. Niger having an initial population of 10^8. In fact it appears probable that the dose of 5 megarads is conservatively high by a factor of about 5 which is equivalent to specifying a heat sterilization cycle five times longer than really necessary. It should be noted that each additional megarad reduces the probability of contamination by a factor of about 10^{10}, based on test data with B. subtilis.

7.4 Convenience and Compatibility with Capsule Assembly Procedures

The application of heat sterilization requires a large furnace and an exposure time of the order of 6 hours at 160°C to 336 hours (14 days) at 105°C. Radiation sterilization of a large capsule requires a large linear accelerator facility, properly shielded for safety, with an exposure time estimated to be 2 days to 14 days. Both radiation and heat sterilizing treatments can be performed within a completely bio-sealed assembly. If one

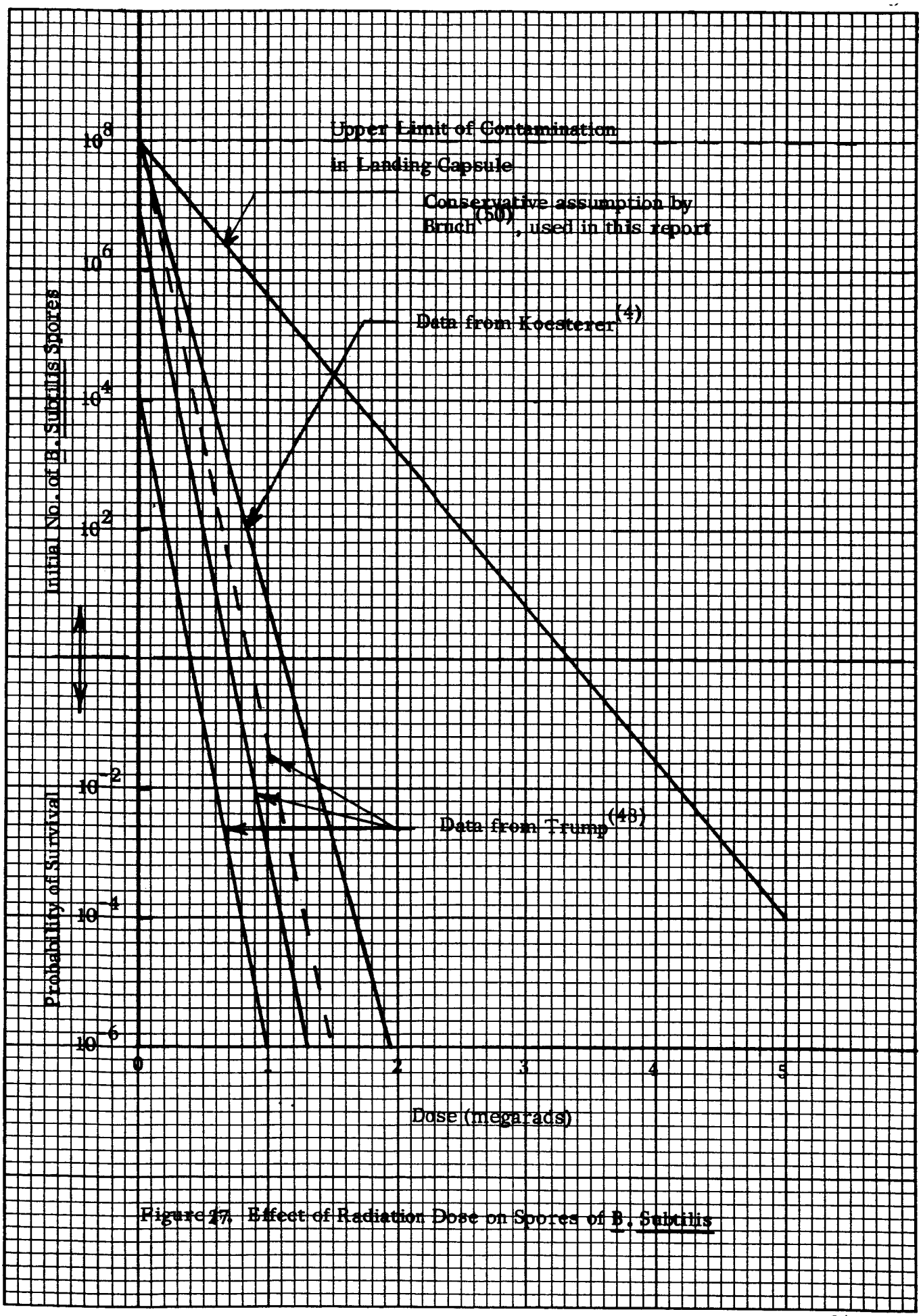

Figure 17. Effect of Radiation Dose on Spores of B. Subtilis

assumed the use of an assembly/sterilizer of the type studied by General Electric[50] in which sterilization would occur at the sub-assembly level in a sterile chamber, followed by sterile assembly, it would be necessary to provide radiation shielding protection of the assembly personnel. However, the use of several relatively small X-ray machines or Cobalt-60 irradiators as part of the facility appears feasible and should not be much more difficult than the use of a collection of small furnaces.

Because of the directional properties of linac X-rays, a machine could be placed external to the sterile assembly area. Sterilization could then be accomplished by bringing the X-ray beam through a bio-barrier to irradiate components, sub-systems, or a complete capsule within an assembly/ sterilizer facility. Personnel would be evacuated or properly shielded during machine operation.

7.5 Cost of Sterilization Equipment and Operation

As indicated in section 6.4, the cost of a 10 MeV linac X-ray facility is estimated to be $450,000. This is considerably greater than the cost of a furnace for heat sterilization. Also the operating costs will be higher.

7.6 Summary Comparison

In summary, it is concluded that there is no outstanding advantage or disadvantage of radiation as compared to heat with respect to effectiveness of sterilization, convenience in operation, or compatibility with capsule assembly procedures. A weight saving would be possible with radiation sterilization by avoiding the gas pressure buildup during heat sterilization. (Alternatively, sterility assurance would be improved by avoiding gas vents.) , Adapting an available linac facility to the task could reduce the radiation sterilization cost significantly. The potential advantage of radiation, which remains to be demonstrated, is that it may not appreciably affect the failure mechanisms which are most likely to cause

part failure during the mission environment. Therefore, there is a definite possibility that a capsule, properly designed for radiation sterilization, could achieve a higher mission reliability than a heat sterilized capsule.

8.0 Conclusions

1. Radiation can be used to sterilize landing capsules and is not incompatible with mission reliability if components are selected to minimize radiation effects, particularly surface effects on transistors.

2. The most suitable radiation sources for sterilizing spacecraft are radioisotopes, notably cobalt-60, or high energy X-ray machines. cobalt-60 gamma rays are suitable for capsule diameters less than about 3 feet and for sterilization of piece-parts. For a 2500 lb. Voyager landing capsule, bremsstrahlung from a 3 to 10 MeV electron accelerator target should be used.

3. The most radiation-sensitive components required in a planetary landing capsule are the transistors. If transistors are carefully selected for stability against surface effects, they can be radiation sterilized by doses of X-rays in the range of 5 to 10 megarads and not lose more than about 10% of their current gain due to degradation of minority carrier lifetime.

4. No experimental data were found on the long-life reliability of electronic parts after being subjected to megarad doses of ionizing radiation. However, for the most critical components, transistors, it is concluded that long-life reliability after irradiation will be controlled by the normal thermal and mechanical failure mechanisms, notably surface degradation. Degradation effects induced by radiation appear immediately, as discussed in section 4, and do not appear to affect the subsequent rate of part deterioration. Transistors should undergo screening tests under both radiation and bias voltage in order to select specific parts and to predict their response to the radiation sterilization dose. Circuit design must tolerate the expected change in performance parameters.

5. The use of radiation sterilization is feasible and has no major disadvantages compared to heat sterilization except for cost. The potential major advantage of radiation sterilization is that the failure mechanisms

activated by the radiation are of a different type from those acting during a flight mission. Therefore the wear-out life of parts in a mission environment should be relatively unaffected by the radiation sterilization treatment and mission reliability should be improved. Also sterility assurance may be improved by avoiding the necessity for venting and refilling with gas, as is usually considered for a heat-sterilized capsule. Alternatively, weight may be saved by avoiding the necessity to design the bio-canister to hold the gas pressure built up during heat sterilization.

6. Radiation damage to components other than transistors can be reduced to an acceptable level by avoiding certain sensitive materials. These include Teflon and other halogen-bearing organic polymers, unfilled polyesters, methyl methacrylate, polymethacrylates, polyacrylates, polyurethane, certain base oils and elastomers (Table 7), lead sulfide and lead telluride sensors, mercury fulminate, some electrolytic capacitors, and some types of radiation sensitive glass.

9.0 Recommendations

1. A study should be directed to an evaluation of the radiation dose, as a function of photon energy, which is required to meet the NASA planetary quarantine criterion. It is expected that dose considerably below 5 megarads will prove adequate. The effects of dose rate and of ambient environment during irradiation should be included in this study.

2. The analysis of the dose distribution in a capsule should be extended with the aid of a more detailed consideration of the capsule geometry, in order to examine more closely the effects of non-homogeneity and to recommend the optimum source arrangement for the sterilization procedure, as well as the preferred photon energy spectrum.

3. The possible synergistic effects of combined radiation and heat sterilization should be explored. This study should include considerations of the heat annealing of radiation-induced damage in semiconductor materials as well as the effects on microorganism destruction.

4. Experimental verification of the predicted high energy bremsstrahlung damage to transistors (section 4.3) should be undertaken. An experimental program to evaluate candidate transistors and semiconductor components for the Mars capsules should be conducted, for the dose levels of 1 to 10 megarads and photon energies of 1 to 10 MeV, which are of interest.

5. Since it appears that some components are more sensitive to radiation damage while others are more sensitive to heat damage, the possibility of component sterilization by a selected mode (radiation or heat) is attractive. A third mode of sterilization -- heat plus radiation -- mentioned above is also possible. The merits of this approach deserve attention.

6. Radiation facilities of the type discussed (electron linear accelerators and cobalt-60 cells) should be investigated as to their availability, costs and suitability for a program of capsule sterilization.

7. An investigation should be made of the feasibility of reducing or eliminating radiation surface effects on transistors by eliminating the surface oxide layers which are presently relied on for passivation but which are primarily responsible for the radiation surface effects. Practical implementation would require evacuation of transistor cans to avoid gas ionization effects, as well as very careful control of surface contamination. The alternate approach which is presently being pursued is to improve the purity and quality of the passivating layer. Radiation testing should be conducted on transistors which are surface-passivated with silicon nitride.

8. Experiments should be performed to determine whether certain critical components like batteries and culture media, which are damaged by heat sterilization, can be satisfactorily sterilized by radiation.

10.0 References

1. Katz, L., Penfold, A.S. "Range-Energy Relation for Electrons and the Determination of Beta-Ray End Point Enzymes", Rev. Mod. Phys. 24, 28(1957).
2. Kock, H.W., Motz, J.W., "Bremsstrahlung Cross-Section Formulas", Rev. Mod. Phys. 31, 920(1959).
3. Katz, L. et. al., "The Photoneutron and Photoproton Cross Sections of Silicon and Magnesium", Can. J. Phys., 32(9/54).
4. Lockheed-Georgia Co., "Georgia Nuclear Laboratories Facility Capabilities", (10/64).
5. Bly, J.H., Burrill, E.A., "High-Energy Radiography in the 6- to 30-MeV Range", Symp. on Nondestructive Testing in the Missile Industry, ASTM Spec. Pub. No. 278 (1959).
6. Evans, R.D., "The Atomic Nucleus". McGraw-Hill (1955).
7. National Bureau of Standards, "Shielding for High-Energy Electron Accelerator Installations", NBS Handbook 97 (After Kirn, J.S., Kennedy, R.J. in Nucleonics 6/64).
8. Crawford, J.G., Zanks, J.F., "The Assembly/Sterilizer - A Facility for the Sterilization and Assembly of Spacecraft", AIAA/AAS Stepping Stones to Mars Meeting, Proceedings, March 28, 1966.
9. Taylor, J.J., "Application of Gamma Ray Buildup Data to Shield Design", WAPD-RM-217 (1/54).
10. Price, B.T., Horton, C.C., and Spinney, K.T., "Radiation Shielding", Pergamon Press (1957).
11. Frank, M., Taulbee, C.D., and Chambers, H.G., "Influence of Operating Conditions on Radiation Damage to Transistor Gain", ASTM Spec. Pub. No. 384 (1964).
12. MacKay, J.W., Klontz, E.E., "Low Temperature Irradiation Semiconductors", Symp. on Phys. of Semiconductors, Paris, 1964. Academic Press (1965).

13. Wertheim, G.K., "Temperature-Dependent Defect Production in Bombardment of Semiconductors", Phys. Rev. 115, No. 3 (8/59).

14. Cooley, W.C., Janda, R.J., "Handbook of Space Radiation Effects on Solar Cell Power Systems", NASA SP-3003 (1963).

15. Anon., "The Energy Dependence of Electron Damage in Silicon", TRW Space Tech. Lab. (9/64).

16. Frank, M., Taulbee, C.D., and Chambers, H.G., "Influence of Operating Conditions on Radiation Damage to Transistor Gain", ASTM Spec. Pub. No. 384 (1964).

17. Sonder, E., Templeton, L.C., "Gamma Irradiation of Silicon", J. Appl. Phys. 31, No. 7 (7/60) and 36 No. 6 (6/65).

18. Messenger, G.C., "Displacement Damage in Transistors", IEEE Trans. on Nuc. Sci., NS-12, No. 2 (4/65).

19. Donaldson, B.J., "General Problems Associated with Electronic System Operation in a Space Environment", IEEE Conf. on Nuc. and Space Radiation Effects (7/65).

20. Flicker, H., Loferski, J.J., and Scott-Monck, J., "Radiation Defect Introduction Rates in n- and p-Type Silicon in the Vicinity of the Radiation Damage Threshold", Phys. Rev. 128, No. 6 (12/62).

21. Brown, R.R., "Proton and Electron Permanent Damage in Silicon Semiconductor Devices", ASTM Spec. Pub. No. 384 (1964).

22. Jet Propulsion Laboratory, "Preferred Parts List: Reliable Electronic Components", JPL Spec. ZPP-2061-PPL-G (7/65).

23. Moll, J.C., Ross, I.M., "The Dependence of Transistor Parameters on the Distribution of Base Layer Resistivity", Proc. IRE, 44, (1/56).

24. Frank, M., Larin, F., "Effect of Operating Conditions and Transistor Parameters on Gain Degradation", IEEE Trans. on Nuc. Sci., Vol. NS-12, No. 5 (10/65).

25. Brucker, G., Denneky, W., and Holmes-Siedle, A., "High Energy Radiation Damage in Silicon Transistors", IEEE Trans. on Nuc. Sci., Vol. NS-12, No. 5 (10/65).

26. Peck, D.S., Blair, R.R., Brown, W.L., and Smits, F.M., "Surface Effects of Radiation on Transistors", Symp. on Protection Against Radiation Hazards in Space, TID-7652, U.S.A.E.C. (11/62).

27. Bostian, C.G., Manning, E.G., "The Selection of Transistors for Use in Ionizing Radiation Fields", IEEE Trans. on Nuc. Sci. (2/65).

28. Battelle Mem. Inst., quoted in "Radiation Effects State-of-the-Art", REIC Report No. 38, Radiation Effects Information Center, (6/65).

29. Bolt, R.O., Carroll, J.G., "Radiation Effects on Organic Materials", Academic Press (1963).

30. Rittenhouse, J.B., Surgletary, J.B., "Space Materials Handbook", NASA SP-3025, 2nd ed. (1964) and suppl. 1 (1966).

31. Avco. Corp., "Comparative Studies of Conceptual Design and Qualification Procedures for a Mars Probe/Lander", RAD-TR-65-29 (10/65).

32. Exotech, Inc., "Definition of Requirements for Advanced Sterilizable Components for Planetary Spacecraft", TR-011 (9/65).

33. Botan, E., et al, "Biological Burden Estimation of Mars Probes and Capsules and a Method of Burden Control", Avco. Corp., (3/66).

34. Burnett, J.R., "Radiation Hardening of an Ion Propulsion System for Snapshot", EOS Report 5370-RT (10/65).

35. Levy, P.W., "Radiation Effects in Glass and Other Materials. Highlights of the 1962 Conference", Phys. Today (9/62).

36. Kreidl, N.J., Hensler, J.R., "Irradiation Damage to Glass", NYO-3780, Bausch and Lomb (11/54).

37. Haynes, G.A., Miller, W.E., "Effects of 1.2 and 0.30 MeV Electrons on the Optical Transmission Properties of Several Transparent Materials", NASA TN D-2620 (3/65).

38. Holmes-Siedle, A.G., "Space Ratiation - Its Influence on Satellite Design", PE-239, Astro-Electronics Div., R.C.A. (1965).

39. Lehr, S.N., Lartire, L.J., and Tronolone, V.J., "Equipment Design Considerations for Space Environment" (2/62).

40. MacMillan, W.D., Howell, D., "The Effect of Reactor Radiation on the Electrical Properties of Electronic Components", Part 4, "Capacitors and Magnetic Cores", Convair, Fort Worth, Texas, NARF-58-6T, MR-N-185, AF 33(600)-32054 (January 23, 1958).

41. Argue, G.R., Recht, H.L., and McCallum, W.A., "Radiation Effects on Silver and Zinc Battery Electrodes. Interim Report, April 1965 to July 1965", AI-65-158 (8/65).

42. Barrett, M.J., "Shielding of Bremsstrahlung from an Electron Accelerator Target", Trans. Am. Nuc. Soc., 8, No. 2 (11/65).

43. Bly, J.H., Applied Radiation Corp. Private communication (3/66).

44. Kukacka, L.E., Manowitz, B., "Estimating Costs for Gamma-Radiation Sprocessing", Nucleonics (1/65).

45. Ketchum, H.W., Osburn, J.W., Jr., and Deitch, J., "Current Status and Commercial Prospects for Radiation Preservation of Food", TID-21431 (1/65).

46. Bruch, Carl, NASA Headquarters, Personal communication.

47. Artandi, C., Van Winkle, W.W., "Sterilization of Pharmaceuticals and Hospital Supplies by Ionizing Radiation", Report from Ethicon, Inc. Somerville, N.J.

48. Trump, J.G., "High Energy Electrons for the Sterilization of Surgical Materials", Sterilization of Surgical Materials Symposium, April 11-13, 1961.

49. Silverman, Paper on radiation sterilization presented at AIBS Meeting, Atlantic City, N.J., 1965.

50. Crawford and Zanks, "The Assembly/Sterilizer - A Facility for the Sterilization and Assembly of Spacecraft", Proc. of AIAA/AAS Stepping Stones to Mars Meeting, Baltimore, Md. March 28-30, 1966.

51. Vette, J.I., "The Space Radiation Environment", IEEE Trans. on Nuc. Sci., NS-12, No. 5, (10/65).

52. Yucker, W.R., Lilley, J.R., "Space Radiation Shielding Analysis by Program Charge", Douglas Paper No. 3415 (6/65).

53. Evans, R.D., "Principles for the Calculation of Radiation Dose Rates in Space Vehicles", Arthur D. Little, Inc. (7/61).

54. Wyatt, M.E., van Lint, V.A.J., "Correlation of Displacement Damage Produced by Electrons and Protons", GA-6703 (9/65).

55. Lockheed-Georgia Co., "Georgia Nuclear Laboratories Facility Capabilities", (10/64).

56. Argone National Laboratory, "Reactor Physics Constants", ANL-5800.

57. Steinberg, M.A., Gaumer, R.E., "Research in Space Materials", IAS Paper No. 62-172 (6/62).

APPENDIX A

Evaluation of Protons and Neutrons as Sterilizing Radiations

A-1 Proton Radiation

To penetrate at all deeply into a capsule, a proton beam must have considerable energy. Below 1 MeV, a proton penetrates less than a millimeter of aluminum. Hence, protons must be accelerated to higher kinetic energies if they are to be useable in capsule sterilization.

Protons are routinely accelerated to MeV energies in existing proton accelerators.[5] Using a 3-stage tandem Van deGraaff electrostatic machine, proton energies up to 30 MeV can be attained. Higher currents at these upper energies can be obtained with a proton linac, and the highest energy that has been achieved (at the University of Minnesota) by such a machine is 70 MeV. Larger machines generate higher energies: the synchrocyclotron accelerates protons to 700 MeV, and the proton synchrotron goes higher. Of these last machines, the huge Cosmotron at Brookhaven National Laboratory can deliver 12 pulses per minute, with 10^{11} protons per pulse, with proton energy in the BeV range. While it may not be practical or economical to sterilize the Mars lander with one of these machines, the point is that a wide range of proton energies is available.

As well, interplanetary space contains a radiation environment which occasionally includes sporadic bursts of high energy protons emanating from spots on the sun and known as "solar flares". These protons, whose energy spectrum can often be fitted by an inverse power (of the form E^{-x}), characteristically have energies of 10 to 100 MeV and higher, thereby suggesting that an evaluation should be made of their possible sterilizing effect.

The nature and statistics of these solar flares have been the subject of considerable study.[51] Roughly, one flare can be anticipated to occur during a six month journey of the spacecraft from Earth to Mars.* Various calculations have been made of the dose distribution with depth into aluminum (the usual spacecraft material) as a result of a solar flare.[52][53] There is a strong decrease in dose with depth, as seen in Figure 2 for one calculation. Depending on the flare magnitude, the exposed surface of the spacecraft might be sterilized, but it is very unlikely that the interior would be. Further, unless the spacecraft is rotating during the flare, only one side may be exposed. Therefore solar flare protons cannot be depended on for inflight sterilization.

The alternative source of sterilizing protons is a linear proton accelerator. This possibility is now investigated.

Consider a lander of a thickness of 92 grams/cm^2. A proton energy E is selected such that the protons penetrate all the way through the lander. This is to avoid the characteristic sharp spike of high dose intensity found at the end of the penetration range of the proton. This spike was not noticeable with a continuous spectrum such as the solar flare of Fig. 3 since successive portions of the spectrum deposit their "spikes" of dose in successively deeper layers, but accelerators produce a line spectrum of protons and the spike does occur. To avoid it, E must be over 360 MeV.

There are several objections to the use of such high energy protons. The first is the requirement that a large machine such as the Cosmotron be used. A second problem is the large number of cascade reactions that occur, resulting in residual radioactivity and in local damage centers such as the "star production" associated with nuclear spallation. A third problem is the secondary neutron emission from these reactions, which leads to radioactivation and radiation damage as discussed in the next section. Finally, because of its mass, the proton is of the order of 30-100 times more damaging than an electron to an atomic lattice[54].

* in a period of comparative solar inactivity. When solar activity is at a maximum, however, about 5 flares can be expected in a 6 month interval.

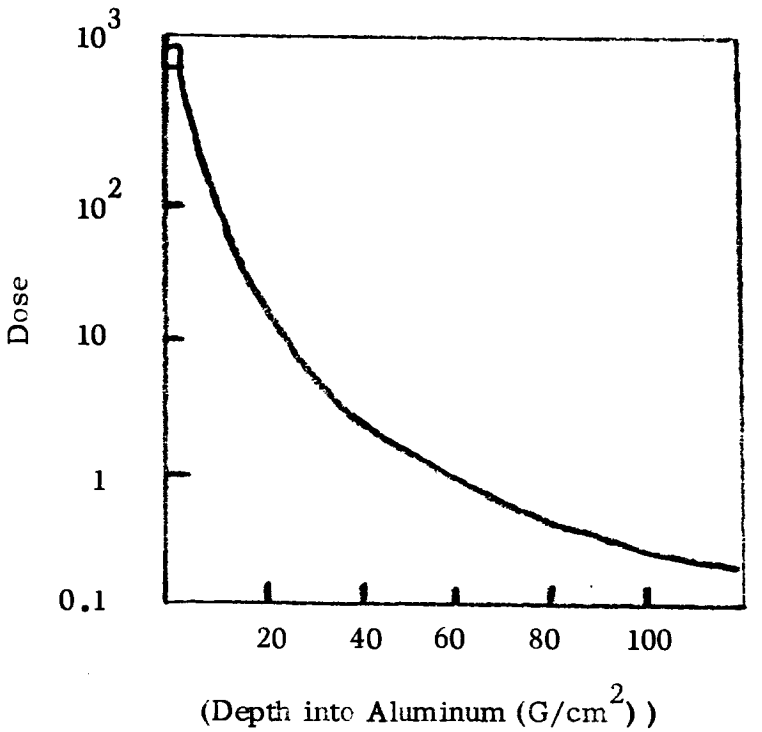

Figure A-1. Dose (in water) from November, 1960, Solar Flare Protons traversing a spherical aluminum shield. (Ref. 5?)

The protons knock nuclei from their lattice positions at a higher rate and thereby introduce more damage per unit dose to transistors and other semiconductors than would be experienced with electrons or high energy photons.

A-2 Neutron Radiation

Of the many ways of obtaining neutrons, the nuclear reactor is most attractive. Megarad doses are readily obtained adjacent to a medium-power (3-5 megawatt) nuclear reactor in less than an hour.[55] The nuclear reactor emits both neutrons and gamma rays and the relative amounts of these can be controlled to some extent by choice of appropriate shielding materials. The energy spectrum of the neutrons incident on the capsule can also be controlled in this way. For example, a boron-loaded filter will transmit only the higher energy portion of the neutron spectrum, with average energies of 1-2 MeV, together with the gamma rays.

Even though such energetic neutrons were to be incident on the capsule, these would be moderated in energy by collisions with the atomic nuclei of the atoms present, until they have thermal energies and are captured. In most materials, very few neutron captures occur at the higher incident energy. In the process of moderation, the fast neutrons travel in a zigzag path; the distance from start to end of the average path is referred to as the slowing down length. In aluminum, this is 60 grams/cm^2 for fission neutrons,[56] so that there is a good chance a fast neutron will not traverse the 92 grams/cm^2 thick capsule before it is reduced to a thermal neutron. Essentially all of the neutrons incident on the capsule are moderated to thermal energies and captured in the capsule.

For a surface dose of 5 megarads, about 2 x 10^{14} fast neutrons should bombard each square centimeter.[55] The dose administered by a nuclear reactor will include some proportion of gamma photons and of thermal neutrons.

For an order of magnitude calculation of neutron effects, the gammas and thermal neutrons are neglected, especially since it is to be recognized that there will be attenuation of the dose with depth into the capsule, so that a surface dose higher than 5 megarads is really required for total capsule sterilization. Furthermore, it is practical to remove the thermal neutron component with a shield of boral or cadmium since they do not have the desirable penetration capability of the fast neutrons and the gamma photons.

A spherical capsule, weighing 2500 lbs. and with a radius of 5 feet will be taken as the model Mars lander in this discussion.

The density of this sphere is 0.0284 that of aluminum. Assuming that the sphere is aluminum with the proper fraction of voids to reduce the density to this value, and using neutron removal cross sections[56], we find that 50% of the fast neutrons will penetrate a diameter of the sphere. The rest lost energy in the sphere, and an upper bound to the activation of the sphere can be found by assuming that all of these thermalize in the sphere and are captured by the material of the sphere. This amounts to 7.3×10^{18} captures.

Typical of such capture reactions is the reaction $Al^{27}(n,\gamma)Al^{28}$. The daughter has a half-life of 2.3 minutes. If all captures were due to this reaction and a two hour cooling period were allowed, the capsule activity would then be about a hundredth of a microcurie, a completely negligible amount.

The capture of neutrons to lead to radioactivity with a half-life on the order of minutes, clearly leads to no radiation hazard, provided that a cooling-off period of a few hours is allowed. As well, elements such as carbon, oxygen, silicon, lithium, and beryllium can be allowed since their neutron absorption cross sections are negligible or (in the case of lithium) lead to no residual activity.

The aluminum alloy X2020-T6 is attractive to spacecraft designers because of its strength, particularly at elevated temperatures.[57] This alloy contains 4.5 percent copper, 1.1 percent lithium, and 0.2 percent cadmium. If the capsule were made of predominately this alloy, some activation would occur during neutron sterilization.

The fraction of the neutrons captured in each element in the alloy is approximately equal to the macroscopic thermal neutron absorption cross section of the element, divided by the total macroscopic cross section. These cross sections are readily available for the pure element.[13] The data for the calculation are tabulated below.

Table 1 Neutron Activation of X2020-T6 Alloy

Element	Al	Cu	Li	Cd
Cross section*:	.0052	.035	.616	17.8
Weight fraction:	.942	.045	.011	.002
Weighted cross section:	.0049	.0016	.0073	.0356
Fraction of neutrons captured:	0.10	.03	.15	.72

* in cm^2/gm

Because of the large cross section, cadmium which is present as only 0.2% of the alloy, accounts for 72% of the neutrons absorbed.

There are eight isotopes present in natural cadmium. About 12.3% of natural cadmium is Cd^{113}, which has a large cross section, around 2.1×10^4 barns, that is responsible for the bulk of the absorptions but produces no residual activity. Also present, about 7.6% is Cd^{116}, which has a cross section around 1.5 barns for the production of Cd^{117}. This product is radioactive, emitting 0.4-1.6 MeV photons, with a half-life of 2.9 hours. Of the captures in cadmium, only 0.45×10^{-2}% are captures in Cd^{116}. This results in about half a curie of activity if a 3 hour cooling period is allowed. A reaction leading to a longer-lived daughter is $Cd^{114}(n,\gamma)$. The half-life is 43 days and about 40 microcuries are formed. Of this small amount of radioactivity, only 1% results in a

gamma emission. Other reactions in cadmium lead to half lives on the order of minutes ($Cd^{106}(n,\gamma)$ and $Cd^{110}(n,\gamma)$) or have small cross sections and negligible photon yields ($Cd^{108}(n,\gamma)$, $Cd^{111}(n,\gamma)$ and $Cd^{112}(n,\gamma)$).

Two isotopes are present in copper. The reaction $Cu^{65}(n,\gamma)\ Cu^{66}$ leads to activity with a half-life of 5 minutes. The reaction $Cu^{63}(n,\gamma)\ Cu^{64}$ leads to activity with a half-life of 12.87 hours, with a photon of 1.34 MeV emitted in a 0.43% of the disintegrations. This amounts to about a third of a curie after irradiation.

The total activity due to this activated aluminum alloy amounts to about one curie at a time of 3 hours after irradiation by fast neutrons. This produces several times the allowable dose rate for men to work at a distance of a few feet from the capsule. If there are appreciable quantities of cobalt in the capsule (e.g., associated with nickel in stainless steel alloys) the radioactivation would be more severe and long-lasting.

These calculations* suggest that for a specific Mars lander design, sterilization by fast neutrons presents a significant radiation hazard. Nuclear reactor radiation, with the thermal neutron portion shielded out, is a combination of gamma photons and fast neutrons, and is therefore a correspondingly smaller source of radioactivation. It is possible that the induced radioactivity from this mode of sterilization would be objectionable if it interfered with nuclear counting experiments installed in the lander.

Another objection to the use of fast neutrons is their high coefficient for damage to silicon semiconductor material. For equal doses, neutrons will cause more displacements in semiconductor materials than will gamma photons. Thus, if reactor radiation is used, it should be shielded so that the fraction of the radiation dose which is produced by neutrons is minimized. However, other radiation sources exist for photons, as discussed in section 2.3.

---

* data are from Ref. 56.